Strål
säkerhets
myndigheten
Swedish Radiation Safety Authority

Research

Identifying radiologically important ESS-specific radionuclides and relevant detection methods

2020:08

Authors: Kristina Eriksson Stenström, Vytenis Barkauskas, Guillaume Pedehontaa-Hiaa, Charlotta Nilsson, Christopher Rääf, Hanna Holstein, Sören Mattsson, Johan Martinsson, Mattias Jönsson, Christian Bernhardsson
Lunds universitet, Lund
Report number: 2020:08
ISSN: 2000-0456
Available at: www.ssm.se

SSM perspective

Background

The European Spallation Source (ESS) facility is under construction in Lund, Sweden. High-energy protons will be accelerated in a linear accelerator and generate neutrons when hitting a rotating target of tungsten. This spallation process will also generate a wide range of different radioactive by-products of which a small part will be released to the environment during normal operation. Furthermore, in case of an accident scenario, gases and aerosols might be released from the tungsten target. Emissions from ESS, both during normal operation or in case of an accident, will differ in radionuclide composition to the environment from those activities with ionising radiation that we have experience from in Sweden today. Thus, the Swedish Radiation Safety Authority has found it of great importance to support the possibilities to increase the knowledge about measurement and analysis of ESS-specific radionuclides that could be useful in the environmental monitoring program when the ESS facility starts to generate neutrons in a few years.

Results

Based on an extensive literature review of ESS-relevant radionuclides the authors concluded that radionuclide production in particle accelerators is well known, while experience with tungsten targets is very limited.

The authors showed a good agreement with results of others, except for ^{148}Gd, and that the calculated radionuclide composition is sensitive to the nuclear interaction models used by developing an independent simplified model of the ESS target sector for the calculations of radionuclide production in the ESS target.

In this report, suggestions of detection techniques of the most relevant ESS-specific radionuclides in environmental samples are given based on a literature review. Liquid scintillation counting (LSC) is suggested as a suitable technique e.g. for the beta emitters ^{3}H, ^{14}C, ^{35}S, ^{31}P and ^{33}P. Alpha spectrometry is seemed promising for the analysis of alpha-emitting lanthanides, in particular for ^{148}Gd. Among the many types of mass spectrometry techniques, inductively coupled plasma mass spectrometry (ICP-MS) and accelerator mass spectrometry (AMS) are seemed to be the most suitable mass spectrometry techniques for the analysis of long-lived ESS radionuclides in environmental samples (e.g. ^{243}Am and possibly lanthanides for ICP-MS and ^{10}Be, ^{14}C, ^{32}Si, ^{36}Cl, ^{60}Fe and ^{129}I for AMS).

Furthermore, this report includes performed experimental parts related to initiation of radioactivity measurements of aerosols at Lund's University, mapping of environmental tritium in the Lund area, and performing a baseline study of the tritium content in urine for persons presently living or working in Lund.

This project has resulted in two scientific publications entitled *Prediction of radionuclide production in European Spallation Source target using FLUKA* (Nuclear Instruments and Methods in Physics Research B) and *Tritium in urine from members of the general public and occupationally exposed workers in*

Lund, Sweden, prior to operation of the European Spallation Source (Journal of Environmental Radioactivity).

Relevance

This report gives insight into techniques useful for measurement and analysis of ESS-specific radionuclides and presents results that are of interest in SSM's regulatory supervision of the licensee ESS.

Need for further research

Initially, it should be mentioned that the licensee ESS has a responsibility to develop an environmental monitoring program near the ESS facility. This includes ensuring the development of the measurement methods that are identified as necessary and to carry out and follow up the monitoring program. However, it could still be of interest for SSM to give future further support to scientific research on development on specific techniques enabling quantification of ESS-specific nuclides like alpha-emitting lanthanides in various samples (^{148}Gd) and radionuclides that are rarely studied and presently in lack of any analytical method.

Furthermore, development of an extraction procedure for subsequent LSC analyse of relevant beta emitters in environmental samples (and in urine) could also be of interest for future research projects especially if it could be connected to the annual follow-ups of urine content of the general public.

Project information

Contact person SSM: Peter Frisk
Reference: SSM 2018-1636 / 703 0237-00

Strål
säkerhets
myndigheten
Swedish Radiation Safety Authority

Authors: Kristina Eriksson Stenström, Vytenis Barkauskas,Guillaume Pedehontaa-Hiaa,
Charlotta Nilsson, Christopher Rääf, Hanna Holstein, Sören Mattsson,
Johan Martinsson, Mattias Jönsson, Christian Bernhardsson
Lunds universitet, Lund

2020:08

Identifying radiologically important ESS-specific radionuclides and relevant detection methods

Date: June 2020
Report number: 2020:08 **ISSN:** 2000-0456
Available at www.stralsakerhetsmyndigheten.se

This report concerns a study which has been conducted for the Swedish Radiation Safety Authority, SSM. The conclusions and viewpoints presented in the report are those of the author/authors and do not necessarily coincide with those of the SSM.

SSM 2020:08

Identifying radiologically important ESS-specific radionuclides and relevant detection methods

Kristina Eriksson Stenström[1], Vytenis Barkauskas[1], Guillaume Pedehontaa-Hiaa[2,1], Charlotta Nilsson[1], Christopher Rääf[2], Hanna Holstein[2], Sören Mattsson[2], Johan Martinsson[2], Mattias Jönsson[2], Christian Bernhardsson[2]

[1]Lund University, Department of Physics, Division of Nuclear Physics

[2]Lund University, Department of Translational Medicine, Medical Radiation Physics, Malmö

Summary

The European Spallation Source (ESS) is under construction in the outskirts of Lund in southern Sweden. When ESS has entered the operational phase in a few years, an intense beam of high-energy protons will not only produce the desired spallation neutrons from a large target of tungsten, but a substantial number of different radioactive by-products will also be generated. A small part of these will be released to the environment during normal operation. During an accident scenario, a wide range of gases and aerosols may be released from the tungsten target. The palette of radionuclides generated in the ESS target will differ from that of e.g. medical cyclotrons or nuclear power plants, thus presenting new challenges e.g. in the required environmental monitoring to ensure that dose limits to the public are not exceeded.

This project (SSM2018-1636), financed by the Swedish Radiation Safety Authority (SSM), aimed to strengthen competence at Lund University for measurement and analysis of ESS-specific radionuclides. First, an extensive literature review, including modelling as well as experimental analyses, of ESS-relevant radionuclides was performed. We found that radionuclide production in particle accelerators is well-known, while experience with tungsten targets is very limited.

As a second part of the project, an independent simplified model of the ESS target sector for the calculations of radionuclide production in the ESS tungsten target was developed using the FLUKA code. We conclude that we have a fairly good agreement with results of other authors, except for ^{148}Gd, and that the calculated radionuclide composition is sensitive to the nuclear interaction models used.

In the third part of the project, known environmental measurement technologies for various ESS-relevant radionuclides were reviewed, focussing on pure difficult-to-measure alpha- and beta-emitters. Liquid scintillation counting (LSC) is a suitable technique e.g. for the important beta emitters ^{3}H, ^{14}C, ^{35}S, ^{31}P and ^{33}P. Several ESS radionuclides of relevance for dose estimates have never been investigated by environmental analytical techniques, due to their absence in the normal environment. Alpha spectrometry seems promising for the analysis of alpha-emitting lanthanides, in particular for ^{148}Gd. Among the many types of mass spectrometry techniques, ICP-MS (inductively coupled plasma mass spectrometry) and AMS (accelerator mass spectrometry) seem to be the most suitable for the analysis of long-lived ESS radionuclides in environmental samples (e.g. ^{243}Am and possibly lanthanides for ICP-MS and ^{10}Be, ^{14}C, ^{32}Si, ^{36}Cl, ^{60}Fe and ^{129}I for AMS).

Three experimental parts were performed during the project, related to initiation of radioactivity measurements of aerosols at Lund University, mapping of environmental tritium in the Lund area, and establishment of a method to measure tritium in urine followed by a study of tritium in persons presently living or working in Lund.

Aerosols were collected at a rural background station (Hyltemossa near Perstorp, northern Skåne) using a high-volume aerosol sampler with automatic

filter change (DHA-80, Digitel). Gamma spectrometry measurements of ^{7}Be agreed rather well with results from a nearby air monitoring station (SSM/FOI).

Tritium (radioactive hydrogen) is expected to dominate the source term from the ESS target station to the environment. We have performed several investigations to monitor the current situation of tritium in Lund using LSC: the matrices investigated included air humidity, precipitation, pond water, indoor air at one accelerator facility and urine from the general public as well as from persons who may be occupationally exposed to tritium. Environmental tritium was generally very low (<3.4 Bq L^{-1}), with somewhat higher concentration in the springtime than during the rest of the year. Tritium in the vast majority of the 55 urine samples was also very low: only a few exposed workers were found to have up to 11 Bq L^{-1} in their urine, which still is very low compared to e.g. reactor workers.

Suggestions for further actions and work related to measurement and analysis of ESS relevant radionuclides are presented.

Sammanfattning

ESS – “European Spallation Source” – är under uppbyggnad i utkanten av Lund. När ESS träder in i den operativa fasen om några år kommer en jonstråle av protoner med hög energi och effekt att träffa ett stort strålmål (”target”) av volfram. Då kommer inte bara de avsedda neutronerna att produceras, utan även ett stort antal radioaktiva restprodukter. En mindre del av dessa kommer att släppas ut till omgivningen vid normal drift. Vid ett olycksscenario kan ett stort antal gas- eller partikelformiga radioaktiva ämnen frigöras och spridas i omgivningen. Paletten av olika radioaktiva ämnen i ESS skiljer sig markant från den som uppträder t ex i cyklotronacceleratorer inom sjukvården eller kärnkraftverk. Nya utmaningar uppkommer därför exempelvis i den miljöövervakning som krävs för att garantera att dosgränser till allmänheten inte överskrids.

Denna rapport sammanfattar ett projekt som finansierats av Strålsäkerhetsmyndigheten (SSM) och som haft för avsikt att stärka kompetensen vid Lunds universitet för mätning och analys av ESS-specifika radionuklider. I projektets första del utfördes en omfattande litteraturstudie, innefattande såväl modellering som experimentella analyser, av det förväntade inventariet av producerade radionuklider inom ESS. Vi kom fram till att radionuklidproduktionen i partikelacceleratorer är välkänd, men att erfarenheten av strålmål av volfram är ytterst begränsad.

I del 2 av projektet gjordes en oberoende simulering med koden FLUKA av radionuklidproduktionen i en förenklad modell av en av ESS strålmålssektioner. Vår slutsats var att överenstämmelsen med andra studier är tämligen god, med undantag för ^{148}Gd, och att beräkningarna av olika isotopförhållanden har hög känslighet för vilken kärninteraktionsmodell som används.

I projektets tredje del gjordes en litteraturöversikt av kända mätmetoder för omgivningsmätningar av olika ESS-relevanta radionuklider, med fokus på svårmätta nuklider och rena alfa- och betastrålare. Mätning med vätskescintillator (LSC) är en lämplig teknik t ex för de för ESS viktiga betastrålarna ^{3}H, ^{14}C, ^{35}S, ^{31}P och ^{33}P. Åtskilliga ESS-radionuklider med relevans för stråldosuppskattningar har aldrig tidigare mätts i miljön (de är varken naturligt förekommande eller släpps ut från vanliga typer av kärntekniska anläggningar). Alfaspektrometri framstår som en lämplig teknik för framtida analys av alfastrålande lantanider, särskilt ^{148}Gd. Av olika masspektrometriska metoder tycks ICP-MS (induktivt kopplad plasmamasspektrometri) och AMS (acceleratormasspektrometri) vara mest lämpliga för analys av långlivade radionuklider i omgivningsprover (t ex ^{243}Am och möjligen lantanider med ICP-MS samt ^{10}Be, ^{14}C, ^{32}Si, ^{36}Cl, ^{60}Fe och ^{129}I med AMS).

Tre experimentella delar utfördes inom projektet: initiering av mätning av radioaktiva aerosoler, kartläggning av tritiumnivåerna i miljön i Lundatrakten, och etablering av en metod för att mäta tritium i urin följt av en studie av tritium i människor som för närvarande arbetar eller bor i Lund.

Aerosoler samlades in på en bakgrundsstation på norra Skånes landsbygd (Hyltemossa utanför Perstorp) med en högvolym-aerosolinsamlare med automatiskt filterbyte (DHA-80, Digitel). Mätningar av ^{7}Be med

gammaspektrometri överensstämde tämligen väl med resultat från en närbelägen luftövervakningsstation (SSM/FOI).

Tritium tros att dominera källtermen från ESS strålmålsstation till omgivningen. Vi har genomfört flera undersökningar av dagens nivåer av tritium i Lund med LSC: undersökta provtyper inkluderar luftfuktighet, nederbörd, vatten från dammar, inomhusluft vid en acceleratoranläggning och urin från allmänhet såväl som potentiellt yrkesmässigt exponerade personer. Tritiumhalten i omgivningsproverna var generellt mycket låg (<3,4 Bq L^{-1}), med något högre nivåer under våren än under övriga året. Majoriteten av urinproven uppvisade också ytterst låga tritiumvärden: endast ett fåtal yrkesmässigt exponerade personer hade upp till 11 Bq L^{-1} in urinen, även det ett lågt yrkesbetingat värde.

Förslag på fortsatt mätning och analys av ESS-relevanta radionuklider presenteras i slutet av rapporten.

Abbreviations and notations

A	Mass number
AMS	Accelerator Mass Spectrometry
δD	delta D, i.e. relative deviation of the $^{2}H/^{1}H$ ratio of a sample compared to that of a standard
DNP	Division of Nuclear Physics, Lund University
DTM	Difficult-To-Measure
E	Energy
EC	Electron Capture
FOI	Swedish Defence Research Agency
GDMS	Glow Charge Mass Spectrometry
GNIP	Global Network of Isotopes in Precipitation
HL	Half-Life
HPGe	High Purity Germanium
HTO	Tritiated water
HWFM	Half Width at Full Maximum
IRMS	Isotope Ratio Mass Spectrometry
ICP-MS	Inductively Coupled Plasma Mass Spectrometry
IT	Isomeric Transition
LSC	Liquid Scintillation Counting
LU	Lund University
MRPM	Medical Radiation Physics, Malmö, Lund University
NAA	Neutron Activation Analysis
OBT	Organically Bound Tritium
PIPS	Passivated Ion-implanted Planar Silicon
PMT	Photo Multiplier Tube
RIMS	Resonance Ionization Mass Spectrometry
SIMS	Secondary Ion Mass Spectrometry
SSM	Swedish Radiation Safety Authority
ST	Source Term
T	Tritium

$T_{1/2}$	Physical half-life
TDCR	Triple-to-Double Coincidence Ratio
TIMS	Thermal Ionization Mass Spectrometry
Z	Atomic number

Contents

1. Introduction

This introductory chapter gives the background to and the objectives of the project SSM2018-1636, financed by the Swedish Radiation Safety Authority (SSM).

1.1. Background

The neutron-based research facility European Spallation Source (ESS) is under construction in the outskirts of Lund in southern Sweden. In the heart of ESS, consisting of a large target of tungsten (atomic number $Z = 74$), proton-induced spallation will not only generate the desired neutrons, but radioactive by-products will also be produced. The main part of these will be of lower Z than the target element itself (see e.g. [2]). The operation of any high-energy accelerator facility inevitably generates radionuclides through nuclear reactions not only in the instrumental parts itself, but also indoor air, surrounding soil and water will be activated [3, 4]. Radioactive gases as well as radioactive aerosols are expected to be formed in the accelerator tunnel during normal operation (see e.g. [5, 6]). Parts of the radionuclides generated during normal operation will be released to the environment e.g. through the ventilation stacks of the ESS facility [6]. During an accident scenario, a wide range of gases and aerosols e.g. from the tungsten target may be released, inhaled by workers as well as by the general public and - in case of aerosols – also deposited on the ground [7].

The palette of radionuclides generated in the ESS target will differ from that of e.g. medical cyclotrons and nuclear power plants, thus presenting new challenges e.g. in the required environmental monitoring to ensure that dose limits to the public are not exceeded. A wide range of alpha and beta emitters are expected to be formed at the ESS, some of which are pure alpha and beta emitters, and which cannot be detected with gamma spectrometry. Examples of pure beta emitters are ^{3}H, ^{14}C, ^{55}Fe, ^{63}Ni, ^{89}Sr and ^{90}Sr. A number of alpha emitters are believed to become of essential importance, due to their radiotoxic effects, such as ^{148}Gd, ^{150}Gd, ^{154}Dy and ^{146}Sm [8, 9].

This report summarizes the activities of a one-year project financed by SSM and related to ESS-specific radionuclides. In the announcement SSM stated that the purpose of the project was to develop competence and knowledge about measurement and analysis of the specific radionuclides that will be generated by ESS. The world-wide experience from operation of high-power spallation facilities such as ESS is very limited, hence the importance of maintaining and developing competence to perform dose assessment through actual measurements.

1.2. Objectives

The objectives of the project were:

- To perform an exhaustive review of the published literature related to the expectation of radionuclides to be formed in the ESS target.
- To perform an independent modelling of the radionuclide content to be produced in the ESS target, using the Monte Carlo-based simulation code FLUKA, and compare the outcome with published data.
- To review and suggest sample detection techniques of the most relevant ESS-specific radionuclides in environmental samples, and to identify the need of development of new techniques. Particular attention was devoted to liquid scintillation counting (LSC).
- To test performance of the aerosol collection instrumentation at the ICOS/ACTRIS rural background site Hyltemossa (near Perstorp in northern Skåne) for assessment of radioactive aerosols, using gamma spectrometry, and to initialize alpha spectrometry measurements of aerosol samples.
- To perform baseline measurements of tritium in environmental samples in Lund, including a one-year study of precipitation and air humidity, and additional surveys of surface waters.
- To map the levels of tritium in humans in the Lund area, including members of the general public, ESS neighbours, ESS personnel and workers currently exposed to tritium, through urinary assessment of waterborne tritium.

The outcome of these tasks is described consequently in the report. In the final part, the work is summarized, and an outlook is provided with suggestions of further actions.

2. Radionuclide production in the ESS facility – a literature review

This section contains a summary of the report "Review of radionuclides in ESS", which is added as an appendix.

The review of radionuclides which may be produced in ESS was performed in accordance with one of the project objectives. The review was based on data in available ESS documentation, as well as on scientific publications, covering not only ESS, but also other spallation sources and linear accelerators. The information provided is based on both modelling and experimental analysis. The list of identified long-lived radionuclides (10 hours and longer half-lives) was made with references where the particular radionuclides were identified. The list is given in Appendix A of Appendix 1.

The current report focusses on laboratory-based methods for assessment of Difficult-To-Measure (DTM) radionuclides. Such techniques have to take time necessary for sampling, sample treatment and measurement into account. Thus, it is difficult to measure short-lived DTM radionuclides, since they may decay significantly before measurement is practically possible. In the literature we limited the half-life of the radionuclides to longer than 10 hours. Thomas and Stevenson [10] are proposing this limit for hydrology studies, since radionuclides with too short a half-life will decay so rapidly as to be of no potential hazard when they reach a public water supply. Their activity is reduced 1000 times in 4 days or faster, i.e. they are relevant only for very specific accident scenarios and their impact for environment is short-term.

The radionuclides are relevant for radioactive waste management issues as well. The most important findings of our study are:

- Experimental data from tungsten spallation targets composition studies exists, but it is limited, and more experimental data is needed to verify existing calculations. Additionally, theoretical spallation models have to be further developed, taking experimental data into account.
- The induced radioactivity in linear accelerators is a well-known phenomenon, described in a number of publications. Radionuclides produced in air, structural elements and soil are also known and listed in those publications. No unique or very rare radionuclides should be generated in the accelerator structures.
- The radionuclides with the highest dose coefficients are the alpha emitters $^{241, 243}$Am, ^{228}Th, $^{150, 148}$Gd, ^{146}Sm, and ^{154}Dy. For most alpha emitters, inhalation dose coefficients are higher than the ingestion ones. Other radionuclides with the high inhalation and ingestion dose coefficients include $^{129, 126, 131, 125}$I and $^{137, 134}$Cs as well as ^{210}Pb, ^{60}Fe, ^{178m}Hf, ^{90}Sr, ^{44}Ti and ^{166m}Ho.

The full report is given in Appendix 1.

3. Modelling the radionuclide content of the ESS target using FLUKA

This section contains a summary of the report "Prediction of radionuclide production in European Spallation Source target using FLUKA", published in Nuclear Instruments and Methods B [11].

An independent, simplified model of the ESS target sector for the calculation of radionuclide production in the ESS tungsten target has been developed. The major components of the ESS target were included in the model, but with simplified geometries. This includes target itself, water pre-moderator, hydrogen moderator, and beryllium reflector. Bulk shielding around the model and moderator-reflector plug were not included in the model.

The FLUKA code was used for calculations. FLUKA is a general-purpose tool for calculations of particle transport and interactions with matter using the Monte Carlo method and it has been used to solve a wide range of particle transport problems. It can be used to calculate radionuclide production in the ESS target, as it is possible to simulate high-energy particle interactions, as well as the behaviour of low-energy neutrons. Ten relevant radionuclides, important immediately after shutdown, and nine radionuclides important after several years of decay, were selected for comparison with the results obtained by other authors. The selection was based on radionuclide dose coefficients and total predicted activities. This was performed in order to verify our model and justify its suitability for this type of calculations. Attention should be paid that radionuclides were selected mainly for the demonstration of model validity, i.e. we were not intending to cover all most relevant radionuclides. One of the important factors for selection was if the activity of the radionuclide was reported in other publications.

The predicted radionuclide production was higher than estimated by other authors for most of the radionuclides considered. The differences between our results and those of Mora et al. [8] are greater than those between our values and those from the PSAR [12] and Kókai et al. [13]. However, the differences were less than a factor of five for all radionuclides analysed, except ^{148}Gd. Evaluation of ^{148}Gd production is not an easy task. The order-of-magnitude errors in the nuclear data available for ^{148}Gd are not surprising, given the spread in available simulation results. Slightly different physical assumptions are used in the various models, and the activities obtained therefore differ, especially in the deep spallation region. FLUKA uses the PEANUT package, which includes a very detailed GINC model and a pre-equilibrium stage model. We believe differences in ^{148}Gd activities predictions can be attributed to differences in spallation and nuclide evaporation models.

The calculated ^{3}H activity was very close to the highest values obtained with other spallation models. Considering impurities that may be present in the tungsten target did not significantly affect the activities of the radionuclides produced in the target. We noticed the impact of impurities for the reduced concentration of ^{90}Sr, but the absolute change of ^{90}Sr concentration is not very significant. Radionuclide production profiles in the target were also investigated and were found to differ depending on the radionuclide.

The relative uncertainty in the estimated activity of ^{90}Sr was highest (65%) among the radionuclides considered in this study. The relative uncertainties for the other radionuclides varied from 0.5% (^{3}H) to 12% (^{60}Co). These uncertainties are only those caused by the statistical nature of Monte Carlo neutron transport calculations. The impact of uncertainties in nuclear data (cross-section) and sensitivity to other parameters were not considered in this study.

The calculated activities can be further used as input for the source term in an accident analysis. Moreover, the model and the results of this study can be used in the coarse radiological characterization of the ESS target.

The full text of the paper, entitled “Prediction of the radionuclide inventory in the European Spallation Source target using FLUKA”, is published in Nuclear Instruments and Methods in Physics Research, Section B [11].

4. Measurement technologies for selected radionuclides

This section starts with a general and very brief introduction to common measurement techniques used for radionuclide-specific measurement of radionuclides mainly present in the environment, but for some cases also for radionuclides produced in the spallation targets. Special attention is devoted to liquid scintillation counting and difficult-to-measure alpha- and beta-emitting radionuclides. Suggestions for measurement methodologies of the selected radionuclides from the review and FLUKA simulations above are briefly described and discussed. The need for development of new methodologies is also discussed.

4.1. Gamma-ray spectrometry

Gamma-ray spectrometry can be referred to as the main technique of radionuclide analysis. In many radioactive decays (e.g. for most alpha and beta emitters), the daughter nucleus emerges in an excited state. Emission of high-energetic electromagnetic radiation in the range of a few keV to several MeV – gamma radiation – is one way for the new-born daughter nucleus to deexcite to a lower energy level or to the ground state. The energy of the gamma radiation emitted corresponds to a difference in energy levels of the nucleus in question, and since the energy levels are nuclide-specific, the energy of the gamma radiation can be used to identify the daughter nuclide, and hence its mother nuclide. This is the basis of gamma-ray spectrometry.

Typical for gamma radiation is its high penetrative power in matter and thus very long range. Detection of gamma radiation is based on its ability to ionize the detector material through the basic interaction processes photoelectric absorption, Compton scattering and pair production. The ultimate gamma-ray detector would completely convert all gamma energy to free electrons in the detector. In reality, however, incomplete absorption and interactions with materials surrounding the detector will produce a background in the detector's energy spectrum. Background may also arise from cosmic radiation and naturally occurring as well as anthropogenic radionuclides (valid for all types of detectors, not only gamma-ray detectors). This background must be corrected for (see e.g. [14, 15]). Furthermore, detector calibration and use of correction factors are essential to ensure high-quality results [16]. Problems to resolve photopeaks in complicated spectra may be a limiting factor, as well as the detection limit [16]. In such cases, other measurement techniques need to be used or radiochemical separations needed, even if the radionuclide of interest emit gamma radiation.

Various types of gamma-ray detectors are available, of which high resolution gamma-ray spectrometry using high-purity germanium (HPGe) detectors is

suitable for many applications including environmental radiology (see e.g. [14, 15] for further information). The energy resolution of HPGe detectors used for environmental radiology can be in the order of 2 keV for 1.33 MeV (^{60}Co) (see e.g. [17]). Detection limits are dependent e.g. on instrument efficiency, background levels and background measurement time. E.g., for laboratory-based large-efficiency detectors (up to 200% relative to 7.6 cm diameter x 7.6 cm long NaI(Tl) detectors), used in measurements of the radionuclide purity of materials, detection limits may typically reach ~1 mBq kg^{-1} [17]. Typical MDAs for *in situ* determination of contemporary radioactivity in soil samples using a 25% relative efficiency p-type HPGe detector (10 min counting time) are about 1.8 Bq kg^{-1} e.g. for ^{60}Co and ^{137}Cs [15].

Using coincidence techniques in gamma spectrometry, it is possible significantly improve the detection limit of the detection system, rejecting events induced by cosmic-rays or by environmental radionuclides. For low-level measurements data acquisition with dual detector systems enables increasing the efficiency by the use of the sum-coincidence method [18, 19].

A benefit of gamma spectrometry is that samples often can be measured without chemical separation. The main limitation of gamma spectrometry lies in that only gamma emitters can be quantified with this technique, and not pure alpha and beta emitters. Additionally, the counting efficiency is generally low and background is often high [20]. The detection limit of gamma spectrometry is usually higher than for alpha spectrometry and beta measurements [20].

4.1.1. Example: gamma-ray spectrometry of various environmental matrices

Bernhardsson et al [21] used *in situ* as well as laboratory-based gamma spectrometry to map the preoperational radiation environment of ESS in the years 2017-2018. See section 5.1 for a summary of this study.

4.1.2. Example: gamma-ray spectrometry of aerosols

The main nuclear analytical technique for assessment of radioactivity in aerosols involves gamma-ray spectrometry, which may be laboratory-based or *in situ* (see e.g. [22-25]). In the present project, gamma spectrometry has been applied to aerosol samples collected at a rural background station (see section 5.2).

4.2. Liquid scintillation counting

Liquid scintillation counting (LSC) is a radiometric technique that may be used for quantification of several ESS-relevant radionuclides. LSC is ideal for beta-emitting radionuclides and instruments equipped with a pulse-shape analyser can also measure alpha emitters in the presence of beta emitters (alpha-beta discrimination). LSC can e.g. also be used for gamma emitters (in particular for low energy), and radionuclides whose decay modes include emission of X-rays, Auger electrons or internal conversion electrons. This report does not aim to give a full description of the LSC technique, but a brief introduction to its principles is provided. For a more detailed description, see e.g. [15] , or [26] (a

recent paper by Hou which summarizes the use of LSC in environmental and nuclear applications, and describes the development of the technique since its infancy in the 1950's).

E.g., for beta emitters, LSC makes use of the fact that the electrons emitted in beta decay are easily stopped in matter, mainly by interactions with other electrons of the stopping material. The basic principle of LSC is usually to first extract the radionuclide of interest (preferably in liquid form) and then mix the sample with a cocktail containing a solvent (to obtain a homogenous counting solution) as well as small amounts of a scintillator. Several types of cocktails are commercially available, designed to fit a specific radionuclide as well as sample type (e.g. aqueous, alkaline or acid solutions). The mixtures of sample and cocktail are placed in transparent vials of glass or plastic (plastic vials generally give lower background than glass vials [15]). The amounts of sample and cocktail used depend on the application and activity concentration. For environmental samples, vials of 20 ml are often used and sample to cocktail ratios vary significantly. For the aqueous tritium samples of the present study the sample to cocktail ratio was 1:1 (10 ml of each). The cocktail is however not always needed. E.g., for high-energy beta particles of energy > 263 keV in aqueous solutions, Cherenkov radiation (photons in the region from ultraviolet to visible wavelengths) is produced, which can be detected by the LSC instrument. Examples of radionuclides that can be detected using Cherenkov radiation are ^{32}P, ^{90}Sr(^{90}Y), ^{86}Rb and ^{89}Sr [15].

The solvents may be aromatic organics such as toluene or xylene, which however are hazardous, or more safe options. The scintillator contains luminescent substances (primary and secondary phosphors). The energy from e.g. a beta particle is transferred to the solvent molecules, which in turn transfer energy to the primary scintillator. Deexcitation of the primary scintillator results in photons, however of unfavourable wavelength for effective detection. A secondary scintillator (wavelength shifter) may therefore be used to transform the light into a wavelength that is suitable to induce photoelectrons in the photocathode of the photo multiplier tube/tubes (PMTs) used in the LSC instrument. The PMT converts the light into a measurable electrical signal. The signal height of the electrical pulse (amplitude) is a measure of the energy deposited, and by using a multichannel analyser, an energy spectrum (and the rate of beta emission) can be obtained. One type of instrument uses two PMTs in coincidence (to only include true signals stemming from the initial ionizing radiation, which are detected in both PMTs). A newer instrument type, called triple-to-double coincidence ratio (TDCR), uses three PMTs giving two different coincident outputs (see e.g. [15, 26]). The TDCR method is used for absolute measurements of pure beta and EC emitters, and does not rely on internal or external radiation sources for determination of the efficiency of the measurement [15, 26].

The counting efficiency in LSC depends on several factors, such as the energy in case of beta emitters (higher efficiency for higher beta energies). The instrument used for the tritium measurements (low-energy beta) in this report (Beckman LS 6500) typically has an efficiency of about 24%. For alpha emitters the efficiency of LSC instruments is usually approximately 100% [15]. The term quenching refers to loss of photons before reaching the PMTs and is thus related to the efficiency of the measurement. Three phenomena exist: chemical quenching,

colour quenching and ionization quenching [15]. Different methods exist to assess the quenching, and hence efficiency, of a sample, see e.g. [15]. In the present study of tritium, Horrocks' method for quenching correction was used [27].

Alpha/beta discrimination in LSC is based on the fact that alpha and beta radiation result in electric signals of different lengths (pulse decay times), with alpha particle pulses being 35-40 ns longer than that of beta particles [15]. The energy spectra may often overlap. Alphas interact less efficiently than betas to transfer energy to the solvent and scintillator, producing a pulse height corresponding to about 10% of its decay energy. Thus, the monoenergetic alpha peaks (original energy in the order of MeV) are recorded at some hundred keV, often overlapping the continuous beta spectrum of some beta emitter (see e.g. Figure 7.2 in [15]). Taking the unique energy of alpha particles as well as the longer pulse duration into account, alpha emitters can often be identified and quantified using LSC. The energy resolution of most commercial LSC systems is however poor (about 20-25%), which makes alpha spectrometry difficult. In environmental LSC, the activity concentrations are of natural and/or anthropogenic radionuclides are generally low, making low instrumental background of utmost importance for measurements of sufficient precision.

Examples of radionuclides which may be quantified by LSC include e.g. tritium, ^{14}C, ^{32}P, ^{33}P, ^{35}S, ^{36}Cl, ^{41}Ca, ^{45}Ca, ^{49}V, ^{51}Cr, ^{55}Fe, ^{59}Fe, ^{63}Ni, ^{65}Zn, ^{67}Ga, ^{86}Rb, ^{89}Sr, ^{90}Sr, ^{90}Y, ^{93}Zr, ^{99}Tc, ^{125}I, ^{129}I, ^{210}Pb and ^{241}Pu [15, 26]. Some positron or EC emitters which may be measured by LSC include ^{18}F, ^{34m}Cl and ^{34}Cl, ^{54}Mn, ^{68}Ga, ^{85}Sr, ^{88}Y, ^{109}Cd, ^{111}In, ^{123}I, ^{125}I, ^{133}Ba and ^{139}Ce [15].

Detection limits and accuracy depend e.g. on radionuclide as well as the instrument used (signal-to-noise ratio), vial type, measurement times and sample volume (see e.g. [15, 20]). A drawback of LSC is the need for time- and labour-consuming quench correction, and not rarely, sample preparation.

4.2.1. Example: Tritium measurements using LSC

LSC is the most common technique for measurement of tritium (pure, low-energy beta-emitter). Alternative measurement methods include ionization chambers and gas proportional counters (to be used mainly in case of high activities) [26]. Accelerator mass spectrometry may also be used, mainly for very small amounts of tritium [28]. Sample preparation methods preceding LSC measurement of environmental samples are outlined e.g. in [1] and are summarized in Figure 1. Electrolytic enrichment (resulting in concentration of tritium in water due to isotope fractionation when water molecules are electrolytically decomposed) may also be used [29]. Environmental tritium is present in low levels, and requires LSC instruments with a low background [29].

LSC has been used in the present study to measure tritium in air humidity, water and urine, see below.

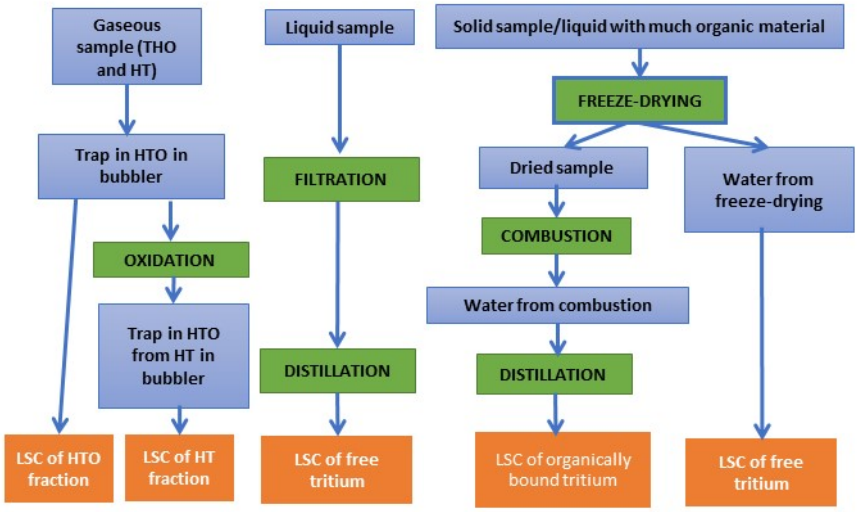

Figure 1: Sample preparation techniques for various environmental matrices before tritium analysis using LSC. Adapted from [1]. Water samples may also be electrolytically enriched prior to LSC measurement.

4.3. ICP-MS and other mass spectrometric techniques

A number of mass spectrometric (MS) techniques are used for quantification of different long-lived radionuclides [15]. The fundamental principle of MS systems is to ionize the sample, accelerate the ions (keV) and make use of magnetic and electrostatic fields to separate different ions depending on mass, energy and charge. Mass spectrometric techniques thus do not rely on detection of the emitted radiation and are instead atom-counting methods. A most useful mass spectrometric technique in environmental measurements of radionuclides is inductively coupled plasma mass spectrometry (ICP-MS), which exhibit extremely low detection limits [15, 30]. The most investigated radionuclides by ICP-MS and laser ablation ICP-MS (LA ICP-MS) include ^{79}Se, ^{90}Sr, ^{99}Tc, ^{210}Pb, ^{226}Ra, ^{228}Ra, ^{230}Th, different uranium and plutonium isotopes and ^{241}Am and ^{243}Am.

In ICP-MS the sample is introduced into the ion source under atmospheric pressure as a nebulized solution (aerosols) or as ablated material [15]. Ions (generally positive) are formed from the sample in a plasma in the ion source and the ions are accelerated to the keV range prior to separation according to mass, energy and charge by a magnetic field (obtaining mass spectra with intensity as a function of the mass-to-charge ratio). The ICP-MS system may be preceded e.g. with liquid chromatography (LC, HPLC), gas chromatography (GC) or supercritical fluid extraction (SFC) [15]. In general, ICP-MS requires significantly less sample preparation than radiochemical techniques, with the exception of the determination of long-lived radionuclides [15]. As summarized in [15], ICP-MS offers simultaneous determination of all-matrix, trace elements and ultratrace elements with very low detection limits (0.001-0.1 pg mL^{-1}). Only very small amounts of analyte are required (< ng) and the precision of trace element determination can be about ±2-5% [15]. Isotope ratio measurements can be very precise (0.001% using multiple ion collectors ICP-MS) [15]. The major

limitation is interference of molecular ions in the mass spectra [15, 20]. This can be exemplified with analysis of ^{14}C, which is hindered by interference from e.g. its molecular isobar ^{13}CH.

Thermal ionization mass spectrometry (TIMS) is another technique used for the determination of isotopic ratios, in particular of long-lived radionuclides [31]. In TIMS, down to 1 μL of the sample solution is dried on a metal filament, usually made of tungsten or rhenium. Generally, a two-filament system is used, one with the sample and one without, their heating in the instrument will evaporate and ionise the nuclides from the sample which will then be analysed by a multi-collector mass spectrometer. The reference method for TIMS measurement is called total evaporation where the full amount of sample on the filament is evaporated in order to avoid isotope fractionation [32]. The main advantage of TIMS is its high accuracy in isotope ratio measurements (0.001% or less) [20]. In addition to U, Th and Pu isotopes, TIMS was used for other radionuclides such as ^{41}Ca, ^{126}Sn, ^{226}Ra, ^{228}Ra, ^{241}Am, ^{243}Am, ^{242}Cm [20, 32].

Glow discharge mass spectrometry (GDMS) is a powerful and efficient analytical method for the direct trace element analysis of solid samples. In GDMS, an argon gas glow discharge is used as an ion source. The cathode surface consisting of the sample material is sputtered by Ar ions, which are formed in a low-pressure argon plasma and accelerated towards the cathode. Sputtered neutral particles of the sample are ionized in the glow discharge plasma (‘negative glow’) by Penning and/or electron impact ionization and charge exchange processes. The analysis of non-conducting materials by GDMS is possible but difficult due to charge-up effects on the sample surface. GDMS were reported for the determination of long-lived radionuclides in biological, geological and environmental samples [31] such as ^{237}Np, ^{137}Cs and ^{90}Sr [20].

Resonance ionisation mass spectrometry (RIMS) is a highly selective and ultrasensitive method for measurement of ultratraces in samples [31]. Atoms of the desired element (or isotope) are selectively excited and ionised by a laser. Undesired ions in the mass spectrometer can be suppressed to a significant extent which leads to less isobaric interferences than ICP-MS or even TIMS [15]. The use of RIMS is limited since it is technically difficult to properly operate and requires a lot of skill and strong technical support. Thus there are fewer examples of its application to environmental samples compared to ICP-MS [15]. RIMS has been used for the determination of long-lived radioisotopes such as $^{238\text{-}244}Pu$, ^{90}Sr and ^{41}Ca [33]. Also noble gases such as ^{39}Ar and $^{81,85}Kr$ have been studied using RIMS [33].

4.3.1. Example: Actinides in environmental samples

ICP-MS is widely used to monitor levels of natural and anthropogenic actinides and their isotopic ratios in the environment. The use of multi-collector ICP-MS is particularly advantageous since it allows the simultaneous measurement of different isotopes at multiple detectors [34]. Chemical separation of the samples is often required to avoid isobaric interferences (isotopes of different elements with the same mass). Actinides have been analysed in all types of environmental samples (e.g. soil, water and biota) with low detection limits.

For example, Varga *et al* [35] selectively separated plutonium and americium from contaminated samples originating from the regions of Chernobyl, Ukraine, and Mayak, Russia. The analysis of the isotopic ratios by ICP-MS provided information about the origin and date of the contamination.

Depending on the complexity of the chemical separation method, pure fractions of many actinides can by extracted from an environmental sample. Harrison *et al* [36] analysed Th, U, Pu and Am from water, soil, sediment, vegetation and seaweed by ICP-MS.

4.3.2. Example: Stable lanthanides in environmental samples

Considering the importance of some lanthanide isotopes, such as ^{148}Gd, in the list of radionuclides which will be produced in the tungsten target of the ESS, it is relevant to consider ICP-MS as a technique for their analysis. In the literature, authors focus mainly on stable lanthanides which are of course much more common than the radioactive ones. The full series of lanthanides, from lanthanum to lutetium, is chemically very homogeneous. Lanthanides can be analysed individually but are more often analysed as a series to detect anomalies in their concentration (lack or excess of one of them compared to the rest of the series) [37].

Stable gadolinium is of particular interest in environmental samples due to its use as a contrast agent for MRI. Hatje *et al* [38] monitored the increase of anthropogenic gadolinium levels in the aquatic environment of the San Francisco Bay, USA, over 20 years. After extraction from the water matrix, the lanthanides were analysed by ICP-MS. In our group, we have shown increased gadolinium levels in *Fucus* from the Swedish west coast during the last ten years (Mattsson S, Long-time variations of radioactive substances and metals in the marine environment of the Swedish west coast as studied by brown seaweed (*Fucus serratus* and *Fucus vesiculosus*), project SSM2018-905). The gadolinium increase in water is attributed to the increasing use of Gd-containing contrast agents for MRI in hospitals.

Gadolinium is not the only lanthanide that can be characterised by ICP-MS. Plausitainis *et al* [39] reported increased levels of erbium in water samples from the Chernobyl exclusion zone. After chemical extraction and pre-concentration, the authors analysed the full series of lanthanides by ICP-MS and observed important concentration anomalies of erbium and smaller ones of cerium and europium.

4.4. Accelerator mass spectrometry

Accelerator mass spectrometry (AMS) is another ultrasensitive mass spectrometric technique, which counts the relative isotopic abundance (stable as well as radioactive isotopes of the same element) in a sample compared to that of a standard. It is particularly useful for a number of long-lived radionuclides at ultralow abundances. One key component of AMS systems is the ion source, which produces singly charged negative ions. This prevents interference of some isobars (e.g. ^{14}N is avoided in case of ^{14}C analysis, since nitrogen does not form

stable negative ions). Another important feature is that AMS systems operate in the energy range of hundreds of keV to several MeV, which allows destruction of molecular isobars using a stripper gas or foil. The general principle of AMS compared to fundamental mass spectrometry is outlined in Figure 2. The AMS technique is described in detail e.g. in [28, 40, 41]. Various radionuclides often require a specific AMS system. Several types of AMS systems exist, e.g. operating at different voltages, employing various electrostatic and magnetic filtering devices for removal of isotopic and isobaric interferences and different ion identification techniques, such as solid state detectors, gas ionization detectors, time-of-flight detectors and X-ray detectors (for the latter, useful for ^{59}Ni, see e.g. [42, 43]).

The main AMS radionuclide is ^{14}C and compared to LSC the AMS technique has the advantage of smaller sample sizes and shorter measurement times (mass < 1 mg and measurement times < 1 h). Samples containing more than ~10 times the contemporary ^{14}C specific activity is not suitable for AMS measurement, due to the risk of contamination of the sample preparation system and the ion source of the AMS instrument.

Other AMS radionuclides are ^{3}H, ^{7}Be, ^{10}Be, ^{22}Na, ^{24}Na, ^{26}Al, ^{32}Si, ^{36}Cl, ^{39}Ar, ^{41}Ca, ^{44}Ti, ^{53}Mn, ^{55}Fe, ^{59}Ni, ^{60}Fe, ^{63}Ni, ^{68}Ge, ^{79}Se, ^{81}Kr, ^{90}Sr, ^{99}Tc, ^{107}Pd, ^{126}Sn, ^{129}I, ^{146}Sm, ^{182}Hf, ^{202}Pb, ^{205}Pb, ^{236}U, ^{237}Np and ^{239}Pu [28, 41]. The AMS technique requires element specific sample preparation, which extracts the element in question into a form that is suitable for ion source of the AMS system [28]. Sample preparation for ^{14}C samples to be used at the Lund AMS facility [44, 45] is e.g. described in [21].

Detection limits and accuracy for a specific radionuclide depend e.g. the instrument used, sample preparation and measurement times. Abundance ratios of 10^{-15} may be achieved e.g. for ^{14}C and ^{36}Cl [28]. Precision of AMS measurements is typically 0.5 to 2% for several radionuclides [28].

4.4.1. Example: ^{14}C analysis using AMS

Analysis of anthropogenic ^{14}C in environmental matrices is well-established. Annual growth rings of trees are e.g. suitable for retrospective dose assessment of airborne $^{14}CO_2$ releases e.g. from nuclear power plants (see e.g. [21, 46]). Figure 3 shows the general methodology for ^{14}C analysis using the Single Stage AMS (SSAMS) facility at Lund University [44, 45], used for samples collected in the vicinity of ESS in a project assessing the preoperational radiation environment of ESS [21]. Graphitization is a process in which the carbon of the sample is extracted as graphite [47, 48] (the ion source at the Lund SSAMS facility requires graphite, but AMS systems may also be equipped with ion sources introducing the sample as CO_2).

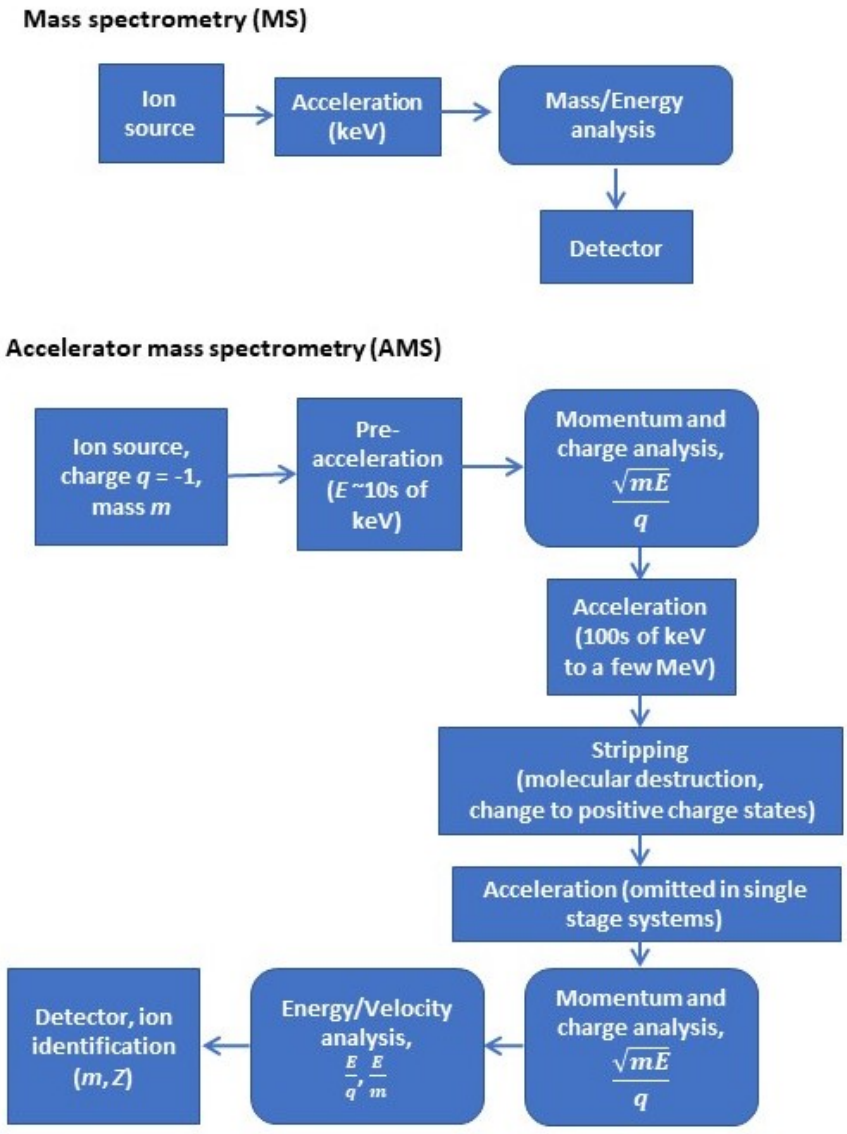

Figure 2: Comparison between mass spectrometry (MS) and accelerator mass spectrometry (AMS).

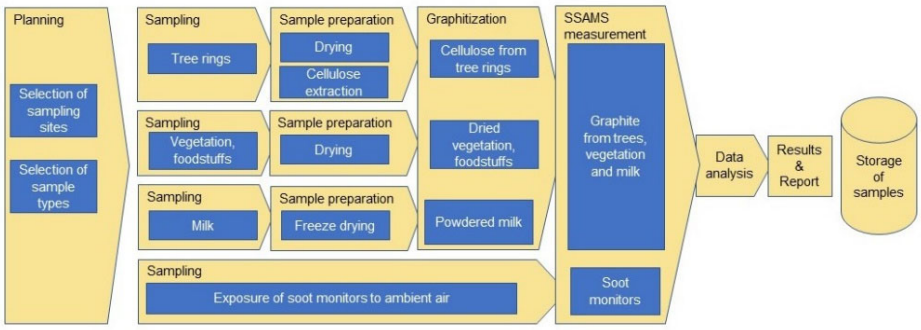

Figure 3: General methodology for ^{14}C AMS analysis of various samples, from [21] with modifications.

AMS may also be used to measure ^{14}C in aerosols (see e.g. [49-52]). Aerosol samples for ^{14}C analysis need to be collected on carbon-free filters (preferably

quartz) using high volume aerosol samplers to obtain sufficient mass of carbon (preferably 100 µg of carbon is required, but some labs can perform measurements of samples of only a few µg of carbon). Samples of activities of more than ~10 times the contemporary ^{14}C concentrations need to be diluted, or be measured with another technique, e.g. LSC.

4.4.2. Example: AMS analysis of other long-lived beta emitters

Refs [53-55] used AMS to measure ^{10}Be, ^{26}Al, ^{129}I, ^{36}Cl, ^{60}Fe and ^{53}Mn in proton-irradiated Pb and Bi targets, with the aim of determining cross sections. Chemical separation procedures for Pb included dissolution of the target in acid and adding of carriers, followed by various extraction techniques (e.g. precipitation, distillation and using ion exchangers) to extract the long-lived radioisotopes (lanthanides were also extracted from the samples, see section 4.5.2) [53, 54]. Ref [56] described AMS measurements of ^{36}Cl and ^{129}I in proton-irradiated targets of Ta.

A previously mentioned, AMS analysis of environmental samples (and all types of samples) requires sample preparation that is element specific (and sometimes dependent on the ion source used). A review of sample preparation techniques for the most common AMS radionuclides can be found e.g. in [28].

4.5. Alpha spectrometry

As described above, alpha emitters can be quantified using LSC, or by using for example gas ionization detectors, ionisation chambers or proportional counters [15, 20]. However, alpha spectrometry is most commonly performed using an external detector, preferably a silicon semiconductor detector, where alphas are completely stopped in Si layers of 100 µm thickness [15]. Passivated ion-implanted planar silicon (PIPS) detectors are most frequently used for alpha spectrometry, since this detector type gives high energy resolution, is robust (entrance window can be cleaned) while still only having a small leakage current [15]. To avoid losses of alphas due to stopping in air, the sample and detector are often placed in vacuum (a drawback of using vacuum is that volatile elements may evaporate, and fractions may be deposited on the surface of the detector). One common problem in alpha spectrometry is recoil nuclei sputtering, meaning that the recoil energy of the daughter nuclide is enough to leave the source and end up on the walls of the vacuum chamber and also contaminating the detector. This may be particularly cumbersome if the daughter nuclide is also an alpha emitter. Various techniques may be applied to avid contamination, e.g. covering the detector with a thin film or applying a voltage between source and detector [57]. Energy and range straggling give rise to broadened (and possibly over-lapped) energy peaks of the initially monoenergetic alphas. In high-resolution alpha spectrometry the energy resolution has fully been fully optimized, e.g. using high vacuum, an ultra-thin detector entrance window, a small detector volume and large distance between source and detector (to have a small solid angle of measurement to reduce straggling, which however reduces the absolute efficiency significantly) [15]. High-resolution alpha spectrometry can result in an energy resolution of less

than 10 keV (the full energy of alphas is normally a few MeV), which is considerably less than for standard alpha spectrometry (typical energy resolution 30-80 keV) [15]. However, high-resolution alpha spectrometry still has a poor energy resolution compared to high-resolution gamma spectrometry.

Sample preparation is usually performed prior to alpha spectrometry. In fact, in high-resolution alpha spectrometry of high quality, the sample preparation is a key parameter. Due to the large stopping power of alpha particles in matter (interactions with electrons in the stopping medium) – and thus very short range – thin samples are required. Radiochemical purification to minimize interference from other radionuclides is usually also necessary [14, 15]. Ideally, the alpha emitters of interest should be homogenously deposited in a single atomic layer, which, however, is difficult to accomplish. Inhomogeneity of the sample will contribute to broadening of the peaks in the alpha spectrum, and may lead to overlapping peaks and difficulties to resolve various alpha-emitting isotopes or nuclides [14].

Sample preparation generally involves a preliminary treatment followed by chemical separation and sample mounting. The preliminary treatment depends on the sample type (e.g. soil, sediment, water) and the radionuclide. It may involve drying and homogenization, sieving or digestion of solid samples. The analyte may also be preconcentrated, which is particularly useful for water samples. A summary of the pretreatment methods can e.g. be found in [15], chapter 6, section V.A, or in [14], chapter 5.3.4. The radiochemical separation is also highly dependent on sample type and radionuclide, see e.g. [15], chapter 6, section V.B, or [14], chapter 5.3. A variety of different procedures may be used, including ion-exchange chromatography, liquid-liquid extraction and precipitation.

Sample mounting, i.e. production of a thin source (sample) of the element/elements of interest, is mainly done either by evaporation, electrodeposition or coprecipitation with a microcrystalline precipitate [15]. In the evaporation technique, the radiochemically separated sample, in liquid form, is deposited onto a disc of stainless steel or platinum, and the sample liquid is removed by evaporation. The recovery is usually high, but issues may arise with the homogeneity of the deposit and its adhesion to the disc [15]. Electrodeposition may be used with high yields (90-99%) for metallic radionuclides such as Cm, Am, Pu, Np, U, Th, Pb and Po [15]. Some elements autodeposit spontaneously on the surfaces of metals such as Ag and Cu in acid solutions [15]. Polonium is such an element. In the co-precipitation method the element of interest is precipitated together with some other element [15].

A disadvantage with alpha spectrometry is the long analysis time, including sample preparation and counting time of several days [20]. Hence, the analytical capacity of alpha spectrometry is usually low, and the technique is not suitable for emergency measurements.

4.5.1. Example: Alpha spectrometry of aerosols

Alpha spectrometry of aerosol samples on filters may be performed using Si semiconductor detectors after radiochemical separation and production of thin targets, or using gas ionization detectors or LSC (e.g. [22, 58]). Pöllanen *et al* [59] have developed a method in which an aerosol sample is collected on a filter and directly analysed by high resolution alpha spectrometry in a vacuum

chamber, without radiochemical sample treatment, which is suitable for quick field measurements. According to the authors, the presence of alpha emitting actinides may be identified to the level of 0.1 Bq m^{-3}. The same group has reported high-resolution alpha spectrometry measurements and modelling at ambient air pressure using collimators [60]. They claim that contamination of 1 Bq cm^{-2} on any smooth and flat surface can be detected in approximately 10 s data acquisition time, but longer time is needed for radionuclide identification. Moreover, the possibility to detect beta active nuclides using the same measurement technique was also reported. Counts originating from alpha and beta particles are mainly at different energies, which make their separation possible. An efficiency of 0.14 was determined for an extended-area (430 cm^2) homogeneous source emitting alpha radiation at the energy of 5–6 MeV, whereas for the beta emitters the efficiencies were 0.07–0.19 depending on the beta-particle emission energies. The use of a collimator reduces the detection efficiencies by a factor of up to ten [61]. The effect of collimators, as well as peculiarities of alpha spectra in aerosol filters are also investigated by other authors [62, 63].

4.5.2. Example: Alpha-spectrometry analysis of ^{148}Gd and ^{154}Dy in lead and tantalum

Talip *et al* report on the alpha spectrometry measurements of ^{148}Gd and ^{154}Dy in proton-irradiated spallation targets of Pb (proton energy from 240 to 2595 MeV), with the primary aim to predict the radionuclide inventory in high-power spallation neutron facilities [57]. According to Artisyuk *et al* [64], the radiotoxicity of ^{146}Sm, ^{148}Gd, ^{150}Gd and ^{154}Dy in Pb and Pb-Bi spallation targets is comparable to that of the polonium produced. ^{148}Gd is pointed out as especially important [64]. Long-lived beta-emitters had previously been extracted from the irradiated targets and measured by AMS (see above) [57]. The separation procedure is complex, e.g. including that the irradiated Pb sample was dissolved in acid, separation of lanthanides was performed using ion exchange resins, carbon foil was used as backing material for molecular plating experiments, and Au was used for vacuum coating experiments [57]. Alpha sources were produced from the lanthanide fractions using molecular plating, which refers to deposition using electrolysis in organic media (with constant current or voltage) [57]. Alpha spectrometry was performed using an alpha spectrometer equipped with a PIPS detector. The sample was coated with a thin layer of gold to prevent contamination of recoil nuclei. Total yields of the chemical separation and deposition was about 70% [57]. Alpha measurements had a full width at half maximum (FWHM) of 26 keV for ^{148}Gd (full alpha energy 3.18 MeV) and 38 keV for ^{154}Dy (full alpha energy 2.87 MeV). Experimental cross sections for ^{148}Gd agreed satisfactory with theoretical predictions calculated using INCL++-ABLA07 code [57]. For ^{154}Dy the experimentally obtained cross sections were higher than predicted [57]. Talip *et al* states in the paper that the developed technique will be used for W, which will be the ESS target material [57].

In another paper by Talip *et al* [56], the alpha emitters ^{154}Dy, ^{148}Gd, ^{150}Gd and ^{146}Sm were extracted from irradiated spallation targets of tantalum (Ta) and measured by alpha spectrometry. According to Kelley *et al* [65], Ta may be used to estimate the radionuclide production in W. Thin samples of proton-irradiated Ta targets were first dissolved in acids (HNO_3 and HF) and then subjected to extraction of long-lived beta-emitters (^{36}Cl and ^{129}I) using distillation for

subsequent measurements with AMS (see above) [56]. The radiochemistry to extract the alpha emitters included precipitation, the use of two types of ion exchange resins followed by molecular plating, gold coating and alpha spectrometry [56]. Total yields of the chemical separation and deposition was between 67 and 97% for ^{148}Gd [66]. The experimental cross section agreed well with theoretical predictions for ^{148}Gd [66]. For ^{154}Dy, the theoretical cross sections were underestimated by a factor of 3 compared to the measurements [66]. ^{146}Sm and ^{150}Gd were not detected in any sample [66]. Hammer *et al* have analysed ^{148}Gd, ^{173}Lu and ^{146}Pm in an irradiated Pb-Bi spallation target by alpha and gamma spectrometry [66].

4.5.3. Example: Alpha spectrometry in environmental samples

Alpha spectrometry is commonly used to analyse natural and anthropogenic radioactivity in the environment. Alpha spectrometry and mass spectrometry are very complementary analytical methods: the radionuclides interfering with each other with one method usually do not with the other. In both cases, chemical separation is required before analysis. When analysing environmental samples, the chemical pre-treatments are necessary to extract the radionuclides from the matrix, to pre-concentrate and to obtain pure fraction of each element. Alpha sources from environmental samples are most commonly prepared by electrodeposition or micro-precipitation [67].

Desideri *et al* [68] analysed the content of natural radionuclides in seaweed products for human consumption. The authors used alpha spectrometry to assess the activity concentration of ^{238}U, ^{234}U, ^{230}Th, ^{210}Po, ^{232}Th, and ^{228}Th in those foodstuffs. Anthropogenic radionuclides can also be measured by alpha spectrometry: e.g. Szufa *et al* [69] analysed plutonium isotopic ratios in various environment samples (e.g. soil, plants, animals) from the Antarctic.

4.6. Activation analysis

Activation analysis is a sensitive method that may be successfully used for quantification of long-lived radionuclides [70, 71]. Activation can be accomplished by neutrons (neutron activation analysis, NAA), photons and protons, and results in transformation of the long-lived radionuclide into a gamma-emitter with a considerably shorter half-life. Neutrons as probe is most common. Examples of radionuclides used in activation analysis include ^{99}Tc, ^{126}Sn, ^{129}I, ^{135}Cs, ^{226}Ra, ^{230,232}Th, ^{235,238}U, ^{237}Np, ^{231}Pa and ^{242}Pu [71]. In NAA, the source of neutrons is most commonly a nuclear reactor, but neutron generators or accelerators may also be used. For environmental samples, pre-separation and pre-concentration are usually required prior to irradiation [71]. Post-irradiation separation may also be required prior to gamma measurement [71].

4.7. Detection techniques for selected ESS radionuclides

During normal operation, important ESS radionuclides related to the dosimetry of workers are believed to be pure beta emitters such as ^{32}P, ^{33}P, ^{35}S, ^{14}C and ^{3}H, and gamma emitters such as ^{39}Cl, ^{29}Al and ^{7}Be [6, 72]. For the general public, the annual effective dose from airborne releases is believed to be dominated by small contributions of ^{13}N, ^{11}C, ^{15}O, ^{41}Ar, ^{125}I, ^{3}H, ^{39}Cl and ^{38}Cl [6]. All but ^{3}H and ^{125}I have half-lives of less than 1 hour and will be very difficult to measure in environmental samples. Other radionuclides that are believed to contribute to a minor extent to the dose to the general public are ^{32}P, ^{7}Be, ^{185}W, ^{172}Hf, ^{60}Co, ^{54}Mn and ^{58}Co [6]. Short-term releases of activated tungsten and stainless steel dust resulting from dismantling in hot cells is believed to become about 10% of the total effective dose resulting from the continuous stack releases [6]. The aerosol ^{7}Be is easily measured with gamma spectrometry, and so is ^{60}Co. ^{54}Mn also releases gamma radiation.

As mentioned above, gamma spectrometry is the workhorse in environmental radiology, and usually has the advantage that no chemical separation techniques are required, and that the activity of many gamma emitters in the sample can be determined simultaneously. A gamma-emitting isotope may be used to estimate the activity levels of some difficult-to-measure radionuclides, if production cross sections are well known. However, this opportunity does not exist for all elements (e.g. hydrogen, carbon). In this section we have on focussed nuclide-specific environmental measurement techniques for pure alpha and beta emitters of relevance for ESS. In section 2 (review of radionuclides) we used a selection criterion of radionuclides of half-lives longer than 10 hours. However, in case of pure alpha and pure beta emitters, we have chosen a more conservative half-life limit of 3 days since these require more sample preparation, often including radiochemical extraction, than gamma emitters. The choice of 3 days stems from an estimated time required for sampling, sample preparation (including radiochemical extraction) and measurement to be one month (30 days), and that samples generally need to be measured within 10 half-lives. We have also included comments on measurement techniques of importance for the radionuclides with the highest dose contributions in an accident scenario according to Ref [7].

4.7.1. Lanthanides

The pure alpha emitters of highest activity according the FLUKA calculations are all lanthanides and are shown in Table 1. Of these, ^{148}Gd is the radionuclide of highest importance for environmental measurements due to its importance in an accident scenario [7]. The radionuclides in Table 1 are not an issue in the operation of nuclear power plants, hence any methods for their quantification in environmental matrices could not be found in the literature. However, as already discussed in section 4.5.2, some studies have been undertaken on how to extract and quantify these alpha emitters in spallation targets using alpha spectrometry [56, 57, 66]. As described above, the preparation methods before analysis of a sample by alpha spectrometry usually consist of three steps: an extraction of the radionuclides from their matrix, a purification of the sample to avoid interferences and finally the preparation of an alpha emitter source (thin layer).

Depending on the nature of the matrix and of the radionuclide each step can be challenging. To our knowledge, there is currently no example of analysis of environmental sample containing radioactive lanthanides in the literature. However, a few articles describe the extraction and analysis of irradiated target materials [56, 57, 66].

Regarding extraction, solid matrixes such as irradiated target materials can simply be dissolved in acid solution. More complex environmental matrixes (e.g. soil, sediments, biological samples) would require more preparation using, for example, acid leaching, ashing or sample fusion procedures.

The second step of the preparation method is usually a chemical separation of the extracted solution in order to obtain different fractions containing the radionuclides of interest. These fractions should be purified of the other chemical species that could interfere during the measurement by alpha spectrometry. Talip *et al* [57] developed a separation procedure consisting of 7 steps to recover a pure lanthanide fraction, plus a final separation on chromatographic resin to separate ^{154}Dy from ^{148,150}Gd. Hammer *et al* [66] also achieved the separation of ^{148}Gd, ^{173}Lu, and ^{146}Pm in about 9 steps in order to measure ^{148}Gd by alpha spectrometry.

The last step of the analytical procedure is the production of sources for alpha spectrometry. The choice of the most suitable method depends mainly of the activity of the sample. Active samples can be analysed by the direct evaporation of the sample solution on a metal or ceramic surface. In order to obtain higher resolution, it is possible to use other methods such as electrodeposition (also called electroplating) or micro-precipitation. Talip *et al* [57] and Hammer *et al* [66] used electrodeposition to prepare their purified radioactive lanthanide sources. Electrodeposition and micro-precipitation would also be the methods recommended for low activity environmental samples.

Table 1: Alpha emitters of relevance for ESS and suggested measurement techniques for lanthanides based on literature.

Nuclide	E_{alpha} (MeV)	$T_{1/2}$	Technique	Refs	Comments
^{148}Gd*	3.183	75 years	Alpha spectrometry	[56, 57, 65, 66, 73]	Not environmental samples
^{150}Gd	2.726	$1.79 \cdot 10^{8}$ years	Alpha spectrometry	[56]	Not environmental samples, not detected.
^{154}Dy	2.870	$3.6 \cdot 10^{6}$ years	Alpha spectrometry	[56, 57]	Not environmental samples
^{146}Sm	2.460	$6.8 \cdot 10^{7}$ years	Alpha spectrometry	[56]	Not environmental samples, not detected.

* Highly relevant at an accident scenario [7].

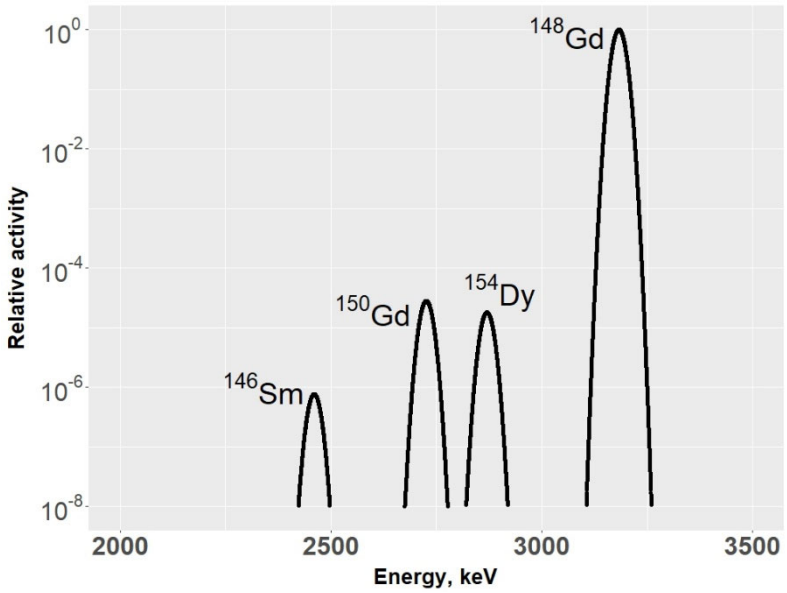

Figure 4: Illustration of principle for expected alpha spectrum of ESS lanthanides using thin targets.

Figure 4 shows a hypothetical spectrum of the pure alpha emitters of highest activity according to the FLUKA simulations (see Table 1). The graph aims to serve as an illustration of principle (the shape of the curves is not realistic and lacks the low-energy tale of alpha spectra). FWHM values for the different peaks have been chosen according to measurements using high-resolution alpha spectrometry of thin targets in Ref [57]. As seen in the figure, the activity of ^{148}Gd is expected to be several orders of magnitude higher than the other lanthanides. Thus, it may be very difficult to observe ^{146}Sm, ^{150}Gd and ^{154}Dy by alpha spectrometry. Removal of Gd by chemical separation could possibly allow for detection of ^{146}Sm and ^{154}Dy. For aerosol samples we suggest to investigate the possibility of direct alpha spectrometry of ^{148}Gd in filters without pretreatment, similar to Ref [74].

ICP-MS is a possible alternative technique for the analysis of these radioactive lanthanide isotopes. Stable lanthanides are commonly analysed using ICP-MS (see section 4.3.2). In environmental samples such as soil or water, the presence of stable lanthanides may create isobaric interferences. For example, stable ^{148}Nd and ^{148}Sm could interfere with the measurement of ^{148}Gd and in a same way ^{150}Nd and ^{150}Sm with ^{150}Gd. The chemical separation of Gd from the rest of the lanthanides present in the matrix may be challenging.

For rapid determination of pure alpha emitters, indirect methods may need to be considered, using e.g. gamma spectrometry. Gamma radiation from ^{146}Gd may possibly be used to estimate the ^{148}Gd content, as suggested in [7]. An alternative would be to investigate the possibility to measure gamma from ^{153}Gd, which has a half-life of 240 days (opposed to ^{146}Gd which has a shorter half-life of 48.2 days).

4.7.2. Other alpha emitters

Table 2 shows some alpha emitters relevant to accelerator components of ESS according to Bungau et al [3]. These may not be of relevance for releases to the environment, however.

Table 2: Alpha emitters accompanied by gamma radiation of relevance for ESS and suggested measurement techniques based on literature.

Nuclide	Main E_{alpha} (MeV)	$T_{1/2}$	Technique	Refs	Sample types	Comments
^{228}Th	5.423 (73.4%)	1.92 years	Alpha spectrometry, Gamma spectrometry, ICP-MS	[36, 68, 75, 76]	Soil, sediments, plants	Actinides are found in one publication only [77], their production in ESS should be investigated more.
^{241}Am	5.486 (84.8%)	432 years	Alpha spectrometry, Gamma spectrometry, ICP-MS, TIMS	[30, 36, 78-82]	Soil, water, biological samples, plants	
^{243}Am	5.275 (86.7%)	7370 years	ICP-MS, Gamma spectrometry, (Alpha spectrometry)	[78, 79, 81, 83]	Soil, biological samples. As a tracer for alpha spectrometry.	

4.7.3. Beta emitters

Table 3 shows some beta emitters of relevance to ESS with well-established methods of separation and quantification according to literature. LSC is suitable for the quantification of several of these beta emitters.

Table 3: Beta emitters of relevance for ESS and suggested measurement techniques based on literature.

Nuclide	Mean E_{beta} (keV)	$T_{1/2}$	Technique	Selection of refs	Example of sample types	Comments
^{3}H	5.68	12.32 years	LSC (AMS, ^{3}He MS)	[15, 21, 26, 84-86]	Water, air, vegetation, milk	Sample preparation, see sections 4.3, 5.3, 5.6
^{10}Be	203	$1.39 \cdot 10^{6}$ years	AMS	[28, 87, 88]	Water, aerosol	
^{14}C	49.5	5730 years	AMS, LSC	[15, 21, 26, 28]	Vegetation, air, water, milk, aerosols	Sample preparation AMS, see section 4.4
^{24}Na	835	15 hours				Too short lived for environmental measurements
^{32}P	695	14.28 days	LSC	[89]	Water, plankton, sediments	
^{33}P	76	25.3 days	LSC	[89]	Water, plankton, sediments	
^{35}S	49	87.3 days	LSC	[90-92]	Aerosols, water	
^{36}Cl	251	$3 \cdot 10^{5}$ years	LSC, AMS	[20, 26, 28, 93, 94]	Water, soil	
^{45}Ca	77	162.7 days	LSC	[95]	Vegetation, soil	
^{63}Ni	17	100 years	LSC, gas flow GM counters, beta-spectrometry with semiconductor detectors, AMS	[20, 26, 96-99]	Water, vegetation	
^{89}Sr	587	50.57 days	LSC (Cherenkov counting), gas flow GM counters	[20, 100, 101]	Soil, sediments, vegetation, water	
^{90}Sr	196	28.9 years	LSC (Cherenkov counting), gas flow GM counters, MS techniques, AMS	[20, 30, 33, 101-103]	Soil, sediments, vegetation, milk, water	
^{90}Y	934	2.7 days	LSC (Cherenkov counting)	[101, 102]	Soil, sediments, vegetation, water	
^{99}Tc	85	$2.1 \cdot 10^{5}$ years	LSC, RIMS, ICP-MS	[20, 30, 104, 105]	Seaweed, soil, vegetation, water	
^{106}Ru	10	374 days	LSC, Gamma	[23, 106]	Aerosols, soil, vegetation	Gamma via daughter ^{106}Rh
^{129}I	40	$1.6 \cdot 10^{7}$ years	AMS, LSC, NAA, ICP-MS	[30, 107-112]	Water, soil, vegetation, milk, aerosol	

Radionuclides from Table 3 with a half-life longer than a few days of particular interest for ESS environmental measurements related to routine releases include ^{3}H, ^{32}P, ^{33}P and ^{35}S [6]. During the current project and during a previous one [21] we have established methods for ^{3}H using LSC in various environmental matrices (and in urine). To include the capability to measure environmental phosphor radioisotopes ^{32}P and ^{33}P, sample preparation would need to be developed similar to the methods reported in Chen *et al* [89], which are based on methods by Waser *et al* [113] and Benitez-Nelson and Buesseler [114]. For ^{35}S, extraction methods similar to those in Hong *et al* [92] would need to be implemented. (^{32}P and ^{35}S may be measured by LSC in urine samples, see e.g. [115]).

Table 4 lists beta emitters that may be more difficult to assess than those in Table 3. For AMS, for example, different instruments and special setups are often required for each radionuclide [28]. The number of laboratories in the world capable of performing AMS analyses of the radionuclides in Table 4 are very limited and are probably not performed on routine basis.

Analysis of the tungsten isotopes is of utmost importance for waste characterization of the irradiated tungsten target. As can be seen in Table 4, there are no developed methods to assess the activities of two tungsten isotopes (^{185}W and ^{188}W), which will be present in the target in high quantities. We believe that some indirect methods (e.g. use of isotope ratios) might be used for assessment, but their validity should be investigated and justified.

Table 4: Other beta emitters of relevance for ESS and suggested measurement techniques based on literature.

Nuclide	Mean E_{beta} (keV)	$T_{1/2}$	Techniques	Selection of refs	Comments
^{39}Ar	219	268 years	Noble gas mass spectrometry, AMS	[116, 117]	
^{31}Si	596	157 min			*
^{32}Si	70	153 years	AMS	[28, 118]	
^{60}Fe	50	$2.6 \cdot 10^6$ years	AMS	[28, 119, 120]	
^{67}Cu	121	62 hours			*
^{77}As	229	38 hours			*
^{79}Se	53	$3.3 \cdot 10^5$ years	ICP-MS, LSC	[121, 122]	
^{85}Kr	252	11 years	RIMS, LSC, proportional counters	[33, 123-125]	
^{91}Y	604	58.5 days	LSC	[126, 127]	
^{93}Zr	19	$1.5 \cdot 10^6$ years	LSC, MS, AMS	[128-130]	No environmental studies
^{107}Pd	9.3	$6.5 \cdot 10^6$ years	ICP-MS, AMS	[28, 131, 132]	No environmental studies
^{115m}Cd	617	44.6 days	Gamma spectrometry		No environmental studies, used as tracer
^{115}Cd	1110	53.5 hours			*
^{121}Sn	116	27 hours			*
^{147}Pm	62	2.6 years	LSC, NAA	[133, 134]	
^{149}Pm	369	53 hours			*
^{151}Sm	20	89 years	LSC	[134, 135]	
^{161}Tb	157	6.9 days	LSC	[136]	
^{169}Er	101	9.4 days	Gamma spectrometry	[137]	No environmental studies. Gamma intensity is very low.
^{170}Tm	323	129 days	Gamma spectrometry? X-ray spectrometry?	[138, 139]	No environmental studies.
^{171}Tm	25	1.9 years	Gamma spectrometry?		No environmental studies.
^{172}Tm	668	63.6 hours			*
^{185}W	127	75.1 days	LSC? Mass spectrometric techniques? Gamma spectrometry?	[140]	Ref [140] gamma spectrometry in tracer studies
^{188}W	100	69.8 days	LSC? Mass spectrometric techniques?		
^{188}Re	795	17 hours			*

*Due to short half-life practically impossible to measure in the environment

4.7.4. Emergency radionuclides

In an SSM report regarding the classification of emergency preparedness planning for ESS [7], the most important radionuclides at an accident scenario are identified (Tables 2 and 3 in [7]). Table 5 below lists the radionuclides that – at the worst case scenario – will mainly contribute to the effective dose from ground deposition for time intervals during the first year after the accidental release [7]. As stated in [7], gamma-emitting radionuclides are believed to mainly contribute to the effective dose from ground deposition. Dose rate measurements and gamma spectrometry of specific radionuclides may thus be used to determine the activity levels of gamma emitters. SSM proposes to use the gamma emitter ^{146}Gd or its daughter ^{146}Eu to estimate the activity concentration of the alpha emitter ^{148}Gd field measurements.

Table 5: Radionuclides that – at the worst case scenario in ref [7] – will mainly contribute to the effective dose from ground deposition for time intervals during the first year after the accidental release and suggested measurement methods.

Nuclide	$T_{1/2}$	Decay mode	Daughter decay	Technique	
^{148}Gd	71.1 y	Pure alpha, 3.183 MeV	None (^{144}Sm)	Gamma spectrometry of other Gd isotope or their daughers. Alpha spectrometry. ICP-MS?	Alpha spectrometry needs to be developed. Gd isotope ratios need to be verified.
^{187}W	24 hours	Beta, gamma	^{187}Re, pure beta, $T_{1/2}$=4·10^{10} y. Granddaughter stable (^{187}Os).	Gamma spectrometry	
^{172}Hf	1.87 years	EC, gamma	^{172}Lu, beta+, gamma, $T_{1/2}$=6.7 d. Granddaughter stable (^{172}Yb).	Gamma spectrometry	
^{182}Ta	111.7 days	Beta, gamma	None (^{182}W)	Gamma spectrometry	
^{178m}Hf	31 years	IT	None (^{178}Hf)	Gamma spectrometry	
^{181}W	121.2 days	EC	None (^{181}W)	Gamma spectrometry	
^{175}Hf	70 days	EC	None (^{175}Lu)	Gamma spectrometry	
^{173}Lu	1.37 years	EC	None (^{173}Y)	Gamma spectrometry	

4.8. Summary and conclusions

The review of the existing analytical techniques developed in this section allow us to sort the radionuclides produced by the ESS into different categories depending on the difficulty to perform the analysis.

Firstly, some of the radionuclides can be considered as easy to analyse. They do not require specific sample preparation before measurement, have well defined reference method of analysis and/or are analysed using widespread techniques. Gamma emitters belong to this category: the samples containing them can be analysed directly *in situ* or in a laboratory with no or very little sample preparation. LSC measurements of ^{3}H is well established for all type of environmental matrices. LSC and AMS are the techniques of reference for ^{14}C

in environmental samples. Alpha emitting actinides also fit this group of radionuclides. They have been widely analysed by alpha spectroscopy due to their importance in the nuclear fuel cycle. Of course, the list of radionuclides belonging to this group can be extended depending on the analytical capabilities of each laboratory.

A second category includes radionuclides that are less often routinely analysed or that are not found in environmental samples. ^{148}Gd and the associated alpha emitting lanthanides belong to this group. Even though some articles describe their analysis by alpha spectrometry, there is no method published for their analysis in the environment. It is important to fill this knowledge back in particular for the radionuclides that will be produced in larger amount and/or are part of the emergency list. This task seems achievable by developing specific methods for their analysis in environmental matrices.

Finally, some of the radionuclides of the lists presented in the section 4 seems very difficult to analyse in the environment. It may not be possible to apply complex and time-consuming analytical procedures (including sampling, extraction and analysis) on the radionuclides with short half-lives before they decay. Moreover, some radionuclides are only described in a couple of research articles. There were never analysed in the environment and the techniques described for their characterisation may not be available in most laboratories. In this last case, the knowledge gap to fill is even bigger that for the other radionuclides due to the lack of available data.

5. Baseline measurements

This chapter begins with a summary of previous baseline measurements around ESS, presented in the report "Assessment of "Zero Point" radiation around the ESS facility" [21]. These measurements did not include aerosol samples, hence the current project has initiated measurements of aerosols collected at the ICOS/ACTRIS rural background site Hyltemossa. The third section of this chapter presents long-term environmental baseline measurements of tritium in the Lund area, including tritium measurements of precipitation, air humidity and pond water. In section 5.4 some measurements on current levels of tritium in HTO in an accelerator facility at the Physics Department are presented. Section 5.5 contains a short investigation of possible leakage of tritium from watches containing tritiated paint. Section 5.6 summarizes the results of a baseline study of the tritium content in urine of 55 subjects living or working in Lund.

5.1. Previous background measurements, a summary

A baseline study of environmental radioactivity and radiation levels around ESS was performed during 2017-2018 in a collaboration project between Lund University (Medical Radiation Physics, Malmö, and the Division of Nuclear Physics) and ESS [21]. More than 40 sampling sites were selected within a few km of the ESS site, covering all wind directions. Sites that were expected to remain the same for an extensive period such as private gardens and parks was chosen carefully. The radionuclides assessed represented natural as well as anthropogenic radionuclides. Special focus was dedicated to gamma-emitting radionuclides, as well as the pure beta emitters ^{3}H and ^{14}C, which both are commonly used as tracers in research and industry, also in the Lund area. The measurements included: ambient equivalent dose rate measurements; *in situ* gamma spectrometry (of ^{7}Be, ^{137}Cs, ^{40}K, ^{226}Ra (^{238}U daughter) and ^{228}Ac (^{232}Th daughter)); gamma spectrometry of sewage sludge, bioindicators, grass, crops and forage, milk and soil profiles (of ^{137}Cs, ^{40}K, ^{226}Ra, ^{228}Ac and ^{131}I); LSC measurements of ^{3}H in ground- and surface water, sewage sludge, bioindicators, crops and milk; AMS measurements of ^{14}C in annual tree rings, grass, bioindicators, milk and in fullerene soot monitors (indicating air-borne ^{14}C).

The *in situ* gamma spectrometry measurements showed only minor variation between sites, with the exception of ^{137}Cs. The average equivalent surface activity of 249 Bq m^{-2} for ^{7}Be and 121 Bq m^{-2} for ^{137}Cs, and observed average activity concentrations (assuming a homogenous distribution in ground) were 407 Bq kg^{-1} for ^{40}K, 42 Bq kg^{-1} for ^{226}Ra and 21 Bq kg^{-1} for ^{228}Ac. The average ambient equivalent dose rate ($\dot{H}^{*}(10)$) at 1 m above ground was 85 ± 17 nSv h^{-1}. The activity concentrations of naturally occurring gamma emitters in the ground displayed only minor geographic variations (average activity concentration in 20 cm deep soil cores were: 75 ± 14 Bq kg^{-1} for ^{226}Ra, 35 ± 2 Bq kg^{-1} for ^{228}Ac and 694 ± 104 Bq kg^{-1} for ^{40}K). ^{137}Cs in soil varied, as expected, with depth as well as in total activity concentration. No unexpected

gamma emitters were found in any sample matrix (however, most of the sewage sludge showed ^{131}I, which is used medically). All samples were dried, homogenized and measured for at least 24 h in a lead shielded HPGe detector.

The ^{3}H activity concentration of all ground water and surface water samples analysed (> 40 samples) was below the Minimum Detectable Activity concentration (MDA) of the measurements (14 Bq L^{-1} and 29 Bq L^{-1} at the time of analysis, which has been reduced for the measurements presented in sections 5.3-5.5). So was the activity concentration of ^{3}H in a limited number of samples of bioindicators, milk and sugar beet (MDA 29 Bq L^{-1}). The activity concentrations of ^{3}H in monthly collected samples of sewage sludge (from April 2017 to April 2018) were mainly below the MDA (varying from 2.6 Bq l^{-1} to 29 Bq L^{-1}). Only two samples displayed ^{3}H activity concentrations above the concurrent MDA: 16 ± 3 Bq L^{-1} in June 2017 (MDA 14 Bq l^{-1}) and 2.9 ± 0.7 Bq L^{-1} in January 2018 (MDA 2.7 Bq L^{-1}).

The ^{14}C measurements showed no evidence of anthropogenic contamination in the Lund area during years 2012 to 2017 (data compared to rural background data from Germany and from Borrby in south-eastern Scania). The average F^{14}C value for all organic year 2017 samples measured for ^{14}C (N = 57) was 1.017 (standard uncertainty of the mean, SUM, 0.001), corresponding to 228 Bq kg^{-1} (using δ^{13}C = -25 ‰).

5.2. Aerosols

Gamma spectrometry measurements of aerosol samples, collected at the ICOS/ACTRIS rural background site Hyltemossa, are presented in this section.

5.2.1. Introduction

An aerosol is defined as a suspension of fine solid or liquid particles in a gas. As in normal operation of any high-energy proton accelerator, radioactive aerosols are expected to be formed in the accelerator tunnel of the ESS (e.g. containing ^{7}Be, ^{10}Be, ^{24}Na, ^{32}P ,^{33}P, ^{35}S) (see e.g. [5]). At the ESS linac, ^{32}P and ^{35}S (both pure beta emitters; $T_{1/2}$ = 14.3 days and 87.4 days, respectively) are believed to become the most important aerosols from a radiological point of view, followed by the more short-lived gamma emitters ^{24}Na ($T_{1/2}$ = 15 h) and ^{28}Mg ($T_{1/2}$ = 20.9 h) [141, 142]. The main fraction of aerosols (99.97%) is expected to be caught in HEPA filters of the ventilation system [6, 141]. Examples of estimated release rates from the linac tunnel – after passage through the HEPA filters – to the environment during 6000 hours of continuous operation are $6.33\cdot10^{5}$ Bq y^{-1} for ^{7}Be, $2.11\cdot10^{5}$ Bq y^{-1} for ^{24}Na, $3.00\cdot10^{4}$ Bq y^{-1} for ^{28}Mg, $9.3\cdot10^{4}$ Bq y^{-1} for ^{32}P, $3.78\cdot10^{4}$ Bq y^{-1} for ^{33}P and $1.46\cdot10^{4}$ Bq y^{-1} for ^{35}S [142].

Furthermore, aerosols containing alkali metals (e.g. Li), alkaline earth metals (e.g. Be and Sr), boron group elements (e.g. Te), transition metals (e.g. Hf, Ta and W), metalloids (e.g. B) and lanthanides (e.g. Gd) may be formed from the spallation reactions as well as from sputtering of the tungsten target during normal operation [2, 6, 141]. These particles will be carried by the gas in the He-cooling loop (the circulating gas may also lead to release of particles from the target by ablation). The helium cooling loop is expected to have a small leakage

rate (of 1 g h^{-1} for the 23 kg of He in the helium cooling loop) [2]. The helium loop will also contain filters to purify the cooling gas from the W dust [6]. The physical and chemical forms of all aerosols are however difficult to predict [141]. Particulate matter may also be formed in and released from hot cells during cutting processes (from tungsten and stainless-steel components) [2]. As stated in ref [2], the experience from and knowledge about the release of radionuclides during irradiation of tungsten at the power levels of ESS is limited, and novel problems may occur.

The source term (ST) of radionuclides released to the environment from target station is estimated by ESS for two cases, one pessimistic and one optimal case [2]. The ST from the helium loop (continuous release) is $6.32 \cdot 10^{11}$ Bq y^{-1} in the pessimistic as well as in the optimal case, and is dominated by ^{3}H ($6.24 \cdot 10^{11}$ Bq y^{-1}), while metalloids contribute with $5.32 \cdot 10^{7}$ Bq y^{-1} and $1.6 \cdot 10^{4}$ Bq y^{-1}, in the pessimistic and optimal case, respectively [2]. The annual effective dose to the general public, however, is believed to be dominated by iodine (gas form) [2]. Short-term release of W and stainless steel dust from the hot cells are estimated to be $6.25 \cdot 10^{11}$ Bq y^{-1} (also containing ^{3}H in dust) [2]. The effective dose from radioactive releases from the hot cells is estimated to small compared to that resulting from the leaking of the helium loop [2].

During an accident scenario, a wide range of aerosols e.g. from the tungsten target may be released to the environment, inhaled by members of the general public and also deposited on the ground [7]. Ref [7] have calculated a representative source term describing the release of radionuclides into the environment for an extreme case scenario, also taking into account estimated uncertainties of the actual radionuclide concentrations in the target. The worst-case scenario occurs after 5 years of operation (before the target is to be exchanged, thus target activity concentration maximized) and at full power (5 MW protons of 2 GeV). The scenario is initialized with a loss of the helium cooling of the target, leading to a series of events, starting with the release of helium and filter particles (containing various radionuclides). Discharge or radionuclides as gas or aerosols will follow resulting from oxidization and melting of the tungsten target, melting of the beryllium reflector, vaporization of the moderator water, and hydrogen gas deflagration [7]. The radionuclides ^{148}Gd (pure alpha, $T_{1/2}$ = 71.1 y), ^{187}W (beta-, $T_{1/2}$ = 24 h), ^{172}Hf (EC, $T_{1/2}$ = 1.87 y), ^{182}Ta (beta- , $T_{1/2}$ =114.7 d) and ^{178m}Hf (IT, $T_{1/2}$ = 31 years) are e.g. expected to dominate the effective dose contribution during the first 7 days: at low wind speeds the inhalation dose is estimated to contribute to more than 50% of the total effective dose [7]. Ground deposition dominates the effective dose on a long-term basis [7]. The particle size distribution at the extreme case scenario, affecting the inhalation dose coefficients as well as dispersion and deposition patterns, is still uncertain [7, 143].

Common methods for environmental radioactive aerosol analysis are described e.g. in Refs [15, 22, 144]. As pointed out in Ref [144], factors such as size range, and physical and chemical concentrations affect the choice of sampling method and measurement technique. Environmental monitoring stations often use high-volume aerosol samplers to collect aerosols on different types of filter material, either batch-wise or on continuously moving filter bands [22]. Some systems separate the aerosols according to size using size-specific inlets (impactors). Nuclear analytical techniques of radioactive aerosols have

traditionally primarily involved gamma spectrometry, which may be laboratory-based or *in situ* (see e.g. [22-25]). Beta spectrometry to identify beta emitters, such as ^{90}Sr, often requires radiochemical separation procedures (e.g. [22, 58, 145]). However, the decay product of ^{90}Sr, ^{90}Y, is a high-energy beta emitter which can be used to directly estimate ^{90}Sr in environmental samples. LSC, also requiring radiochemical pre-treatment, may also be efficient in beta spectrometry of radioactive aerosols [22, 26]. Pure beta emitters such as ^{14}C can be measured by accelerator mass spectrometry (AMS) (e.g. [50, 51, 146-150]). As described above in section 4.5.1, alpha spectrometry of aerosols samples on filters may be performed using Si semiconductor detectors after radiochemical separation and production of thin targets, or using gas ionization detectors or LSC (e.g. [22, 58]). High-resolution alpha spectrometry of aerosol filters without radiochemical sample treatment has also been demonstrated [59].

In the present SSM project, we have initialized gamma spectrometry measurements of aerosol samples collected at a rural reference station, Hyltemossa, that is used e.g. by Lund University for climate-related studies of green-house gases and aerosols. The type of aerosol sampler used (Digitel DHA-80) has previously been tested with satisfactory results in extreme weather conditions at the Jungfraujoch High Altitude Research Station by the Swiss Federal Office of Public Health (natural ^{7}Be and ^{210}Pb easily detectable and detection limit of artificial ^{137}Cs of 2 μBq m^{-3}) [151]. In the present project, we compare gamma spectrometry data from aerosol filters collected during 14 weeks at our station at Hyltemossa to data collected at SSM's environmental monitoring station for gamma-emitting aerosols at Ljungbyhed (operated by the Swedish Defence Research Agency, FOI), located about 38 km north of the ESS and approximately 12 km west (260 °) of Hyltemossa.

5.2.2. Location and methods

The ICOS/Actris[1] site Hyltemossa, a combined atmosphere and ecosystem station, is located a few km south of Perstorp, in northern Scania (56°06′N, 13°25′E, 115 m asl). Aerosol samples were collected on quartz fibre filter of 150 mm diameter (Advantec QR-100) using a high-volume aerosol sampler, DHA-80 (Digitel, [152]), equipped with automatic filter change. The DHA-80 has a capacity of 15 filters and maximum flow rate 1000 L min^{-1}, however, the flow meter at the time of sampling had a maximum flow rate of 600 L min^{-1}. The DHA-80 sampler was situated at the roof top of one of the buildings at Hyltemossa (see Figure 5). Filters were mounted on filter holders using forceps according to the operation instructions of the DHA-80 sampler [153]. The sampling time for each filter was 3.5 days using a flow rate of 500-600 L min^{-1} during the periods 22 March to 1 July 2019. Filters were removed from the DHA sampler (29 March, 25 April, 10 May and 1 August), wrapped in aluminium foil, labelled and placed in Ziplock bags, and transported to Medical Radiation Physics, Malmö. Filters were then prepared for measurement by gamma spectrometry according to the method proposed in Flury and Völke [151] with some modifications (see Figure 6). Four to five filters, corresponding to 2-2.5 weeks of aerosol sampling time, were pressed into a puck with a diameter of 40-50 mm and a height of 10 mm by using a 10-ton hydraulic press

[1] ICOS: Integrated Carbon Observation System, https://www.icos-ri.eu/ ; ACTRIS: the European **Research Infrastructure** for the observation of **Aerosol, Clouds, and Trace gases,** https://www.actris.eu/

(Hamron, Item no. 619550). The head of the hydraulic press was covered with aluminium foil in order to protect the filters from contamination. A pressure of 4-6 tonnes was used for compressing the filters. The compressed filters were then placed in a 60 ml petri dish. The filters were finally measured by gamma ray spectrometry by using a liquid nitrogen cooled HPGe detector (ORTEC p-type HPGe, model GM55-P4, SN 45-PT22044A). The counting time was one to two weeks. The results were corrected for the time between aerosol sampling and gamma ray spectrometry measurement.

Figure 5: *Left:* The DHA-80 sampler on the roof of the Hyltemossa site. *Right:* Interior of the DHA-80 sampler, showing the filters mounted on filter holders.

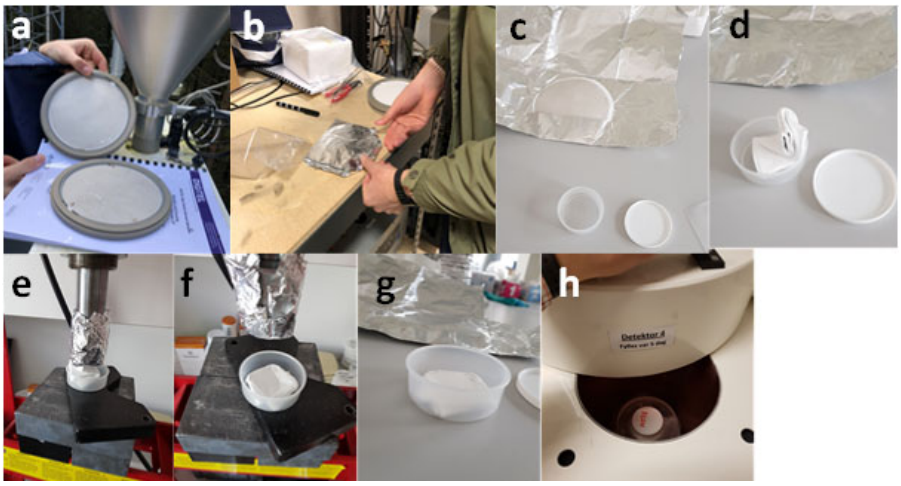

Figure 6: Procedure of sampling and gamma-ray spectrometry measurements of ambient aerosols. a). Aerosols were sampled on quartz fibre filter using a high-volume sampler. b). The filters were dismounted from the sampler and wrapped in aluminium foil. c). At the laboratory, the filters were unpacked and put into a 60 ml petri dish (d.). e-g). The filters were pressed to a cylindrical puck by a hydraulic press. h). The filters were finally measured by gamma-ray spectrometry.

The results from the gamma spectrometry measurements were compared to data from the SSM/FOI station at Ljungbyhed, located about 12 km from Hyltemossa. The procedure for the SSM/FOI filters are described e.g. in Ref [23, 154]. The flow rate of the aerosol sampler at the Ljungbyhed station is approximately 1000 m^3 h^{-1}, i.e. significantly higher than the DHA-80 sampler

used at Ljungbyhed (36 m^3 h^{-1} for the samples collected in the study). The filters used at Ljungbyhed are glass fibre filters of about 60 cm x 60 cm collected in 3.5 day periods, and samples are pooled into weekly samples, which are measured 4-5 days after collection on shielded HPGe detectors [154].

5.2.3. Results and discussion

Figure 7 shows the filters after collection of particulate matter during 3.5-day intervals from 22 March to 1 July 2019. As seen in the figure the sampled material varies with season (e.g. pollen in spring). The two dark filters in the period ending 8 April were collected during easterly winds, carrying polluted air from Eastern Europe. Previous measurements performed in southern Sweden have shown that air masses from eastern and southern Europe usually carry more particulate matter, hence can be said to be more polluted, than air masses from west and north [147, 155, 156]. It can further be visually seen that the aerosol collected on filters between 22 April and 6 May is darker in colour compared to neighbouring dates (190408-190422 and 190506-190520, Figure 7). This might be due to the tradition on Walpurgis Night when bonfires are lightened all around the country during the evening of 30th of April leading to enhanced emissions of biomass burning aerosols [157].

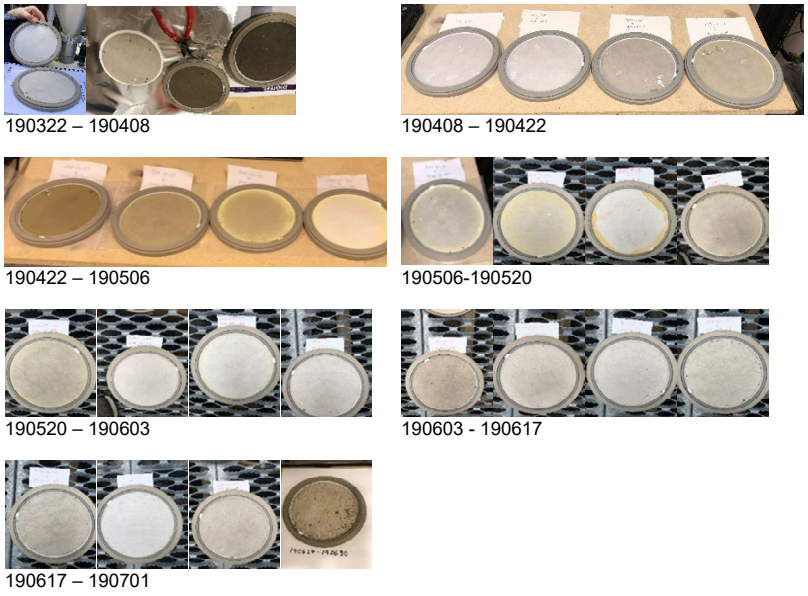

Figure 7: Filters sampled in 3.5-day intervals from 22 March to 1 July 2019.

The results of the gamma spectrometry measurements are shown in Table 6. Time between sampling and measurement was too long for several samples, resulting in difficulties to quantify radionuclides with relative short half-lives. Due to missing data we have focussed mainly on ^{7}Be and ^{40}K in this evaluation. ^{7}Be has a mean value of 4.58 mBq m^{-3} (standard deviation of 2.22 mBq m^{-3}) which is in line with the ^{7}Be measurements of aerosol filters from the Swedish Defence Research Agency measurement site in Ljungbyhed, 12 kilometers west of Hyltemossa (see Figure 8). ^{40}K displays a mean activity of 76 µBq m^{-3} (standard deviation of 41 µBq m^{-3}).

Table 6: Results from gamma spectrometry measurements of aerosol filters collected in Hyltemossa. HL: half-life. Uncertainties represent 2σ.

M578	190322 – 190329	6087	0.003	(2.58±0.01)·10^3	52	0.22·10^3	0.16·10^3	53	0.24·10^3	65	99	<MDA
M579	190322 – 190408	12240	0.0075	(5.28±0.02)·10^3	96	98	39	31	70	32	48	820
M583	190408 – 190422	10080	0.0058	(8.27±0.03)·10^3	74	11·10^3	33	33	<MDA	43	64	<MDA
M584	190422 – 190506	10080	0.0066	(6.83±0.19)·10^3	144	11·10^3	81	<MDA	<MDA	67	<MDA	<MDA
M595	190506 – 190520	12096	0.0062	(2.83±0.13)·10^3	25	>12 HL	<MDA	<MDA	>12 HL	<MDA	<MDA	<MDA
M596	190520 – 190603	12096	0.0062	(1.69±0.12)·10^3	103	>12 HL	>12 HL	>12 HL	>12 HL	>12 HL	0.11·10^3	<MDA
M597	190603 – 190617	12096	0.0062	(4.66±0.06)·10^3	72	>12 HL	>12 HL	>12 HL	>12 HL	>12 HL	>12 HL	<MDA
M598	190617 – 190701	12096	0.0062	(4.55±0.14)·10^3	18	>12 HL	>12 HL	>12 HL	>12 HL	>12 HL	<MDA	<MDA

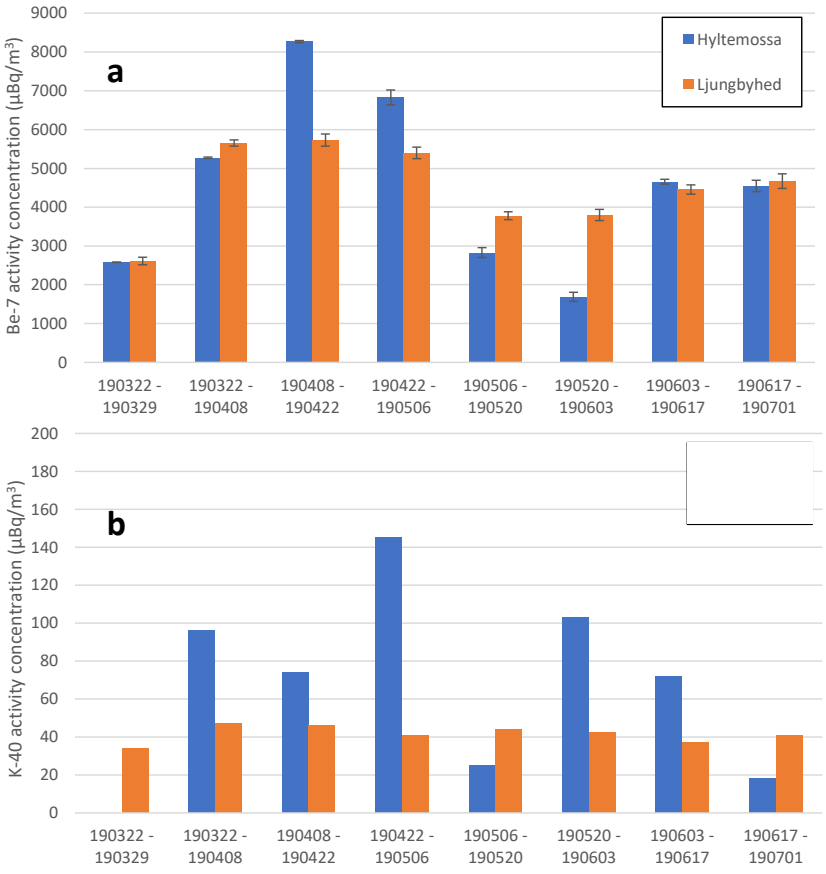

Figure 8: Activity concentrations of ^{7}Be (a) and ^{40}K (b) from the Hyltemossa measurement station and the Ljungbyhed measurement station (FOI/SSM). Data from the Ljungbyhed measurement station has been pooled in pairs in order to perform this comparison. Error bars represents 2σ. No measurement uncertainty was available for the ^{40}K measurements at Hyltemossa.

5.2.4. Conclusion and outlook

A measurement campaign on radionuclides in aerosols was initiated at the Hyltemossa measurement station. Activity concentrations of common aerosol radionuclides such as ^{7}Be and ^{40}K were quantified and compared to the FOI measurement site in Ljungbyhed, 12 km west of Hyltemossa. The comparison showed good agreement in ^{7}Be activity concentration, despite significantly lower flow rate with the DHA-80 sampler employed at Hyltemossa. Time between collection and measurement needs to be decreased for upcoming measurements at Hyltemossa.

As a next step we propose to evaluate expected detection limits in environmental monitoring of the most relevant gamma-emitting ESS radionuclides using a DHA-80 sampler and gamma spectrometry. With knowledge of expected source terms [2, 141], stack dimensions, exhaust speed from the stacks (can be found in [142]) and meteorological data, the average expected ambient radionuclide concentrations at various locations can be evaluated (e.g. using the free software SCREEN View), and expected detection limits can be assessed. The outcome will reveal if the DHA-80 sampler would be suitable to be used e.g. in central Lund for environmental monitoring and inhalation dose assessments.

We also propose to investigate the possibility to establish detection methods for direct radionuclide-specific alpha spectrometry measurements of aerosol samples, similar to Ref [74]. Conventional alpha spectrometry and liquid scintillation counting techniques require chemical pre-treatment of the samples. I.e. those methods are relatively slow and time consuming. The establishment of direct methods would be useful for emergency preparedness as well as regular environmental monitoring. To justify validity of the method the background levels of alpha emitters in the aerosol filters should be measured using the same measuring technique.

5.3. Tritium in the environment

In this section results of a one-year study of tritium in precipitation continuously collected at the ESS site are presented. Results of tritium in grab samples of air moisture, collected once a month during one year at two sites (at ESS and in the northern parts of the city of Lund), are presented. In addition, the tritium levels have been monitored on a monthly basis in 3 ponds (one at ESS, one at MaxIV and one in the northern parts of Lund) during 4 months. A procedure for the measurements is presented as an appendix. Furthermore, data of the stable hydrogen isotope composition of the samples is presented (an additional description about the use of stable isotopes related to radioactivity measurements, and the use as carriers of other information about the sample, is presented in an appendix).

5.3.1. Introduction

The low-energy pure beta emitter tritium (also denoted ^{3}H or T, $T_{1/2}$ = 12.3 years) will be produced in ESS from proton beam-loss reactions, from spallation reactions in the target and from neutron activation of ^{2}H and ^{3}He. According to our FLUKA calculations, the target will contain $9.8 \cdot 10^{14}$ Bq tritium after 5 years of operation [11]. This is similar to values reported by others [13, 158]. According to ESS, tritium is expected to dominate the source term from the ESS target station to the environment with an estimated release rate of ~1 TBq year^{-1} during normal operation [2, 6]. Releases of tritium from the accelerator tunnel to the environment are estimated to become in the order of 10^{8} Bq year^{-1} [6]. Tritium may also be formed in construction materials and soil [159].

Tritium is a naturally occurring radionuclide, which mainly appears in the environment in the form of water (and to a smaller fraction as gaseous tritium (HT)). Thus, tritium has a very high environmental mobility due to its participation in the hydrological cycle. The natural production – originating from nuclear reactions involving gases in the atmosphere and cosmic radiation – results in tritium activity concentrations of between 0.1 to 0.6 Bq L^{-1} of water [1]. The global inventory of naturally produced tritium is about 10^{18} Bq [160, 161]. Tritium that has been incorporated into organic compounds is denoted organically bound tritium (OBT), which can be either exchangeable (when bound to oxygen, nitrogen or sulphur), or non-exchangeable (when covalently bound to carbon). The OBT fraction is of particular interest due to the longer biological half-life of OBT (40 days) compared to that of HTO (10 days) [161]. The dominant pathway of natural tritium to man is through drinking water and food (the latter containing HTO as well as OBT), resulting in global individual average annual effective dose of 0.01 μSv year^{-1} [161].

Anthropogenic tritium mainly stems from the atmospheric testing of nuclear weapons during the last century: ~$2 \cdot 10^{20}$ Bq of tritium has been added to the worldwide hydrological cycle [162]. The highest concentrations of tritium in rainwater was observed in 1963, containing > 400 Bq L^{-1} [1, 163]. The main part of the bomb-tritium has now (year 2019) decayed, and current levels of tritium in rainwater are typically single Bq or less [163]. Seasonal as well as geographical variations can be observed in tritium in air humidity and in precipitation. These are described in section 6.3 in Appendix 3 (see Fig. 6b in

Appendix 3). Appendix 3 also discusses the effect of isotope fractionation on tritium measurements and describes how measurements of isotope fraction of the stable hydrogen isotopes can reveal not only the history and the source of natural waters, but also be used for quality control in sampling and sample preparation related to tritium measurements. Figure 9 shows the stable isotope ratios ($^2H/^1H$, expressed as isotope fractionation δD, see definition in Appendix 3) in precipitation collected at two German monitoring stations in the programme Global Network of Isotopes in Precipitation (GNIP) [163]. The variation in $^2H/^1H$ ratio mainly depends on temperature, hence the seasonal variations [164]. Variations between sites depend on several factors such as elevation, latitude and amount of precipitation (see also Figure 2 in Appendix 3) [164].

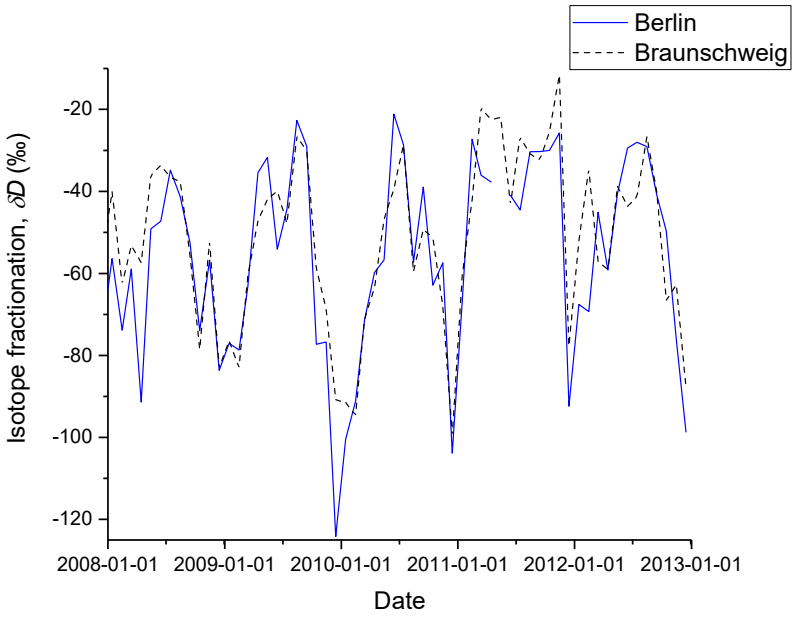

Figure 9: Stable isotope fractionation in precipitation at two German stations participating in the monitoring programme Global Network of Isotopes in Precipitation (GNIP) [163].

The nuclear power industry produces substantial amounts of tritium, of which parts are released continuously to the environment during operation. The amount produced and released varies significantly between different reactor types: heavy-water moderated reactors are known to release approximately 10 times more tritium than light-water reactors [165]. A typical release rate of tritium from a heavy water reactor of 1 GW_{el} is $7.4 \cdot 10^{14}$ Bq $year^{-1}$ as gaseous effluents and $1.8 \cdot 10^{14}$ Bq $year^{-1}$ as liquid discharges [165]. Fuel reprocessing plants release about 10^{16} Bq $year^{-1}$ [166]. An example of the amount of excess tritium that can be found in the environment of nuclear facilities is given in Ref [167]: 95% of the tritium in the lower Phone River (up to 10 Bq L^{-1}) is of nuclear-facility origin.

Tritium is also produced in significant amounts - in some countries - in industrial reactors for military as well as civilian purposes (e.g. to be used as tracer in radiolabelled substances or as ingredient is luminous paint or gas). Tritium is used at some nuclear physics research laboratories in neutron generators and fusion-based test reactors use tritium as part of the fuel. Despite the fact that the amount of tritium released to the environment from commercial

and research applications is small compared to the total global inventory, significant excess of tritium may arise in the local environment and biota [161, 168].

Contamination of the local environment by tritium has also occurred after nuclear accidents and incidents [161]. E.g., releases in the order of 10^{16} Bq of tritium have been reported from the US [161]. Environmental contamination with tritium was substantial after the Chernobyl accident in 1986 as well as the Fukushima accident in 2011 [169]. As an example, the tritium concentration was over 100 times higher than background in water from a plant collected 20 km from the Fukushima site one month after the accident [169]. Figure 10 shows tritium activity concentrations in precipitation from three European stations participating in the GNIP monitoring programme [163]. The Swiss station Bern is clearly influenced either by local releases of tritium, or the samples have been contaminated during collection. No recent Swedish (or Danish) data is available in the GNIP database.

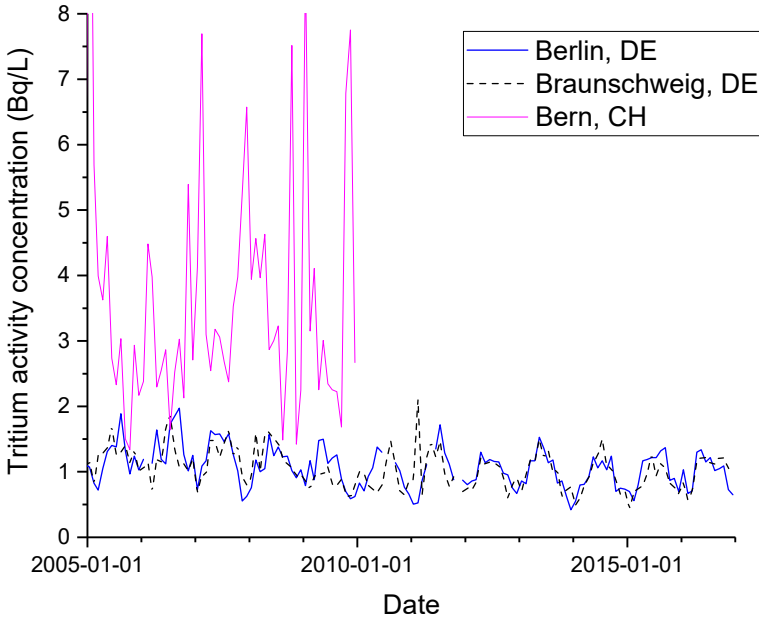

Figure 10: Tritium activity concentration in precipitation at three station participating in the monitoring programme Global Network of Isotopes in Precipitation (GNIP) [163].

Environmental levels of tritium in Swedish drinking water and sea water are monitored by SSM [170, 171]. Six waterworks are monitored since 2001 [170], none however in southernmost Sweden (the closest waterwork is Alelycka/Göta Älv, located about 220 km from ESS). Activity concentrations are often below the detection limits of a few Bq L^{-1}. At six other stations SSM monitors surface sea water since 2011, as part of the national programme for environmental control at the nuclear power plants [171]. The sea water station closest to ESS is located 8.2 km outside Ringhals nuclear power plant, 170 km from ESS. Most values are below the detection limit (generally a few Bq L^{-1}) [171].

The city of Lund hosts several activities using tritium-labelled compounds and tritium-containing materials, as well as accelerators handling tritium targets and

which may produce tritium from varying activation reactions. Therefore, we have performed several investigations to monitor the current situation of tritium in Lund: the matrices investigated include air humidity, precipitation, pond water, indoor air at one accelerator facility and urine from the general public as well as from persons who may be occupationally exposed to tritium. In this process, we have developed our competence in tritium measurements using LSC, we have continuously lowered our detection limit using our existing LSC counter, and we have established protocols for distillation of water samples and purification of urine.

5.3.2. Environmental tritium measurements in the Lund area

Locations and methods

Four sites were used (see Table 7, Figure 11 and Figure 12):

- Site T0, located ~13.8 km from ESS (~193°): Water from the deep well Grevie PV5 (depth 71-72 m), operated by VA Syd, serve as background water. A previous studies by Åkesson *et al* has demonstrated that the tritium concentration of this well is about 0.02 TU, corresponding to 0.002 Bq L^{-1} [172].
- Site T1, located ~4.3 km from ESS (~246°): This site in the north of Lund serves as a rural background site. Air humidity was collected at T1a (Timjanvägen 5) and pond water at T1b (Monument park). Public tap water was also collected at this site.
- Site T2, located inside the fenced ESS area: At site T2a, located ~ 0.29 km from the ESS target (342°) precipitation and air humidity were collected. At T2b, located ~ 0.25 km from the ESS target (329°), pond water was collected (ESS pond 4).
- Site T3, located at MaxIV, ~ 0.86 km from the ESS target (223°): At this site pond water was collected.

Table 7: List of sites for sampling of environmental samples (precipitation, air humidity and pond water) for tritium measurements.

Site	Description	GPS coordinates	Deep well	Precipitation	Air humidity	Pond water
T0	Grevie PV5 well	N55.6131 E13.1970	x			
T1a	Timjanvägen 5, Lund	N55.71861 E13.18278			x[2]	
T1b	Monument park, pond	N55.7182 E13.1851		x[1]		x[3]
T2a	ESS	N55.7366 E13.2455			x[2]	
T2b	ESS, pond 4	N55.7359 E13.2446				x[3]
T3	MaxIV, pond	N55.7283 E13.2376				x[3]

[1] Monthly samples of total precipitation, May 2018-April 2019
[2] Grab samples once a month, May 2018-April 2019
[3] Grab samples once a month, January 2019-April 2019

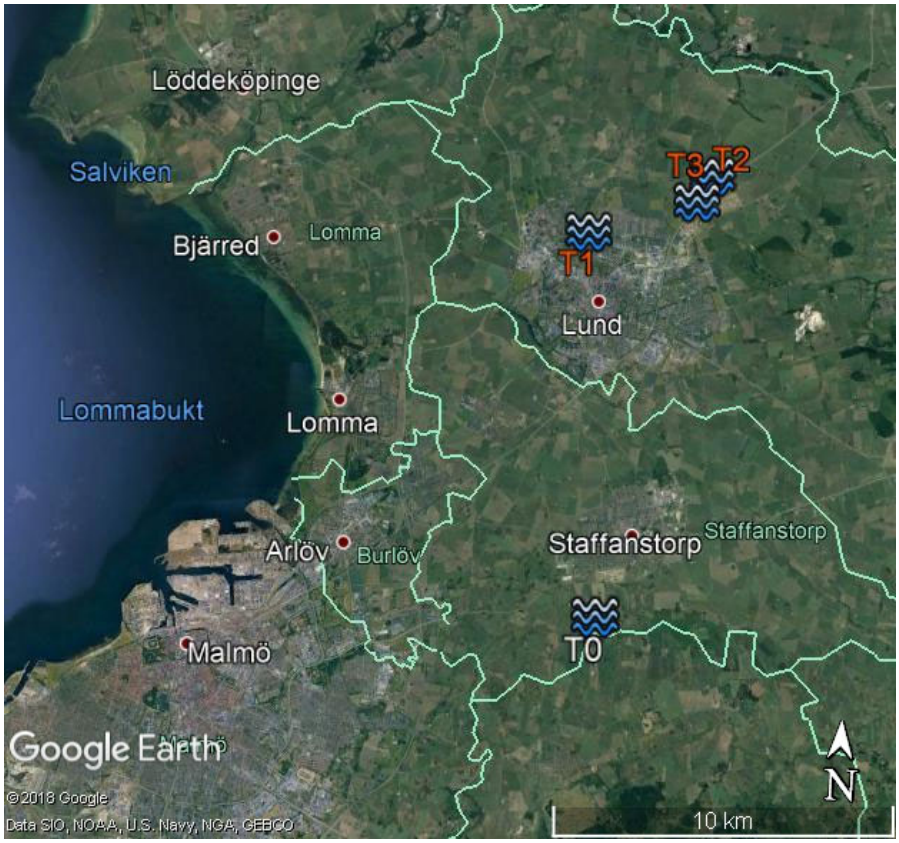

Figure 11: Sampling sites for environmental tritium in the Lund area according to Table 7, including the Grevie well (T0) used as background.

Figure 12: Sampling sites for environmental tritium in the Lund area according to Table 7.

The sample collection and sample preparation procedures for precipitation samples and air humidity samples are described in Appendix 2. In brief, precipitation samples were collected on a monthly basis using a rain collector from Palmex (Croatia) (Standard Rain Sampler RS1, including a siphon inlet). The sampler and the samplings followed the recommendations of the IAEA/GNIP precipitation sampling guide [173]. Air humidity was collected using condensation of water vapor.

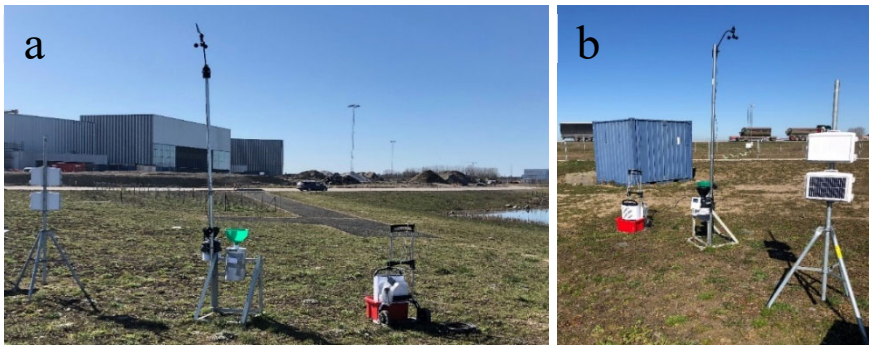

Figure 13: a) Weather station, precipitation collector (green funnel) and air dehumidifier at site T2a. The pond at site T2b is shown to the far right. **b)** Site T2a and the power station (blue building) used to power the air dehumidifier during air humidity sampling. The console for viewing data from the weather station is located in the white upper box mounted on the tripod to the far right. The Davis Weather Envoy with the USB data logger is placed in the lower solar-powered box mounted on the tripod. Pictures taken 1 April 2019.

The ESS site T2a was equipped with a solar-powered weather station (Davis Vantage Pro2, Davis Instruments), installed in the end of September 2018, see Figure 13. Weather data was displayed using a wireless console and stored on a WeatherLink® USB Data Logger, Windows, using a wireless solar-powered Davis Weather Envoy (both mounted on a tripod in universal shelters). Data was logged every 30 minutes including e.g. temperature, wind speed, wind direction, air humidity and precipitation rate. Data was transferred to a laptop computer once a month using the software WeatherLink®. The precipitation data was used to ensure that no losses occurred during precipitation sampling using the Palmex rain sampler (e.g. from stop in the siphon inlet).

The Grevie background water and the pond water samples were collected in the same bottles as the air humidity samples and were subjected to distillation prior to LSC measurement. For the pond water, samples of water not subjected to distillation were also measured to investigate the effect of distillation. All LSC measurements were performed using a Beckman LS 6500 LSC multipurpose liquid scintillation counter according to Appendix 2. All samples were measured at least 1200 minutes.

The $^{2}H/^{1}H$ ratio of part of the samples was measured using Isotope Ratio Mass Spectrometry (IRMS) at the Stable Isotope Service Lab, Department of Biology, Lund University. For each collected sample of water, duplicate of triplicate aliquots of 1 ml was transferred to 1.5 ml HPLC vials with a screw caps (VWR1548-14888, VWR) using a pipette. Samples of tap water collected in March 2018, October 2019 and January 2019 as well as water from the Grevie well collected in October 2018 were also subjected to IRMS analysis. Additionally, some commercial bottled waters were analysed.

Results and discussion

Tritium activity concentrations

The results of the tritium measurements of the precipitation samples are shown in Table 8. Nine of the twelve samples also include data of the stable isotope composition (the final three samples have not yet been measured at the time of finalizing this report). Average temperatures from before the installing of the Davis weather station was taken from SMHI open data, station Lund (N55.693, E13.229) [174].

Table 8: Results of tritium activity concentration ($A_{tritium}$) and stable isotope data (δD) of precipitation sampled from May 2018 to April 2019 at the ESS site T2a. $T_{average}$ is the average temperature during the sampling period, m_{water} is the sampled mass of water, R_{prec} is the precipitation during the period expressed in mm, $t_{tritium}$ is the LSC measurement time and *MDA* is the minimum detectable activity concentration. Values in red italic style are below the *MDA* and are thus not relevant.

ID	Sampling interval	$T_{average}$ (°C)	m_{water} (g)	R_{prec} (mm)	δD (‰)	$t_{tritium}$ (min)	$A_{tritium}$ (Bq L^{-1})	*MDA* (Bq L^{-1})
P9	2018-05-03 – 2018-06-04	17.4	18	0.4	-32.7±2.7	1800	3.4±0.5	1.4
P10	2018-06-04 – 2018-07-05	18.6	746	18.0	-55.7±3.2	4680	2.3±0.3	1.0
P11	2018-07-05 – 2018-08-13	21.9	2607	62.7	-58.6±0.4	2400	1.5±0.4	1.2
P12	2018-08-13 – 2018-08-31	17.6	1950	46.9	-49.9±2.3	2400	2.3±0.4	1.2
P13	2018-08-31 – 2018-10-01	14.1	1057	25.4	-55.2±0.7	1200	1.9±0.5	1.6
P14	2018-10-01 – 2018-11-01	10.6	2200	53.0	-50.2±0.8	3000	*0.6±0.3*	1.1
P15	2018-11-01 – 2018-11-30	5.2	1131	27.2	-59.4±0.6	1200	*0.1±0.5*	1.6
P16	2018-11-30 – 2019-01-02	3.5	2812	67.7	-69.4±0.6	3600	1.5±0.3	1.0
P17	2019-01-02 – 2019-01-31	1.0	1658	39.9	-58.6±1.9	1200	*0.6±0.5*	1.5
P18	2019-01-31 – 2019-02-28	3.8	2121	51.0		1200	*1.0±0.5*	1.6
P19	2019-02-28 – 2019-04-01	4.9	4060	97.7		1200	2.1±0.5	1.6
P20	2019-04-01 – 2019-04-30	8.2	283	6.8		1200	*1.3±0.5*	1.7

Figure 14 shows the precipitation and average temperature at the ESS site T2 during the sampling period. Note the very dry beginning and end of the sampling period.

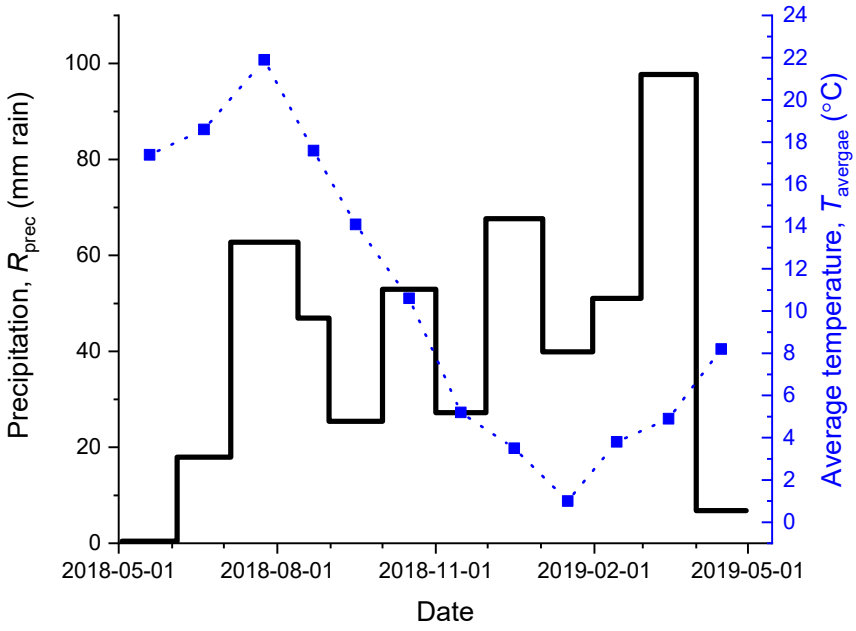

Figure 14: Average temperature and precipitation during the sampling period at the ESS site T2b. Temperature data until September 2018 are taken from SMHI open data [174].

As seen in Figure 15, the tritium activity concentration seems higher during the spring 2018 than during the rest of the sampling period. Higher values during spring than during the rest of the year is expected since water vapour from the stratosphere (with a relatively higher tritium activity concentration than in the troposphere) enters the troposphere each spring when the tropopause breaks up between 30° and 60° north [175]. The highest tritium activity concentration was in the sample with very little precipitation (0.4 mm for approximately one month in May and beginning of June 2018). The range of activity concentrations is somewhat higher than the German data in Figure 10.

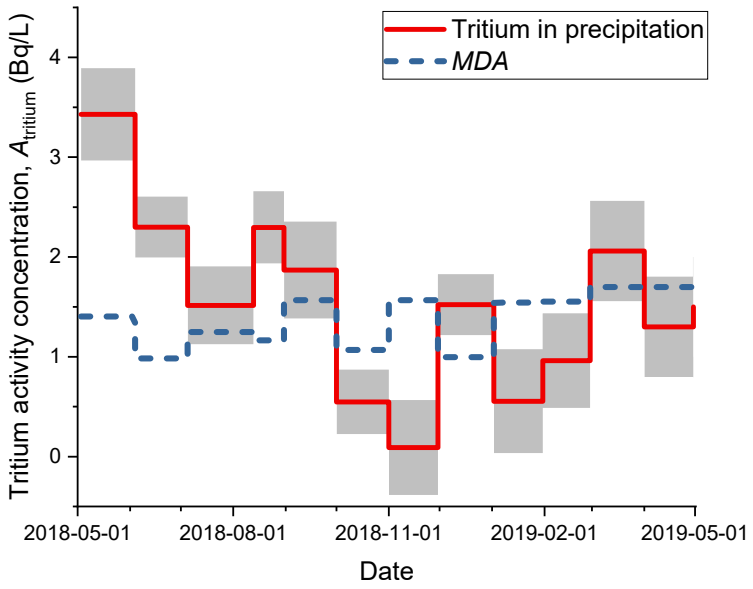

Figure 15: Activity concentration of tritium in precipitation sampled at the ESS site T2a during one year. Tritium values below the *MDA* are not relevant. Uncertainties (marked in grey) represent 1 σ.

The tritium activity concentration of the air humidity samples collected approximately once a month at the ESS site T2a is shown in Table 9, including other relevant data from the sampling occasion and measurements of the stable isotope ratio (expressed as δD, see definition in Appendix 3).

Table 9: Results of tritium activity concentration ($A_{tritium}$) and stable isotope data (δD) of air humidity sampled as water from May 2018 to May 2019 at the ESS site T2a. *T* is the temperature, *RH* is the relative humidity during the sampling time *t* and *v* is the wind speed. m_w is the sampled mass of water, $t_{tritium}$ is the LSC measurement time and *MDA* is the minimum detectable activity concentration. Values in red italic style are below the *MDA* and are thus not relevant.

ID	Sampling date	*T* (°C)	*RH* (%)	*v* (m s^{-1})	Wind dir.	*t* (hh:mm)	m_w (g)	δD (‰)	$t_{tritium}$ (min)	$A_{tritium}$ (Bq L^{-1})	*MDA* (Bq L^{-1})
H7	2018-05-03	16	52	7	NW	01:06	49	-100.1±1.8	3000	1.9±0.3	1.1
H8	2018-06-04	22	59	6	W	00:40	109	-55.7±2.2	2400	3.3±0.4	1.2
H10	2018-07-05	20	58	5	W	00:40	88	-72.5±1.3	2400	1.8±0.4	1.2
H12	2018-08-13	22	78	4	SSE	00:40	174	-71.6±3.8	2400	1.4±0.5	1.2
H15	2018-10-01	12	66	4	W	01:10	53	-46.1±1.0	1200	*1.0±0.6*	1.6
H17	2018-11-01	10	86	5	E	03:15	269	-83.4±0.8	1800	*0.8±0.5*	1.3
H18	2018-11-30	2	88	5	SSE	01:30	39	-43.5±0.6	1200	*1.0±0.5*	1.6
H20	2019-01-08	5	95	3	NNW	01:25	>34	-98.6±0.7	1200	2.2±0.5	1.5
H22	2019-01-31	1	87	5	ESE	05:40	45	-104.7±0.6	1200	*-0.2±0.5*	1.6
H25	2019-02-28	7	70	5	NW	04:20	131	No data	1200	1.9±0.5	1.6
H27	2019-04-05	14	50	8	E	01:40	31	No data	1200	*0.7±0.5*	1.6
H28	2019-04-30	15	50	2	SW	01:06	49	No data	1200	*0.9±0.5*	1.6

Table 10 shows the corresponding values for air humidity collected at the urban reference site T1a (sampling was however not performed in May 2018). The required time of sampling using the air dehumidifier strongly depends on temperature and outdoor air humidity. The cooler and dryer, the longer collection time is required. Attempts on sampling at temperatures < 1 °C with dry conditions (RH~50%) failed.

Table 10: Results of tritium activity concentration ($A_{tritium}$) and stable isotope data (δD) of air humidity sampled as water from June 2018 to May 2019 at the urban background site T1a. *T* is the temperature, *RH* is the relative humidity during the sampling time *t* and *v* is the wind speed. m_w is the sampled mass of water, $t_{tritium}$ is the LSC measurement time and *MDA* is the minimum detectable activity concentration. Values in red italic style are below the *MDA* and are thus not relevant.

ID	Sampling date	*T* (°C)	*RH* (%)	*v* (m s^{-1})	Wind dir.	*t* (hh:mm)	m_w (g)	δD (‰)	$t_{tritium}$ (min)	$A_{tritium}$ (Bq L^{-1})	*MDA* (Bq L^{-1})
H9	2018-06-04	22	58	6	W	00:40	103	-51.4±3.3	1200	3.3±0.4	1.7
H11	2018-07-05	20	59	5	W	00:50	137	-76.5±3.5	2400	1.8±0.5	1.2
H13	2018-08-13	20	88	3	SSE	00:40	145	-72.3±3.5	1200	*1.1±0.5*	1.7
H14	2018-10-01	7	96	1	WNW	00:57	74	-61.2±1.5	1200	*0.3±0.5*	1.6
H16	2018-11-01	7	86	4	E	02:00	68	-92.7±0.6	1200	*0.4±0.5*	1.6
H19	2018-11-30	3	40	5	SSE	02:00	40	-82.0±3.0	1200	*1.2±0.5*	1.6
H21	2019-01-08	3	96	6	NW	05:20	51	-100.3±1.5	1200	2.0±0.8	1.6
H23	2019-01-31	1	88	3	ESE	03:45	32	No data	1200	*0.8±0.5*	1.6
H24	2019-02-28	5	97	5	NW	02:00	47	No data	1200	1.9±0.5	1.6
H26	2019-04-05	14	55	7	E	04:42	142	No data	1200	*-0.4±0.5*	1.7
H29	2019-04-30	15	48	4	SSW	02:20	82	No data	1200	*0.9±0.5*	1.6

The tritium activity concentration in air humidity at the two sites samples (ESS site T2a and urban background site T1a) are graphically presented in Figure 16. The trend is the similar to that of precipitation (Figure 15) with higher tritium concentrations in June 2018 (westerly winds) than during the rest of the sampling period, and with the same range of activity concentrations. Most wind directions have been represented during the sampling period.

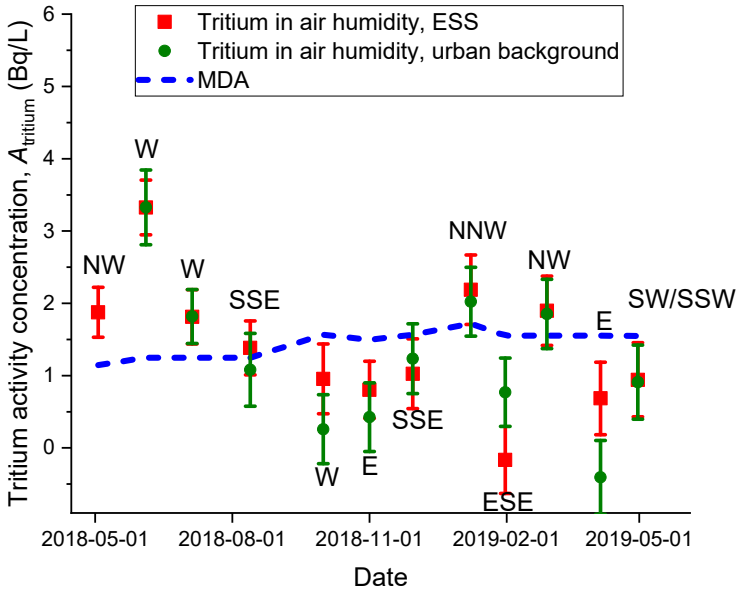

Figure 16: Activity concentration of tritium in air humidity sampled at the ESS site T2a and urban background site T1a. Tritium values below the *MDA* are not relevant. Uncertainties (marked in grey) represent 1 σ.

The results of the tritium measurements of the 3 ponds monitored are shown in Table 11. The tritium activity values are mean of the LSC measurements of samples distilled and not distilled: a paired sample t test showed no significant difference between distilled and not distilled samples at the 0.05 level. No interference from other radionuclides is thus apparent, and the fraction of organically bound tritium in the pond water is insignificant. Only 2 samples showed tritium activity concentration above the MDA. The relatively lower values of the pond water compared to air humidity and precipitation may be a result of groundwater in the ponds.

Repeated measurements of the Lund tap water revealed an average tritium concentration of 1.5 ± 0.6 Bq L^{-1} (MDA = 1.2 Bq L^{-1}).

Table 11: Results of tritium activity concentration ($A_{tritium}$) and stable isotope data (δD) of pond water sampled from January to April 2019 at the urban background site T1b, the ESS site T2b and the MaxIV site T3. *T* is the temperature at the time of sampling, $t_{tritium}$ is the LSC measurement time and *MDA* is the minimum detectable activity concentration. Values in red italic style are below the *MDA* and are thus not relevant.

ID	Site	Sampling date	*T* (°C)	δD (‰)	$t_{tritium}$ (min)	$A_{tritium}$ (Bq L^{-1})	*MDA* (Bq L^{-1})
Pond-1	T2b	2019-01-08	4,5	-56.2±2.2	2400	*0.6±0.4*	1.2
Pond-2	T3	2019-01-08	4,5	-64.8±1.3	2400	*0.4±0.4*	1.2
Pond-3	T1b	2019-01-08	4,5	-55.7±2.7	2280	*1.2±0.4*	1.2
Pond-4	T2b	2019-01-31	1	-70.3±1.5	1800	*0.6±0.4*	1.3
Pond-5	T3	2019-01-31	1	-61.4±4.4	1800	*1.2±0.4*	1.3
Pond-6	T1b	2019-01-31	1	-76.0±2.3	2400	*0.5±0.4*	1.2
Pond-7	T2b	2019-02-28	5	No data	2400	1.5±0.4	1.2
Pond-8	T3	2019-02-28	5	No data	3000	2.5±0.4	1.1
Pond-9	T1b	2019-02-28	5	No data	2400	*0.7±0.4*	1.2
Pond-10	T2b	2019-04-01	7	No data	2400	*0.7±0.4*	1.2
Pond-11	T3	2019-04-01	7	No data	2400	*0.6±0.5*	1.2
Pond-12	T1b	2019-04-02	7	No data	2400	*0.9±0.5*	1.2

Stable isotope data

Figure 17 shows the measured δD values in precipitation from May 2018 to January 2019 as well as average temperature during this period. As the isotope fractionation is affected by the condensation temperature, and hence the ground temperature, the isotope fractionation is expected to be correlated with temperature. The variation in δD does not follow the temperature variations as distinctly as reported e.g. in [176] (see also Figure 3 in Appendix 3). One reason may be that the δD value in May 2018 is affected by the low precipitation rate during that specific period (see Table 8 and Figure 14) [164]. Not only the stable hydrogen isotopes, but also the tritium concentration is of course subjected to isotope fractionation. This is demonstrated in Figure 18, in which δD and the tritium activity concentration (only values above the *MDA*) have been plotted for the precipitation samples. A high degree of correlation is observed between the isotope fractionation of the stable isotopes and the tritium activity concentration ($R = 0.94$, $p = 0.006$). It should however be remembered that the current data set is very limited. Furthermore, and more importantly, the isotope fractionation effect is on the order of percent and does not explain the larger relative variations in the tritium activity concentration. Instead, the spring leak is expected to be the reason for the increase in tritium concentration during spring.

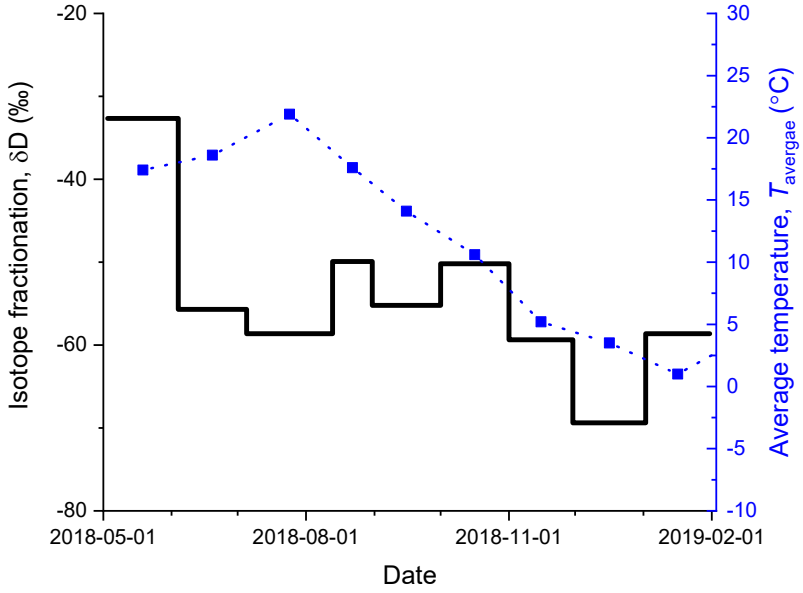

Figure 17: Isotope fractionation of stable hydrogen isotopes (δD) in precipitation collected at the ESS site T2a and average temperature.

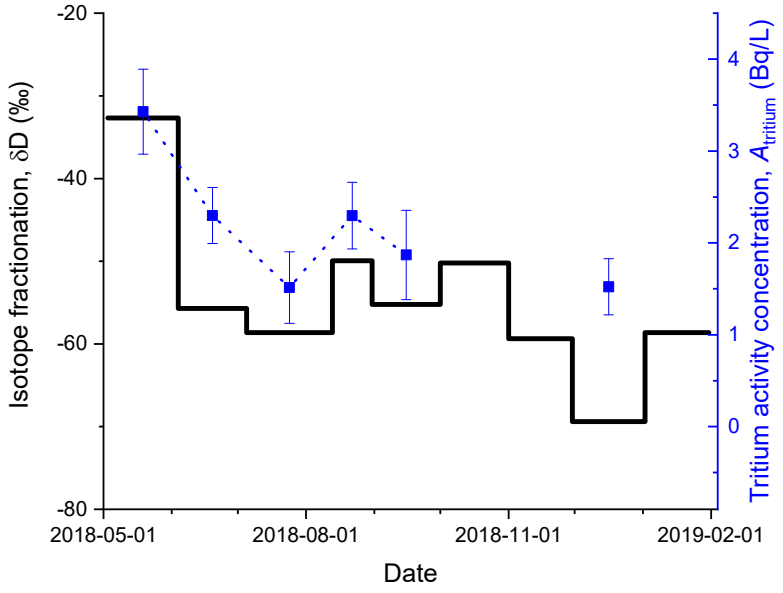

Figure 18: Isotope fractionation of stable hydrogen isotopes (δD) and tritium activity concentration in precipitation collected at the ESS site T2a. Only tritium values above the MDA have been included.

Figure 19 shows stable isotope data and outdoor temperature for the water collected from air moisture at the ESS site T2a and the urban background site T1a. Some rough trend can be seen in correlation between δD and temperature. It must be noted that it is not the δD value of the air moisture itself that is measured, but the δD of the water that has been condensed during sampling. The

condensation itself introduces isotope fractionation, which may be affected not only by outdoor temperature, but also on factors such as wind speed, and details in the sampling, such as thawing time if the air dehumidifier not only condensates, but also freezes the air moisture. However, the δD data reveals that this isotope fractionation will not significantly influence the measured tritium concentrations (see also Appendix 3, section 5.1).

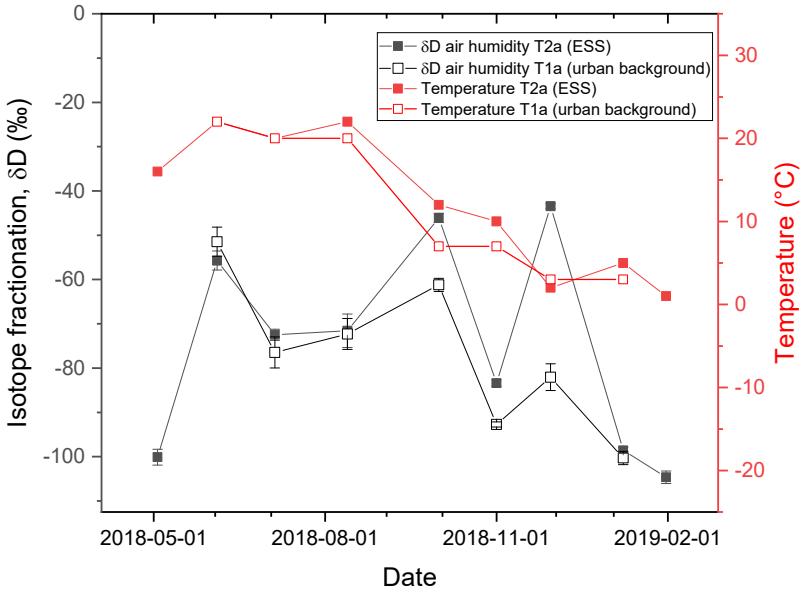

Figure 19: Isotope fractionation data (δD) for condensed air moisture and temperature at the time of sampling at the ESS site T2a and the urban background site T1a.

The results of IRMS measurements of some bottled water, distilled Grevie water (site T0) and tap water from Lund are shown in Table 12. The tap water in Lund mainly originates from Lake Bolmen (N56.850, E13.682) and occasionally from Lake Vomb (N55.678, E13.597) [177]. Thus, the public tap water in Lund is surface waters. The Grevie water and the bottled waters are ground waters, which all display lower δD values than Lund tap water.

Table 12: Isotope fractionation data for some bottled commercial waters, distilled water from the Grevie well (site T0) and tap water from Lund.

Sample	No of replicates	δD (‰)
Bottled sparkling water, brand 1 (Coop)	2	-72.8 ± 0.2
Bottled sparkling water, brand 2 (Ramlösa)	2	-58.0 ± 1.3
Bottled sparkling water, brand 3 (Loka)	2	-66.6 ± 0.9
Distilled Grevie well water, October 2018	3	-65.9 ± 0.2
Lund tap water, March 2018	3	-50.4 ± 2.2
Lund tap water, October 2018	6	-42.2 ± 2.6
Lund tap water, January 2019	6	-50.5 ± 0.8

δD values of precipitation, pond water, Lund tap water (surface water) and Grevie deep aquifer water (ground water) are shown in Figure 20. The three tap water samples are enriched in the heavier isotope compared to all precipitation samples, except the one collected during the very dry month of May 2018. This is consistent with the common knowledge that evaporation from surface waters

favours vaporization of the lighter isotopes, leaving the surface water isotopically heavier [164]. The relatively low δD values of the pond waters may indicate groundwater inflow to the ponds, which would be consistent with the low tritium values observed (see Table 11).

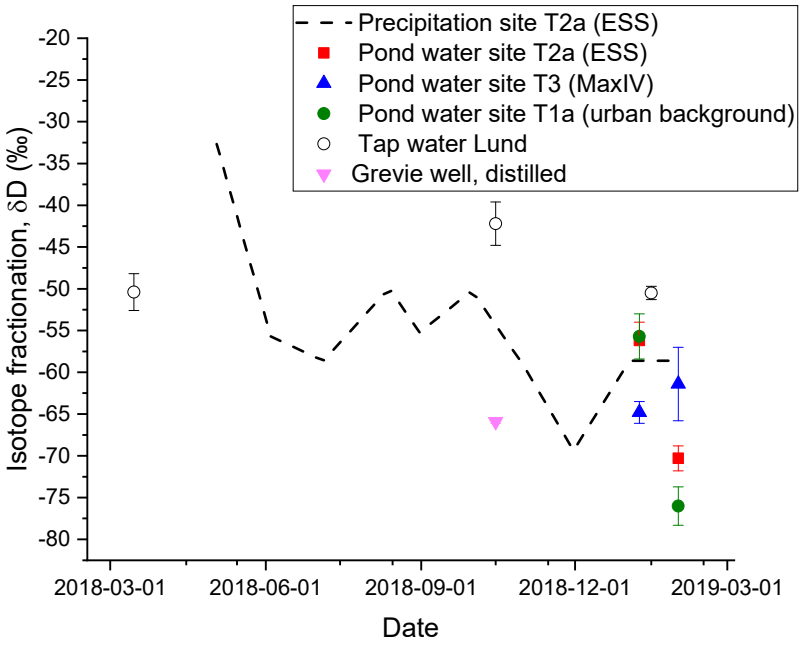

Figure 20: Stable isotope data for precipitation, pond water, tap water and deep aquifer water from the Grevie well (ground water of low tritium content).

Conclusions and outlook

Sampling using the rain collectors worked well, and the Davis weather station has proven reliable for collection of weather data. The precipitation sampler needed to be cleaned occasionally to prevent clogging of the dip-in tube. The collection of air humidity sampler using a dehumidifier worked well when not raining and not too cold and dry. A commercial collector of airborne tritium, located indoors, would be preferable to obtain continuous sampling. Furthermore, a sampler equipped with a catalyst to enable trapping not only water but also other hydrogen-containing gases, is desirable. For the pond samples analysed in this study, distillation did not affect the measured tritium concentration. When ESS is in operation, this may be the case.

The *MDA* of the tritium activity concentration measurements was in the range of 1.0-1.6 Bq L^{-1}. To obtain these MDAs the measurement time had to be very long (10s of hours). Tritium in monthly samples of precipitation collected at the ESS site showed values from below the *MDA* (4 of 12 samples) to a maximum of 3.4±0.5 Bq L^{-1}, observed in the dry month of May 2018. Tritium in air humidity was sampled approximately once a month during one year at the ESS site and at an urban background site located ~4.3 km from the ESS site. 43% of the 23 samples were below the *MDA*, and the maximum concentration was 3.3 Bq L^{-1} (observed in 3 samples). The maximum observed tritium activity concentrations in precipitation and air humidity are somewhat higher than other background data (see e.g. the German data in Figure 9 and other GNIP data [163]). This could be due to local or regional effluents of anthropogenic tritium. However, it

should be remembered that the values are all close to the detection limit of the instrument used.

The GNIP data base contains no recent Swedish data on either tritium or stable hydrogen and oxygen isotopes [163]. We propose to use the Hyltemossa station for precipitation monitoring of stable hydrogen and oxygen isotope ratios as well as tritium. We also propose to continue the precipitation collection at ESS to analyse the tritium levels as well as stable isotope data. For future measurements we also see the need of a new LSC instrument with a lower background, which would not only reduce the detection limit and increase the precision and accuracy of the measurements, but would also give the possibility to measure other radionuclides than tritium of relevance for ESS. As a next step we propose to prepare for OBT measurements, which requires the capability to separate HTO from OBT, preferably by a commercial instrument. Funding for such an instrument is however yet not available.

5.4. Tritium as water vapour inside an accelerator facility

In this section we report on tritium in HTO collected at an accelerator laboratory at the Physics Department at Lund University.

Indoor air humidity samples were collected close to the 3 MV electrostatic accelerator of the Lund Ion Beam Analysis Facility (LIBAF) between March and September 2019. This date range covers periods of inactivity, experiments with proton and deuterium beams and maintenance operation. For comparison purposes, samples were also collected in another room of the Physics Department located about 100 m from the accelerator. All these samples were collected with the same types of air dehumidifiers used for outdoor measurements. The samples were analysed by LSC without pre-treatment according to the operating conditions describes in Appendix 2.

Activity concentrations from 1.9 to 8.3 $Bq \cdot L^{-1}$ were measured in the accelerator hall while the maximum values measured indoor and outdoor were 2.6 $Bq \cdot L^{-1}$ and 2.9 $Bq \cdot L^{-1}$, respectively, during the same time period.

The values which were higher than the environmental values indicate that the accelerator can release some tritium in the air. However, these quantities are too small to be detected locally in Lund once diluted in the environment.

The measurement campaign is still ongoing at the time of publishing this report.

5.5. Tritium in luminous objects

This section contains a short investigation of possible leakage of tritium from watches containing tritiated paint.

The tritium concentration in humans may vary depending on natural variations as well as addition of artificial tritium. Examples from the literature show that tritium in members of the general public may be higher than in drinking water (the main transfer path of tritium to man) [178-181]. A common explanation found in the literature is that the elevated tritium levels observed in urine have other sources than drinking water, e.g. food or tritiated luminous products [168, 182]. Highly elevated tritium activity concentrations have been found in urine of persons constantly wearing tritium-containing plastic case wristwatches [168, 182]. Leakage rates of up to 162 kBq day^{-1} was found in one of the studies, and levels in urine of up to over 1 kBq L^{-1} [168].

Both these studies, [168, 182], are over 20 years old, and therefore we did a trial with a more modern tritium-containing watch, a Luminox (series 7050). Other contemporary brands that produce tritium-containing wathches include Ball, Isobrite, Traser, Marathon, Nite, Deep Blue and Yelang [183]. The Luminox watch was placed in a 100 ml plastic jar (a urine sampling jar seen in Figure 21) filled with 50 ml of water and the lid was closed. The watch was above the water surface for 20 hours (bracelet in the water). After 18 hours the jar was shaken a few times and the whole watch encountered the water. The watch was removed from the jar and 10 ml of the water was taken for LSC analysis. The

tritium activity concentration was not distinguishable from the background (< a few Bq L^{-1}), and any leakage of tritium would be insignificant. A study of tritium in air humidity in a watch shop selling tritium-containing watches was also planned, but not performed, since the one watch shop asked for participation in the study turned out not to have any such watches in store [183].

5.6. Tritium in man

A baseline study of the tritium content in urine of 55 subjects living or working in Lund is presented in this section. The subjects of the study are the general public in Lund (N = 17), ESS neighbours (N = 10), occupationally exposed workers (N = 18) and ESS personnel (N = 10). Method development for sample preparation (filtration with active charcoal and distillation) is presented. The full article has been published in the journal "Environmental Radioactivity" [184].

5.6.1. Purpose of the study

In this part of the project, a preoperational baseline study of the urinary tritium levels in four different groups of people were investigated: ESS employees, members of the public in a range of 2 km from the ESS (referred to as ESS neighbours), workers presently exposed to tritium and the general public in the city of Lund (living from 2 to 15 km from ESS). A baseline study of tritium in humans is motivated since the tritium concentration in humans may vary between individuals depending on several factors. Drinking habits, e.g. the relative amounts of water consumed originating from tritium-depleted groundwater and from tritium-containing surface water, may be reflected in the urinary tritium content. Additionally, the presence of anthropogenic sources of tritium (industries, hospital and academic research laboratories and accelerators), as well as tritium used in certain luminous objects, may also contribute to individual variations [161].

Tritium is mainly transferred to humans via drinking water and food as tritiated water (HTO) and organically bound tritium (OBT) [161]. Excretion of HTO occurs not only in urine and faeces, but also in sweat and exhaled water vapour. Some HTO can be incorporated into tissue as OBT. The biological half-time in adult humans is generally considered to be 10 d for HTO and 40 d for OBT [161]. The global individual average annual effective dose around the year 2000 was only about 0.01 µSv [161] (in 1962, the corresponding value for bomb-related tritium was about 7.2 µSv [161]).

Inhalation, skin absorption and inadvertent ingestion may be relevant exposure routes for workers handling tritium-labelled organic material. Excretion may partly occur as HTO, but some fraction of the tritium-labelled organic compounds may be incorporated in the body as OBT [185]. The resulting effective dose is strongly dependent on the type of compound [185].

The ESS is expected to release tritium mainly as HTO. In this study, we therefore analysed the HTO content in urine. These data may serve as basis for future assessments of the radiological impact of the ESS.

5.6.2. Sample collection

After approval of the study by the Regional Ethics Review Board at Lund University (No. 2018/296), participants from the general public were recruited by post. Participants from the ESS or the exposed worker category were recruited directly. Appendix 4 shows the recruitment material as well as other documents used in the communication with the ESS neighbours. Slightly different versions were used for the other groups.

The participants received a sampling kit (Figure 21) and were asked to collect morning urine at home in a 100 mL sterile urine beaker. The urine sample was stored in a cooling bag until the sample was transferred to Lund University. Samples were stored in a refrigerator at 4 °C until sample pretreatment and ^{3}H measurement.

The participants were also asked to fill in a questionnaire providing data on age, weight, gender and address, as well as information about possible known exposure to tritium and their beverage consumption during the day before sampling.

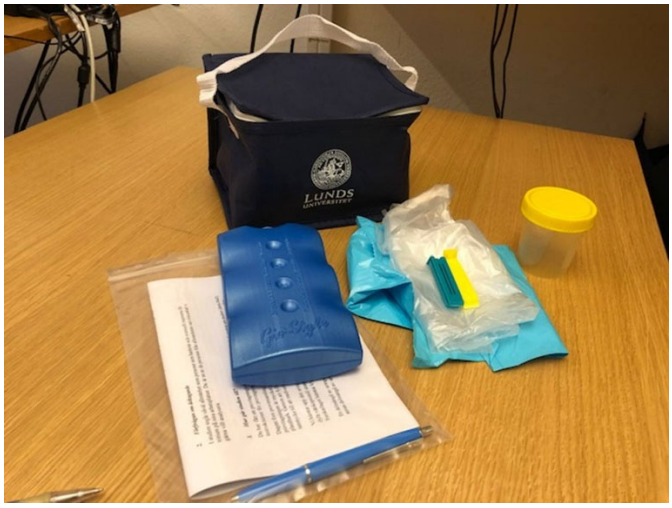

Figure 21: Sampling kit including a sample bottle, a cooling bag and a questionnaire to fill in.

In total 55 volunteers (32 men and 23 women), living or working in Lund, participated in the study and samples were collected between September and December 2018. Seventeen individuals were classified as members of the general public, 10 individuals were ESS neighbours, 10 were ESS employees and 18 persons were categorized as occupationally exposed workers. Fourteen individuals in the latter category were actively handling ^{3}H-labelled substances or ^{3}H-containing materials; the other 4 being employees who may be passively exposed to tritium. Several of the ESS employees have previously been employed at, or have recently visited, workplaces with excess levels of tritium.

Activity concentration of tritium in tap water from Lund was also measured.

5.6.3. Analytical method

The full pretreatment and measurement procedure is described in Appendix 5.

5.6.4. Results

The average tritium concentration in tap water in Lund, measured between October 2018 and January 2019, was 1.5 ± 0.6 Bq L^{-1} (MDA = 1.2 Bq L^{-1}).

The average reported volume of beverages consumed by the volunteers was 2.1 ± 0.8 L day^{-1} (information was provided by 54 of the 55 participants). Tap water accounted for, on average, 78 ± 17% (mean ±1 SD) of the total drinking volume. Average age, weight, volume of beverages consumed and HTO activity concentrations for each group of participants are summarised in Table 13.

Table 13: Age (range), weight, volume of beverages consumed, urinary HTO activity concentration and MDA for the four categories of participants (mean ± 1 σ) [184].

Group (*N*)	Age (y)	Weight (kg)	Volume of beverages consumed (L)	HTO activity conc. (Bq L^{-1})	MDA (Bq L^{-1})
General public (17)	51.7 (29-77)	80.3 ± 16.1	1.9 ± 0.7	<MDA	2.1
ESS neighbours (10)	50.7 (25-59)	75.0 ± 15.8	1.6 ± 0.5	<MDA	1.4-2.1
ESS employees (10)	46.0 (31-58)	88.7 ± 26.8	2.5 ± 0.9	<MDA	2.1
Other exposed workers (18)	39.4 (26-63)	73.9 ± 11.4	2.1 ± 1.0	2.6 ± 1.0	1.4-2.1

The average urinary HTO activity concentrations found in the general public, the ESS employees and ESS neighbours, were all below the MDA. Only one value from a member of the general public was slightly above the MDA; 2.2 ± 1.3 Bq L^{-1} (however, not significantly different from the activity concentration of Lund tap water). The group of exposed workers had an average HTO urinary activity concentration of 2.6 ± 1 Bq L^{-1}.

Figure 22 shows the urinary HTO activity concentration in workers. Subject number 1-4 are bystanders, i.e. individuals not handling tritium-labelled materials themselves, and subject number 5-18 are workers who actively handle tritiated material, or work at facilities where tritium is produced (particle accelerators). Five of the workers actively handling tritium-containing materials had values above the MDA that were significantly different from that in Lund tap water. Additionally, 3 workers had values above the MDA, however not significantly different from the activity of Lund tap water. The remaining 6 workers actively exposed to tritium-containing materials had urinary tritium activity concentrations below the MDA and so did all 4 bystanders.

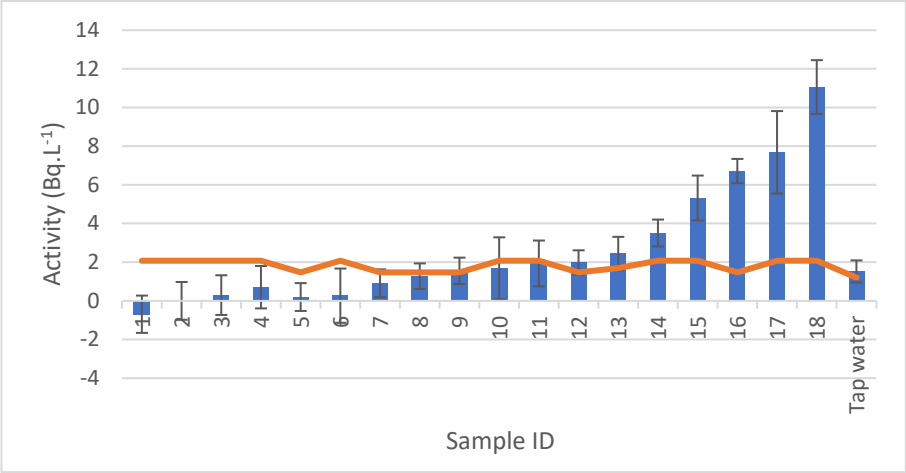

Figure 22: Urinary HTO activity concentration in bystander workers (number 1-4) and active workers (number 5-18) [184]. (The error bars correspond to the confidence interval).

5.6.5. Discussion

The HTO concentration in Lund tap water is very low (1.5 ± 0.4 Bq L^{-1}), as compared to the European Union limit of tritium in drinking water of 100 Bq L^{-1}. The finding that the urinary HTO levels were below the MDA of 2.1 Bq L^{-1} for the 38 participants that were not actively working with tritium, follows the global trend (most of the bomb-tritium produced in the 1960ies have now decayed).

Only 5 of the 18 exposed workers showed elevated levels of urinary HTO (3.5-11 Bq L^{-1}). Those concentrations are very low compared to values presented in other occupational studies. As an example, workers at a research reactor in Denmark showed urinary HTO concentrations of up to 120 000 Bq L^{-1} [85]. In Swedish studies from the 1980ies, tritium-handling workers from different hospital services and research laboratories displayed urinary HTO concentrations from background levels up to 720 Bq L^{-1} (tap water 6 Bq L^{-1}) [186, 187]. Workers at Ringhals nuclear power plant had an average HTO activity concentration of 47 Bq L^{-1} (0-165 Bq L^{-1}; $N = 18$); the corresponding values were 24 Bq L^{-1} (0-144 Bq L^{-1}; $N = 75$) for hospital employees and 149 Bq L^{-1} (30-720 Bq L^{-1}; $N = 32$) for accelerator facility employees, respectively [186, 187].

In the current study, the five occupationally exposed workers with elevated levels of tritium were working with ^{3}H-leucine, ^{3}H-thymidine, ^{3}H-acetate or methyl-^{3}H-thymidine (Figure 23). The route of contamination could e.g. be direct contamination from the organic tritium-labelled compounds followed by their degradation in the digestive system or inhalation of HTO vapour (from degradation of the compounds).

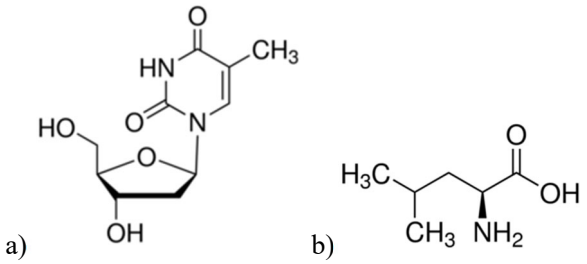

Figure 23: Examples of amino-acids used by the exposed workers: a) thymidine, b) leucine.

Tritium-containing luminous wristwatches may leak, leading to elevated tritium levels in the body that can be measured in urine [168]. This source of contamination was however not apparent for any of the participants in the current study.

According to the questionnaires, tap water was the main source of water intake for the majority of the participants. It should be noted that the origin of this tap water, and hence the tritium activity concentration of the tap water, varies among the participants. As an example, the tap water distributed in the central parts of Malmö, where some of the participants work, is tritium-depleted groundwater [188]. The Lund public trap water is however surface water of higher tritium activity concentration than ground water.

According to the ICRP, the committed effective dose coefficients of HTO are $2.0 \cdot 10^{-11}$ Sv Bq^{-1} for inhalation [189] and $1.8 \cdot 10^{-11}$ Sv Bq^{-1} for ingestion, respectively [190]. The annual effective dose from HTO in Lund drinking water would thus be about 21 nSv $year^{-1}$ (using a HTO concentration of 1.5 Bq L^{-1} for Lund tap water and an average estimated drinking volume of 2.1 L day^{-1}). Intake of OBT will result in a larger dose than from intake of HTO, by a factor of 2-2.5 [161, 189]. For occupational exposure of tritium-labelled organic compounds, the internal dose to tissue is usually up to ten times higher than the dose from an equal amount of HTO. It should also be noted that the absorbed dose to the nuclei of proliferating cells may be higher by one to two orders of magnitude than the dose from the intake of the same amount of HTO [161]. This is valid for both acute and prolonged intake of tritiated DNA precursors (e.g. ^{3}H-thymidine, ^{3}H-desoxycitidine) [161].

5.6.6. Conclusion

The baseline of HTO in humans in Lund was established using urine samples from 55 individuals divided in four groups: the general public (N =17), ESS staff members (N =10), ESS neighbours (N =10) and occupationally exposed workers (N =18). For the first three categories, no elevated levels of urinary tritium were detected as compared to Lund tap water and most of the values were found below the MDA. Thus, it can be concluded that there is currently no source of tritium contamination in Lund.

All cases of observed tritium contamination belonged to the occupationally exposed category: only 5 workers, actively handling tritium-labelled organic compounds during the study, were found to have elevated levels of tritium in their urine. The tritium activity concentrations observed were very low

compared to other studies. The preoperational baseline data presented here will be used as a reference to individual monitoring of tritium in the local population during the operational phase of ESS.

6. Summary and conclusions

This project financed by SSM aimed to strengthen competence at Lund University for measurement and analysis of ESS-specific radionuclides. In the first part of the project an extensive literature review concerning radionuclides which may be produced in ESS was performed. The information provided was based on both modelling and experimental analysis. We found that radionuclide production effects in particle accelerators are well-known, while experience with tungsten targets is very limited. As a second part of the project, an independent simplified model of the ESS target sector for the calculations of radionuclide production in the ESS tungsten target was developed using FLUKA code. The predicted radionuclide production was higher than estimated by other authors for most of the radionuclides considered. However, the differences were less than a factor of five for all radionuclides analysed, except for ^{148}Gd. The reason for this is different spallation and nuclide evaporation models used.

In the third part of the project a review was performed regarding the techniques already used to analyse the radionuclides that will be produced in the ESS tungsten target. The two main categories are the radiometric techniques (liquid scintillation, alpha and gamma spectrometry) and mass spectrometry techniques. Gamma-ray spectrometry can be referred to as the main technique of radionuclide analysis since most of the ESS specific radionuclides will be gamma-emitter. Our research groups have extensive experience in gamma spectrometry measurement in environmental matrices such as soil, water, vegetation and aerosol samples. Special attention was given to the pure alpha- and beta-emitters that are considered as difficult to measure. Liquid scintillation counting methods have already been developed by us to analyse releases of tritium in the environment, but the technique is also of interest for the analysis of other important ESS beta-emitters like ^{14}C, ^{35}S, ^{31}P and ^{33}P in environmental samples. Finally, alpha spectrometry is extensively used to measure alpha-emitter occurring naturally or produced in the nuclear fuel cycle. It can be used for the measurement of environmental matrix including the direct measurement of aerosols. Alpha spectrometry also seems a promising technique for the analysis of the alpha-emitting lanthanides that will be produced in the ESS target, and in particular for ^{148}Gd. Compared to gamma spectrometry, both LSC and alpha spectrometry analysis require sample preparation steps (extraction, pre-concentration, chemical separation…).

Mass spectrometry techniques are complementary to the radiometric techniques. Among the many types of MS techniques, ICP-MS and AMS seem to be the most suitable for the analysis of environmental samples. ICP-MS is suitable for the analysis of many radionuclides and can be hyphenated with several extraction or separation techniques such as laser ablation or gas chromatography. The possible drawback of the technique is the presence of isobaric interferences. AMS is ultrasensitive, since it can remove interfering isobars, but usually requires more complex sample preparations. It is commonly used for ^{14}C analysis and our group has a long experience with this type of

measurement. However, there are examples of its use for the analysis of several other radionuclides.

It is also possible to use techniques like neutron activation analysis (NAA) to analyse ESS specific radionuclides but these techniques are usually not widely available.

Several of the ESS radionuclides are very specific and have so far never or rarely been investigated by analytical techniques. Since they do not exist in the environment, the only available data regarding their analysis comes from other fields of research (e.g. medicine, nuclear physics).

In brief, this literature survey allowed us to sort the ESS specific radionuclides in three categories:

- Radionuclides that can be considered as the easiest to analyse: gamma emitters, common alpha- and beta- emitters (actinides, tritium, ^{14}C…)
- Radionuclides for which analytical methods were already developed but never or rarely applied to environmental samples
- Radionuclides that were too rarely studied and presently in lack of any analytical method

If the first category should not pose a problem, the knowledge gaps existing for the two other categories should be filled, in particular for most radiotoxic ESS radionuclides such as ^{148}Gd.

Three experimental parts were performed during the project, related to radioactivity measurements of aerosols, mapping of environmental tritium in the Lund area, and establishment of a method to measure tritium in urine followed by a study of tritium in persons presently living or working in Lund.

In a previous project performed by Lund University, the radiation levels around ESS was monitored in years 2017-2018 by ambient equivalent dose rate measurements, *in situ* gamma spectrometry, gamma spectrometry of various environmental samples, LSC of tritium in ground- and surface water and environmental samples, and AMS measurements of ^{14}C vegetation. Aerosol measurements were not included. However, during an accident scenario, a wide range of aerosol particles e.g. from the tungsten target may be released to the environment. Hence, we initiated gamma spectrometry measurements of aerosols which were collected at a rural background site, Hyltemossa, located close to SSM's environmental monitoring station for gamma-emitting aerosols at Ljungbyhed (operated by the Swedish Defence Research Agency, FOI). Aerosol samples were collected on quartz filters using a DHA-80 high-volume aerosol sampler (600 L min^{-1}) with automatic filter change in 3.5 day periods. Samples were pooled into 2-week collections times and measured with gamma spectrometry at Lund University. Measurements of ^{7}Be on the collected aerosols agreed fairly well with FOI results from Ljungbyhed, despite significantly higher flowrates, and hence sampled aerosol mass, at Ljungbyhed. In conclusion, the DHA-80 sampler worked well and has the potential to be used for upcoming radioactive aerosol measurements (flow rate can be increased up to 1000 L min^{-1}). In particular, the automatic filter change is most beneficial. In future measurements, a routine must be implemented which shortens the time

between end of sample collection and start of gamma measurement to a few days, to be able to measure more short-lived radionuclides.

Tritium (radioactive hydrogen) is expected to dominate the source term from the ESS target station to the environment with an estimated release rate of ~1 TBq $year^{-1}$ during normal operation. Tritium is very mobile in the environment, and is easily incorporated into living matter, including humans. Tritium is commonly used as a tracer in research and industry and may also be used as target material in accelerator facilities or being produced in nuclear reactions in these laboratories. Local contamination of tritium in the Lund area is thus possible already prior to the start of ESS. In the previous project performed during 2017-2018, tritium was mapped in several environmental matrices, however not precipitation, air and humans. During the present SSM project, we have performed several investigations to monitor the current situation of tritium in Lund using LSC: the matrices investigated included air humidity, precipitation, pond water, indoor air at one accelerator facility and urine from the general public as well as from persons who may be occupationally exposed to tritium. We have also reduced our detection limits of tritium considerably.

The results of the tritium measurements of monthly samples of precipitation collected at the ESS site for one year (May 2018-April 2019) displayed low activity concentrations (<3.4 Bq L^{-1}), with somewhat higher concentration in the spring of 2018 than during the rest of the year. The values were close to the detection limit (1.0-1.6 Bq L^{-1}, depending on sample measurement time), but occasionally slightly higher than reported at other European stations according to the IAEA GNIP database. Tritium in grab samples of air humidity (collected once a month at the ESS site and at an urban background site in Lund for a year) showed similar activity concentrations and trends as precipitation. Grab samples of pond water, collected once a month for 4 months at 3 different sites (ESS, MaxIV and an urban background site in Lund), showed tritium activity concentrations below the detection limit (~1.2 Bq L^{-1}) in 83% of the samples, which may possibly be explained by inflow of groundwater into the ponds.

The baseline of tritium levels in Lund population was assessed by measuring urine samples from 55 volunteers. Activity concentration of tritium in the inhabitants of Lund were found lower than our 2.1 Bq L^{-1} minimum detectable activity. By comparison, during the sampling period (September to December 2018), the activity concentration of tritium in Lund tap water was 1.5 Bq L^{-1}. There are currently no increased tritium levels even in the people working at the ESS or living in a 2 km range from the facility. Some exposed workers were found to have up to 11 Bq L^{-1} in their urine but those values are still very low compared to reactor workers for example.

7. Outlook

The independent modelling of the radionuclide production in the ESS target was started in this project. We propose to continue this activity as modelling results might be very useful identifying the most important radionuclides in other structures as well. E.g. modelling of other components such as the beam dump or air in the tunnel may help assessing radionuclide activities and doses during the commissioning. Simulations may be further used for evaluation, justification, and expansion of indirect measurement methods of difficult-to-measure radionuclides. For example, simulations of Gd isotopes ratios may link actual dose measurements with the source of exposure during normal operation and accidents. In this specific project, we planned that modelling would be performed by one person only. It is necessary to keep this competence and also to expand the capabilities to perform modelling with different tools.

We propose to continue the current project by developing techniques based on alpha spectrometry to be able to quantify alpha-emitting lanthanides like ^{148}Gd in various environmental samples, such as soil and vegetation, but also in aerosol samples. We plan to increase the flow rate of the DHA-80 sampler from 600 L min^{-1} to 1000 L min^{-1}. Chemical extraction of lanthanides may be based on the work performed for spallation targets [56, 57, 66] and extended into environmental samples. New chemical separation methods and deposition techniques for the production of thin alpha sources for actinides and ^{210}Po analysis are under development in other SSM-financed projects (Sören Mattsson: SSM2018-905 and SSM2020-797). In 2018, we initiated a new collaboration with the Department of Radiation Physics of the University of Gothenburg. It consists in laboratory training and sharing of experience on new radiochemistry and alpha spectrometry techniques. By strengthening the network of Swedish environment radioactivity groups, we hope to help to develop and maintain competence in our field of research.

For aerosol samples we also propose to investigate the possibilities of direct alpha spectrometry measurements according to the principles of Pöllenen [61] and determine detection limits when using different types of aerosol collectors and sampling intervals. We also suggest to thoroughly investigate the use of mass spectrometric techniques, such as ICP-MS, for determination of lanthanides in environmental samples. This study is part of another SSM-finance project focusing on radioecology (Christian Bernhardsson: SSM2019-1010). We plan to assess the existing concentrations of lanthanides in order to establish the equilibrium distribution of these elements in soil in the vicinity of the ESS and in the locally produced foodstuff. This project also includes the development of methods for the chemical extraction of these elements.

Furthermore, we propose to set up extraction procedures primarily for ^{32}P, ^{33}P and ^{35}S in different environmental matrices (and in urine) for subsequent LSC analysis. LSC techniques for other relevant ESS beta-emitters, and alpha emitters, will require a newer LSC instrument than what we are presently equipped with.

We also propose to estimate detection limits for ESS-relevant gamma emitters in environmental samples, including aerosols, for laboratory-based gamma spectrometry available at Lund University.

For tritium, we suggest that Lund University continues to perform independent measurements of the environmental tritium levels. We suggest setting up a station in the centre of Lund to collect samples of precipitation on a monthly basis, and to continuously sample air humidity (we have funding to purchase a sampler for continuous collection of separate fractions of HTO and HT). We also propose to investigate the feasibility of passive tritium samplers (see e.g. [191]). Additionally, we propose to use the rural background station Hyltemossa for precipitation monitoring of stable hydrogen and oxygen isotope ratios as well as tritium. Currently, no Swedish data is reported to the IAEA database Global Network of Isotopes in Precipitation (GNIP). We also wish to equip the proposed central station in Lund with a DHA-80 sampler for aerosol collection.

We propose annual follow-ups of the tritium levels in urine of the general public in Lund with a reduced number of participants. We also suggest to further survey indoor tritium levels in various chemical forms at existing accelerator facilities in Lund (at Lund University and at the Skåne University Hospital).

We hope that the competence gained during this project will get the opportunity to be further developed, maintained and expanded, as ESS within a few years enters its operational phase.

8. Acknowledgement

This study was financed by the Swedish Radiation Safety Authority SSM (SSM2018-1636). Several people have been most helpful during the project. We especially thank Peter Andersson at Skanska, Johan Kastlander at FOI, all participants in the tritium-in-man study, VA Syd, Klockmaster B Larssons klockor and the Environment, Safety & Heath group at ESS, Mattias Olsson at the ^{14}C laboratory at Lund University, Rimon Thomas and Juan Mantero at Department of Radiation Physics at University of Gothenburg.

9. References

[1] IRSN. *Tritium and the environment*. Available at http://www.irsn.fr/EN/Research/publications-documentation/radionuclides-sheets/environment/Pages/Tritium-environment.aspx. 2012. Accessed: 2018-02-01.

[2] Ene, D. *Source Term to the Environment from the ESS Target Station*. Nuclear Energy Agency. NEA/NSC/R(2018)2, p. 32-47. 2018.

[3] Bungau, C., Bungau, A., Cywinski, R., Barlow, R., Edgecock, T.R., Carlsson, P., Danared, H., et al. *Induced activation in accelerator components.* Physical Review Special Topics-Accelerators and Beams, 17(8): 084701, 2014.

[4] R. Stevenson, G. *Induced activity in accelerator structures, air and water.* Radiation protection dosimetry, 96(4): 373-379, 2001.

[5] Endo, A., Oki, Y., Kanda, Y., Kondo, K. *Characterization of ^{11}C, ^{13}N and ^{15}O produced in Air through Nuclear Spallation Reactions by High Energy Protons.* P-6a-336. 2000.

[6] Ene, D., Avila, R., Hjerpe, T., Bugay, D., Stenberg, K. *Assessment of environmental consequences of the normal operations of the ESS facility.* Journal of Physics: Conference Series, 1046(1): 012018, 2018.

[7] Blixt Buhr, A.M., Johansson, J., Kock, P., Karlsson, S., Lindgren, J., Tengborn, E. *Underlag till beredskapsplaneringen kring ESS.* SSM2018:02. Swedish Radiation Safety Authority (SSM). 2018.

[8] Mora, T., Sordo, F., Aguilar, A., Mena, L., Mancisidor, M., Aguilar, J., Bakedano, G., et al. *An evaluation of activation and radiation damage effects for the European Spallation Source Target.* Journal of Nuclear Science and Technology, 55(5): 548-558, 2018.

[9] Ene, D. *Assessment of environmental consequences of the normal operations of ESS facility. Part #1 Input data Source Term. Breakdown of radionuclides & Related basic information.* ESS-0028551. 2016.

[10] Thomas, R.H., Stevenson, G.R., *Radiological Safety Aspects of the Operation of Proton Accelerators*. International Atomic Energy Agency. 1986.

[11] Barkauskas, V., Eriksson Stenström, K. *Prediction of the radionuclide inventory in the European Spallation Source target using FLUKA.* Nuclear Instruments and Methods B 471: 24-32, 2020.

[12] *ESS Preliminary Safety Analysis Report.* ESS-0000002. 2012.

[13] Kókai, Z., Török, S., Zagyvai, P., Kiselev, D., Moormann, R., Börcsök, E., Zanini, L., et al. *Comparison of different target material options for the European Spallation Source based on certain aspects related to the final disposal.* Nuclear Instruments and Methods B, 416: 1-8, 2018.

[14] Isaksson, M., Rääf, C.L., *Environmental radioactivity and emergency preparedness*. CRC Press. 1315372878, 2017.

[15] L'Annunziata, M.F., *Handbook of radioactivity analysis*. Academic press. 0123848741, 2012.

[16] Anagnostakis, M.J. *Environmental radioactivity measurements and applications–difficulties, current status and future trends.* Radiation Physics and Chemistry, 116: 3-7, 2015.

[17] Povinec, P., Benedik, L., Breier, R., Ješkovský, M., Kaizer, J., Kameník, J., Kochetov, O., et al. *Ultra-sensitive radioanalytical technologies for underground physics experiments.* Journal of Radioanalytical and Nuclear Chemistry, 318(1): 677-684, 2018.

[18] Mattsson, L.S. *Sodium-22 in the food-chain: lichen-reindeer-man.* Health Physics, 23(2): 223-230, 1972.

[19] Markovic, N. *Coincidence methods in gamma-ray spectrometry for radioecological applications.* DTU Nutech. 2018.
[20] Hou, X., Roos, P. *Critical comparison of radiometric and mass spectrometric methods for the determination of radionuclides in environmental, biological and nuclear waste samples.* Analytica Chimica Acta, 608(2): 105-139, 2008.
[21] Bernhardsson, C., Eriksson Stenström, K., Jönsson, M., Mattsson, S., Pedehontaa-Hiaa, G., Rääf, C., Sundin, K., et al. *Assessment of "Zero Point" radiation around the ESS facility.* Report MA RADFYS 2018:01, Report BAR-2018/04. Lund University, Sweden. https://portal.research.lu.se/portal/sv/publications/assessment-of-zero-point-radiation-around-the-ess-facility(2153e07c-b465-4191-abc3-dbfcaf28b85b).html. 2018.
[22] IAEA. *Radioactive Particles in the Environment: Sources, Particle Characterization and Analytical Techniques.* IAEA-TECDOC-1663. INTERNATIONAL ATOMIC ENERGY AGENCY (IAEA), Vienna. https://www-pub.iaea.org/MTCD/Publications/PDF/TE_1663_web.pdf. 2011.
[23] Ramebäck, H., Söderström, C., Granström, M., Jonsson, S., Kastlander, J., Nylén, T., Ågren, G. *Measurements of ^{106}Ru in Sweden during the autumn 2017: Gamma-ray spectrometric measurements of air filters, precipitation and soil samples, and in situ gamma-ray spectrometry measurement.* Applied Radiation and Isotopes, 140: 179-184, 2018.
[24] Kastlander, J., Söderström, C. *Evaluation of an early warning system for airborne radionuclides.* Applied Radiation and Isotopes, 126: 228-231, 2017.
[25] Zhang, W., Bean, M., Benotto, M., Cheung, J., Ungar, K., Ahier, B. *Development of a new aerosol monitoring system and its application in Fukushima nuclear accident related aerosol radioactivity measurement at the CTBT radionuclide station in Sidney of Canada.* Journal of Environmental Radioactivity, 102(12): 1065-1069, 2011.
[26] Hou, X. *Liquid scintillation counting for determination of radionuclides in environmental and nuclear application.* Journal of Radioanalytical and Nuclear Chemistry, 318(3): 1597-1628, 2018.
[27] Horrocks, D.L. *A new method of quench monitoring in liquid scintillation counting: The H number concept.* Journal of Radioanalytical Chemistry, 43(2): 489-521, 1978.
[28] Tuniz, C., Kutschera, W., Fink, D., Herzog, G.F., Bird, J.R., *Accelerator mass spectrometry: ultrasensitive analysis for global science*. CRC press. 0-8493-4538-3, 1998.
[29] Douglas, M., Bernacki, B.E., Erchinger, J.L., Finn, E.C., Fuller, E.S., Hoppe, E.W., Keillor, M.E., et al. *Liquid scintillation counting of environmental radionuclides: a review of the impact of background reduction.* Journal of Radioanalytical and Nuclear Chemistry, 307(3): 2495-2504, 2016.
[30] Roos, P. *Analysis of radionuclides using ICP-MS*, in *Radioactivity in the Environment*, P.P. Povinec, Editor. 2008, Elsevier. p. 295-330.
[31] Becker, J.S. *Mass spectrometry of long-lived radionuclides.* Spectrochimica Acta Part B: Atomic Spectroscopy, 58(10): 1757-1784, 2003.
[32] Quemet, A., Ruas, A., Dalier, V., Rivier, C. *Americium isotope analysis by Thermal Ionization Mass Spectrometry using the total evaporation method.* International Journal of Mass Spectrometry, 431: 8-14, 2018.
[33] Erdmann, N., Passler, G., Trautmann, N., Wendt, K. *Resonance ionization mass spectrometry for trace analysis of long-lived*

radionuclides, in *Radioactivity in the Environment*, P.P. Povinec, Editor. 2008, Elsevier. p. 331-354.

[34] Qiao, J., Lagerkvist, P., Rodushkin, I., Salminen-Paatero, S., Roos, P., Lierhagen, S., Jensen, K.A., et al. *On the application of ICP-MS techniques for measuring uranium and plutonium: a Nordic inter-laboratory comparison exercise.* Journal of Radioanalytical and Nuclear Chemistry, 315(3): 565-580, 2018.

[35] Varga, Z., Surányi, G., Vajda, N., Stefánka, Z. *Determination of plutonium and americium in environmental samples by inductively coupled plasma sector field mass spectrometry and alpha spectrometry.* Microchemical journal, 85(1): 39-45, 2007.

[36] Harrison, J.J., Zawadzki, A., Chisari, R., Wong, H.K. *Separation and measurement of thorium, plutonium, americium, uranium and strontium in environmental matrices.* Journal of Environmental Radioactivity, 102(10): 896-900, 2011.

[37] Gonzalez, V., Vignati, D.A., Leyval, C., Giamberini, L. *Environmental fate and ecotoxicity of lanthanides: are they a uniform group beyond chemistry?* Environment international, 71: 148-157, 2014.

[38] Hatje, V., Bruland, K.W., Flegal, A.R. *Increases in anthropogenic gadolinium anomalies and rare earth element concentrations in San Francisco Bay over a 20 year record.* Environmental Science & Technology, 50(8): 4159-4168, 2016.

[39] Plausinaitis, D., Prokopchik, A., Karaliunas, A., Bohdan, L., Balashevska, Y. *Erbium concentration anomaly as an indicator of nuclear activity: Focus on Natural waters in the Chernobyl exclusion zone.* Science of The Total Environment, 621: 1626-1632, 2018.

[40] Hellborg, R., Skog, G., Stenström, K. *Accelerator Mass Spectrometry and its Applications.* digital Encyclopedia of Applied Physics: 503-534, 2003.

[41] Kutschera, W. *Accelerator mass spectrometry: state of the art and perspectives.* Advances in Physics: X, 1(4): 570-595, 2016.

[42] Persson, P., Kiisk, M., Erlandsson, B., Faarinen, M., Hellborg, R., Skog, G., Stenström, K. *Detection of ^{59}Ni at the Lund AMS facility.* Nuclear Instruments and Methods in Physics Research Section B: Beam Interactions with Materials and Atoms, 172(1–4): 188-192, 2000.

[43] Persson, P., Erlandsson, B., Freimann, K., Hellborg, R., Larsson, R., Persson, J., Skog, G., et al. *Determination of the detection limit of ^{59}Ni at the Lund AMS facility by using characteristic projectile X-rays.* Nuclear Instruments and Methods in Physics Research Section B: Beam Interactions with Materials and Atoms, 160(4): 510-514, 2000.

[44] Skog, G. *The single stage AMS machine at Lund University: Status report.* Nuclear Instruments and Methods in Physics Research Section B: Beam Interactions with Materials and Atoms, 259(1): 1-6, 2007.

[45] Skog, G., Rundgren, M., Sköld, P. *Status of the Single Stage AMS machine at Lund University after 4 years of operation.* Nuclear Instruments and Methods in Physics Research Section B: Beam Interactions with Materials and Atoms, 268(7-8): 895-897, 2010.

[46] Stenström, K., Skog, G., Nilsson, C.M., Hellborg, R., Leide-Svegborn, S., Georgiadou, E., Mattsson, S. *Local variations in ^{14}C – How is bomb-pulse dating of human tissues and cells affected?* Nuclear Instruments and Methods in Physics Research Section B: Beam Interactions with Materials and Atoms, 268(7–8): 1299-1302, 2010.

[47] Wacker, L., Němec, M., Bourquin, J. *A revolutionary graphitisation system: Fully automated, compact and simple.* Nuclear Instruments and

Methods in Physics Research Section B: Beam Interactions with Materials and Atoms, 268(7): 931-934, 2010.
[48] Adolphi, F., Muscheler, R., Friedrich, M., Güttler, D., Wacker, L., Talamo, S., Kromer, B. *Radiocarbon calibration uncertainties during the last deglaciation: Insights from new floating tree-ring chronologies.* Quaternary Science Reviews, 170: 98-108, 2017.
[49] Genberg, J., Stenström, K., Elfman, M., Olsson, M. *Development of graphitization of μg-sized samples at Lund University.* Radiocarbon, 52: 1270-1276, 2010.
[50] Genberg, J. *Source apportionment of carbonaceous aerosol. Measurement and model evaluation.* 978-91-7473-428-7. PhD thesis, Lund University, Sweden. 2013.
[51] Glasius, M., Hansen, A.M.K., Claeys, M., Henzing, J.S., Jedynska, A.D., Kasper-Giebl, A., Kistler, M., et al. *Composition and sources of carbonaceous aerosols in Northern Europe during winter.* Atmospheric Environment, 173: 127-141, 2018.
[52] Salazar, G., Zhang, Y., Agrios, K., Szidat, S. *Development of a method for fast and automatic radiocarbon measurement of aerosol samples by online coupling of an elemental analyzer with a MICADAS AMS.* Nuclear Instruments and Methods in Physics Research Section B: Beam Interactions with Materials and Atoms, 361: 163-167, 2015.
[53] Schumann, D., David, J.-C. *Cross sections and excitation functions for the production of long-lived radionuclides in nuclear reactions of lead and bismuth with protons.* Nuclear Data Sheets, 119: 288-291, 2014.
[54] Schumann, D., Neuhausen, J., Michel, R., Alfimov, V., Synal, H.-A., David, J.-C., Wallner, A. *Excitation functions for the production of long-lived residue nuclides in the reaction natBi (p; xn, yp) Z.* Journal of Physics G: Nuclear and Particle Physics, 38(6): 065103, 2011.
[55] Schumann, D., Michel, R., Korschinek, G., Knie, K., David, J.-C. *Excitation functions for the production of ^{60}Fe and ^{53}Mn in the reaction natPb (p, xp/yn) Z.* Nuclear Instruments and Methods in Physics Research Section A: Accelerators, Spectrometers, Detectors and Associated Equipment, 562(2): 1057-1059, 2006.
[56] Talip, Z., Dressler, R., David, J.C., Vockenhuber, C., Müller Gubler, E., Vögele, A., Strub, E., et al. *Radiochemical Determination of Long-Lived Radionuclides in Proton-Irradiated Heavy-Metal Targets: Part I - Tantalum.* Anal Chem, 89(24): 13541-13549, 2017.
[57] Talip, Z., Pfister, S., Dressler, R., David, J.C., Vögele, A., Vontobel, P., Michel, R., et al. *Analysis of the ^{148}Gd and ^{154}Dy Content in Proton-Irradiated Lead Targets.* Anal Chem, 89(12): 6861-6869, 2017.
[58] Baeza, A., Rodríguez-Perulero, A., Guillén, J. *Anthropogenic and naturally occurring radionuclide content in near surface air in Cáceres (Spain).* Journal of Environmental Radioactivity, 165: 24-31, 2016.
[59] Pöllänen, R., Siiskonen, T. *High-resolution alpha spectrometry under field conditions – fast identification of alpha particle emitting radionuclides from air samples.* Journal of Environmental Radioactivity, 87(3): 279-288, 2006.
[60] Pöllänen, R., Peräjärvi, K., Siiskonen, T., Turunen, J. *High-resolution alpha spectrometry at ambient air pressure—Towards new applications.* Nuclear Instruments and Methods in Physics Research Section A: Accelerators, Spectrometers, Detectors and Associated Equipment, 694: 173-178, 2012.
[61] Pöllänen, R. *Performance of an in-situ alpha spectrometer.* Applied Radiation and Isotopes, 109: 193-197, 2016.

[62] Geryes, T., Monsanglant-Louvet, C., Gehin, E. *Experimental and simulation methods to evaluate the alpha self-absorption factors for radioactive aerosol fiber filters.* Radiation Measurements, 44(9): 763-765, 2009.
[63] Pripachkin, D.A., Aron, D.V., Budyka, A.K., Khusein, Y.N. *Collimator Effect on Semiconductor α-Spectrometer Characteristics in Measurements of Radioactive Aerosols.* Atomic Energy, 125(2): 119-123, 2018.
[64] Artisyuk, V., Saito, M., Stankovskii, A., Korovin, Y., Shmelev, A. *Radiological hazard of long-lived spallation products in accelerator-driven system.* Progress in Nuclear Energy, 40(3-4): 637-645, 2002.
[65] Kelley, K., Hertel, N., Pitcher, E., Devlin, M., Mashnik, S. *^{148}Gd production cross section measurements for 600-and 800-MeV protons on tantalum, tungsten, and gold.* Nuclear Physics A, 760(3-4): 225-233, 2005.
[66] Hammer, B., Neuhausen, J.r., Boutellier, V., Wohlmuther, M., Türler, A., Schumann, D. *Radiochemical Determination of Rare Earth Elements in Proton-Irradiated Lead–Bismuth Eutectic.* Anal Chem, 87(11): 5656-5663, 2015.
[67] Lee, M., Park, J.-H., Song, K. *Determination of plutonium, uranium and americium/curium isotopes in environmental samples with anion exchange, UTEVA, Sr and DGA resin.* Proceedings in Radiochemistry A Supplement to Radiochimica Acta, 1(1): 189-194, 2011.
[68] Desideri, D., Cantaluppi, C., Ceccotto, F., Meli, M.A., Roselli, C., Feduzi, L. *Radiochemical Characterization of Algae Products Commercialized for Human Consumption.* Health Physics, 111(3): 256-264, 2016.
[69] Szufa, K.M., Mietelski, J.W., Anczkiewicz, R., Sala, D., Olech, M.A. *Variations of plutonium isotopic ratios in Antarctic ecosystems.* Journal of Radioanalytical and Nuclear Chemistry, 318(3): 1511-1518, 2018.
[70] Greenberg, R.R., Bode, P., Fernandes, E.A.D.N. *Neutron activation analysis: a primary method of measurement.* Spectrochimica Acta Part B: Atomic Spectroscopy, 66(3-4): 193-241, 2011.
[71] Hou, X. *Activation analysis for the determination of long-lived radionuclides*, in *Radioactivity in the Environment*, P.P. Povinec, Editor. 2008, Elsevier. p. 371-405.
[72] Rääf, C., Almén, A., Sundin, K., Johansson, L., Eriksson Stenström, K. *In-vivo measurement of pre-operational spallation source workers: Baseline body burden levels and detection limits of relevant gamma emitters using high-resolution gamma spectroemtry.* Journal of Radiological Protection, Submitted, 2019.
[73] Titarenko, Y.E., Batyaev, V., Titarenko, A.Y., Butko, M., Pavlov, K., Florya, S., Tikhonov, R., et al. *Measurement and Simulation of the Cross Sections for the Production of ^{148}Gd in thin natW and ^{181}Ta Targets Irradiated with 0.4- to 2.6-GeV Protons.* Physics of Atomic Nuclei, 74(4): 573-579, 2011.
[74] Pöllänen, R., Peräjärvi, K., Siiskonen, T., Turunen, J. *In-situ alpha spectrometry from air filters at ambient air pressure.* Radiation Measurements, 53: 65-70, 2013.
[75] Oliveira, J., Carvalho, F. *Sequential extraction procedure for determination of uranium, thorium, radium, lead and polonium radionuclides by alpha spectrometry in environmental samples.* Czechoslovak Journal of Physics, 56(1): D545, 2006.
[76] Murray, A., Marten, R., Johnston, A., Martin, P. *Analysis for naturally occuring radionuclides at environmental concentrations by gamma*

spectrometry. Journal of Radioanalytical and Nuclear Chemistry, 115(2): 263-288, 1987.

[77] Bungau, C., Bungau, A., Cywinski, R., Barlow, R., Edgecock, T.R., Carlsson, P., Danared, H., et al. *Induced activation in accelerator components.* Phys. Rev. ST Accel. Beams, 17: 084701-084701, 2014.

[78] IAEA. *A Procedure for the Sequential Determination of Radionuclides in Environmental Samples. Liquid Scintillation Counting and Alpha Spectrometry for ^{90}Sr, ^{241}Am and Pu Radioisotopes.* IAEA Analytical Quality in Nuclear Applications Series No. 37. IAEA/AQ/37. 2014.

[79] Yamato, A. *An anion exchange method for the determination of ^{241}Am and plutonium in environmental and biological samples.* Journal of Radioanalytical Chemistry, 75(1-2): 265-273, 1982.

[80] Stricklin, D., Tjärnhage, Å., Nygren, U. *Application of low energy gamma-spectrometry in rapid actinide analysis for emergency preparedness.* Journal of Radioanalytical and Nuclear Chemistry, 251(1): 69-74, 2002.

[81] Agarande, M., Benzoubir, S., Bouisset, P., Calmet, D. *Determination of ^{241}Am in sediments by isotope dilution high resolution inductively coupled plasma mass spectrometry (ID HR ICP-MS).* Applied Radiation and Isotopes, 55(2): 161-165, 2001.

[82] Wang, J.-J., Chen, J., Chiu, J.-H. *Sequential isotopic determination of plutonium, thorium, americium, strontium and uranium in environmental and bioassay samples.* Applied Radiation and Isotopes, 61(2-3): 299-305, 2004.

[83] Truscott, J.B., Jones, P., Fairman, B.E., Evans, E.H. *Determination of actinide elements at femtogram per gram levels in environmental samples by on-line solid phase extraction and sector-field-inductively coupled plasma-mass spectrometry.* Analytica Chimica Acta, 433(2): 245-253, 2001.

[84] Vichot, L., Boyer, C., Boissieux, T., Losset, Y., Pierrat, D. *Organically bound tritium (OBT) for various plants in the vicinity of a continuous atmospheric tritium release.* Journal of Environmental Radioactivity, 99(10): 1636-1643, 2008.

[85] Hou, X. *Analysis of urine for pure beta emitters: methods and application.* Health Physics, 101(2): 159-169, 2011.

[86] Ducros, L., Eyrolle, F., Vedova, C.D., Charmasson, S., Leblanc, M., Mayer, A., Babic, M., et al. *Tritium in river waters from French Mediterranean catchments: Background levels and variability.* Science of The Total Environment, 612(Supplement C): 672-682, 2018.

[87] Dibb, J.E., Meeker, L.D., Finkel, R.C., Southon, J.R., Caffee, M.W., Barrie, L.A. *Estimation of stratospheric input to the Arctic troposphere: ^{7}Be and ^{10}Be in aerosols at Alert, Canada.* Journal of Geophysical Research: Atmospheres, 99(D6): 12855-12864, 1994.

[88] Padilla, S., López-Gutiérrez, J., Manjón, G., García-Tenorio, R., Galván, J., García-León, M. *Meteoric ^{10}Be in aerosol filters in the city of Seville.* Journal of Environmental Radioactivity, 196: 15-21, 2019.

[89] Chen, M., Yang, Z., Zhang, L., Qiu, Y., Ma, Q., Huang, Y. *Determination of cosmogenic ^{32}P and ^{33}P in environmental samples.* Acta Oceanologica Sinica, 32(6): 18-25, 2013.

[90] Deinhart, A., Bibby, R., Roberts, S., Tompson, A., Esser, B. *The Analysis of Sulfur-35 as a Young Groundwater Tracer at E-Tunnel, Rainier Mesa, Nevada National Security Site.* Lawrence Livermore National Lab.(LLNL), Livermore, CA (United States). 2017.

[91] Lin, M., Thiemens, M., Shaheen, R., Biglari, S., Crocker, D., Zhang, Z., Tao, J., et al. *Cosmogenic ^{35}S as a Novel Detector of Stratospheric Air*

at the Earth's Surface: Key Findings from the Western United States and New Insights into the Seasonal Variations of Ozone and Sulfate in East Asia.

[92] Hong, Y.-L., Kim, G. *Measurement of cosmogenic ^{35}S activity in rainwater and lake water.* Anal Chem, 77(10): 3390-3393, 2005.

[93] Zulauf, A., Happel, S., Mokili, M., Bombard, A., Jungclas, H. *Characterization of an extraction chromatographic resin for the separation and determination of ^{36}Cl and ^{129}I.* Journal of Radioanalytical and Nuclear Chemistry, 286(2): 539-546, 2010.

[94] Tolmachyov, S., Ura, S., Momoshima, N., Yamamoto, N., Maeda, Y. *Determination of ^{36}Cl by liquid scintillation counting from soil collected at the Semipalatinsk Nuclear Test Site.* Journal of Radioanalytical and Nuclear Chemistry, 249(3): 541-545, 2001.

[95] Videla, X., Rojas-Silva, X., Nario, A., Arias, M.I., Bonomelli, C. *Calcination Method of ^{45}Ca Samples for Isotope Ratio Analysis via Liquid Scintillation.* Communications in soil science and plant analysis, 50(4): 412-420, 2019.

[96] Song, L., Ma, L., Ma, Y., Yang, Y., Dai, X. *Method for sequential determination of ^{55}Fe and ^{63}Ni in leaching solution from cement solidification.* Journal of Radioanalytical and Nuclear Chemistry, 319(3): 1227-1234, 2019.

[97] Huang, F.-Y.J., Su, T.-Y., Tsai, T.-L., Chao, J.-H. *Analysis of ^{63}Ni in radwastes by extraction chromatography and radiometric techniques.* Journal of Radioanalytical and Nuclear Chemistry, 314(2): 879-886, 2017.

[98] Hou, X., Togneri, L., Olsson, M., Englund, S., Gottfridsson, O., Forsstrom, M., Hirvonen, H. *Standardization of radioanalytical methods for determination of ^{63}Ni and ^{55}Fe in waste and environmental samples, .* NKS-356, Nordic Nuclear Safty Research. 2015.

[99] Gudelis, A., Druteikienė, R., Lukšienė, B., Gvozdaitė, R., Nielsen, S.P., Hou, X., Mažeika, J., et al. *Assessing deposition levels of ^{55}Fe, ^{60}Co and ^{63}Ni in the Ignalina NPP environment.* Journal of Environmental Radioactivity, 101(6): 464-467, 2010.

[100] Grahek, Ž., Karanović, G., Nodilo, M. *Rapid determination of $^{89,90}Sr$ in wide range of activity concentration by combination of yttrium, strontium separation and Cherenkov counting.* Journal of Radioanalytical and Nuclear Chemistry, 292(2): 555-569, 2011.

[101] Casacuberta, N., Masqué, P., Garcia-Orellana, J., García-Tenorio, R., Buesseler, K.O. *Sr-90 and Sr-89 in seawater off Japan as a consequence of the Fukushima Dai-ichi nuclear accident.* Biogeosciences, 10(6): 3649-3659, 2013.

[102] Olfert, J.M., Dai, X., Kramer-Tremblay, S. *Rapid determination of $^{90}Sr/^{90}Y$ in water samples by liquid scintillation and Cherenkov counting.* Journal of Radioanalytical and Nuclear Chemistry, 300(1): 263-267, 2014.

[103] Betti, M., Giannarelli, S., Hiernaut, T., Rasmussen, G., Koch, L. *Detection of trace radioisotopes in soil, sediment and vegetation by glow discharge mass spectrometry.* Fresenius' journal of analytical chemistry, 355(5-6): 642-646, 1996.

[104] Guérin, N., Gagné, A., Kramer-Tremblay, S. *A rapid method for the routine monitoring of ^{99}Tc by liquid scintillation counting.* Journal of Radioanalytical and Nuclear Chemistry, 314(3): 2009-2017, 2017.

[105] Lindahl, P., Ellmark, C., Gäfvert, T., Mattsson, S., Roos, P., Holm, E., Erlandsson, B. *Long-term study of ^{99}Tc in the marine environment on*

the Swedish west coast. Journal of Environmental Radioactivity, 67(2): 145-156, 2003.

[106] Jakab, D., Endrődi, G., Kocsonya, A., Pántya, A., Pázmándi, T., Zagyvai, P. *Methods, results and dose consequences of ^{106}Ru detection in the environment in Budapest, Hungary.* Journal of Environmental Radioactivity, 192: 543-550, 2018.

[107] Gómez-Guzmán, J., Holm, E., Enamorado-Báez, S., Abril, J., Pinto-Gómez, A., López-Gutiérrez, J., García-León, M. *Pre-and post-Chernobyl accident levels of ^{129}I and ^{137}Cs in the Southern Baltic Sea by brown seaweed Fucus vesiculosus.* Journal of Environmental Radioactivity, 115: 134-142, 2013.

[108] Remenec, B., Dulanská, S., Horváthová, B., Mátel, Ľ. *Determination of ^{129}I using volatilization method and liquid scintillation spectrometry.* Journal of Radioanalytical and Nuclear Chemistry, 311(3): 1649-1655, 2017.

[109] Tsukada, H., Ishida, J., Narita, O. *Particle-size distributions of atmospheric ^{129}I and ^{127}I aerosols.* Atmospheric Environment. Part A. General Topics, 25(5-6): 905-908, 1991.

[110] Englund, E., Aldahan, A., Hou, X., Possnert, G., Söderström, C. *Iodine (^{129}I and ^{127}I) in aerosols from northern Europe.* Nuclear Instruments and Methods in Physics Research Section B: Beam Interactions with Materials and Atoms, 268(7-8): 1139-1141, 2010.

[111] Jabbar, T., Wallner, G., Steier, P. *A review on ^{129}I analysis in air.* Journal of Environmental Radioactivity, 126: 45-54, 2013.

[112] Parry, S., Bennett, B., Benzing, R., Lally, A., Birch, C., Fulker, M. *The determination of ^{129}I in milk and vegetation using neutron activation analysis.* Science of The Total Environment, 173: 351-360, 1995.

[113] Waser, N., Bacon, M. *Cosmic ray produced ^{32}P and ^{33}P in Cl, S and K at mountain altitude and calculation of oceanic production rates.* Geophysical research letters, 21(11): 991-994, 1994.

[114] Benitez-Nelson, C.R., Buesseler, K.O. *Measurement of cosmogenic ^{32}P and ^{33}P activities in rainwater and seawater.* Anal Chem, 70(1): 64-72, 1998.

[115] Challeton-de Vathaire, C., Crescini, D., Remenieras, J., Biau, A., Dubuquoy, E., Cassagnou, H., Bourguignon, M., et al. *Monitoring of workers occupationally exposed to radionuclides in France: results from February to August 1997 in the non nuclear energy field.* Radiation protection dosimetry, 79(1-4): 145-148, 1998.

[116] Mark, D., Barfod, D., Stuart, F., Imlach, J. *The ARGUS multicollector noble gas mass spectrometer: Performance for ^{40}Ar/^{39}Ar geochronology.* Geochemistry, Geophysics, Geosystems, 10(10), 2009.

[117] Collon, P., Bichler, M., Caggiano, J., DeWayne Cecil, L., El Masri, Y., Golser, R., Jiang, C.L., et al. *Development of an AMS method to study oceanic circulation characteristics using cosmogenic ^{39}Ar.* Nuclear Instruments and Methods in Physics Research Section B: Beam Interactions with Materials and Atoms, 223-224: 428-434, 2004.

[118] Treacy, D.J., Knies, D.L., Grabowski, K.S., Hubler, G.K., DeTurck, T.M., Mignerey, A.C. *Determination of ^{32}Si by AMS at the US Naval Research Laboratory.* Nuclear Instruments and Methods in Physics Research Section B: Beam Interactions with Materials and Atoms, 172(1): 321-327, 2000.

[119] Ayranov, M., Schumann, D. *Preparation of ^{26}Al, ^{59}Ni, ^{44}Ti, ^{53}Mn and ^{60}Fe from a proton irradiated copper beam dump.* Journal of Radioanalytical and Nuclear Chemistry, 286(3): 649-654, 2010.

[120] Knie, K., Korschinek, G., Faestermann, T., Wallner, C., Scholten, J., Hillebrandt, W. *Indication for supernova produced ^{60}Fe activity on Earth.* Physical Review Letters, 83(1): 18, 1999.
[121] Aguerre, S., Frechou, C. *Development of a radiochemical separation for selenium with the aim of measuring its isotope 79 in low and intermediate nuclear wastes by ICP-MS.* Talanta, 69(3): 565-571, 2006.
[122] Dewberry, R.A., Leyba, J.D., Boyce, W.T. *Observation and Measurement of 79Se in Savannah River Site High Level Waste Tank Fission Product Waste.* Journal of Radioanalytical and Nuclear Chemistry, 245(3): 491-500, 2000.
[123] Huang, Y.-J., Guo, G.-Y., Chen, C.-F., Yang, L.-T., Shang-Guan, Z.-H., Sha, X.-D., Yao, J.-L., et al. *Automated separation and analysis of krypton-85 from low-volume gaseous effluent of nuclear power plant.* Journal of Radioanalytical and Nuclear Chemistry: 1-10, 2019.
[124] Tertyshnik, E., Ivanov, V., Abduragimov, E. *Measurement of Krypton-85 in samples of atmospheric with Quantulus 1220 device without using a liquid scintillator.* arXiv preprint arXiv:1510.03151, 2015.
[125] Schlosser, C., Bollhöfer, A., Schmid, S., Krais, R., Bieringer, J., Konrad, M. *Analysis of radioxenon and Krypton-85 at the BfS noble gas laboratory.* Applied Radiation and Isotopes, 126: 16-19, 2017.
[126] Tomasz, P., Katarzyna, C., Małgorzata, D., Jakub, O., Zbigniew, H. *Assessment of occupational internal exposure to beta emitters from the nuclear reactor primary coolant circuit.* Polish Journal of Medical Physics and Engineering, 18(2): 41-47, 2012.
[127] Dion, M.P., Eiden, G.C., Farmer, O.T., Finch, Z., Liezers, M., Thomas, M.-L. *Quantification techniques of mass-separation and ion yield for the detection of radioactive isotopes.* Journal of Radioanalytical and Nuclear Chemistry, 319(3): 937-944, 2019.
[128] Cassette, P., Chartier, F., Isnard, H., Fréchou, C., Laszak, I., Degros, J.P., Bé, M.M., et al. *Determination of 93Zr decay scheme and half-life.* Applied Radiation and Isotopes, 68(1): 122-130, 2010.
[129] Oliveira, T., Monteiro, R., Oliveira, A. *A selective separation method for ^{93}Zr in radiochemical analysis of low and intermediate level wastes from nuclear power plants.* Journal of Radioanalytical and Nuclear Chemistry, 289(2): 497-501, 2011.
[130] Deneva, B. *Development of accelerator mass spectrometry for ^{93}Zr.* Maier-Leibnitz Laboratorium in Garching, Technische Universitat at Munchen, Deutschland, 2015.
[131] Asai, S., Yomogida, T., Saeki, M., Ohba, H., Hanzawa, Y., Horita, T., Kitatsuji, Y. *Determination of 107Pd in Pd Recovered by Laser-Induced Photoreduction with Inductively Coupled Plasma Mass Spectrometry.* Analytical Chemistry, 88(24): 12227-12233, 2016.
[132] Korschinek, G., Faestermann, T., Kastel, S., Knie, K., Maier, H., Fernandez-Niello, J., Rothenberger, M., et al. *AMS for M> 36 with a gas-filled magnetic spectrograph.* Nuclear Instruments and Methods in Physics Research Section B: Beam Interactions with Materials and Atoms, 92(1-4): 146-152, 1994.
[133] Broderick, K., Lusk, R., Hinderer, J., Griswold, J., Boll, R., Garland, M., Heilbronn, L., et al. *Reactor production of promethium-147.* Applied Radiation and Isotopes, 144: 54-63, 2019.
[134] Sumiya, S., Hayashi, N., Katagiri, H., Narita, O. *A radioanalytical method for samarium-151 and promethium-147 in environmental samples.* Science of The Total Environment, 130: 305-315, 1993.

[135] Bé, M.-M., Isnard, H., Cassette, P., Mougeot, X., Lourenço, V., Altzitzoglou, T., Pommé, S., et al. *Determination of the 151Sm half-life*, in *Radiochimica Acta*. Report, p. 619,2015.
[136] Jiang, J., Davies, A., Arrigo, L., Friese, J., Seiner, B.N., Greenwood, L., Finch, Z. *Analysis of 161Tb by radiochemical separation and liquid scintillation counting.* Applied Radiation and Isotopes, 2015.
[137] Chakravarty, R., Chakraborty, S., Chirayil, V., Dash, A. *Reactor production and electrochemical purification of 169Er: A potential step forward for its utilization in in vivo therapeutic applications.* Nuclear Medicine and Biology, 41(2): 163-170, 2014.
[138] Schock, H. *Comparison of a coaxial Ge (Li) and a planar Ge detector in instrumental neutron activation analysis of geologic materials.* Journal of Radioanalytical and Nuclear Chemistry, 36(2): 557-564, 1977.
[139] Laul, J.C., Nielson, K.K., Wogman, N.A. *Trace rare earth analysis by neutron activation and γ-ray/x-ray spectrometry.* CONF-771072--. United States. http://inis.iaea.org/search/search.aspx?orig_q=RN:10447740. 1977.
[140] Thomasson, W.N., Bolch, W.E., Gamble, J. *Uptake and Translocation of ^{134}Cs, ^{59}Fe, ^{85}Sr and ^{185}W by Banana Plants and a Coconut Plant Following Foliar Application.* BioScience, 19(7): 613-615, 1969.
[141] ESS. *Assessment of environmental consequences of the normal operations of ESS facility. Part #1 Input data Source Term. Breakdown of radionuclides & Related basic information.* ESS-0028551. 2016.
[142] Ene, D. *Envronmental and radiological impacts of the activated air inside the tunnel of ESS accelerator.* ESS-0018010. 2015.
[143] Nilsson, P. *Tungsten Oxidation and AeroSol Transport (TOAST).* ESS-0151001. 2018.
[144] Papastefanou, C. *Radioactive aerosol analysis*, in *Handbook of Radioactivity Analysis*. 2012, Elsevier. p. 727-767.
[145] Irlweck, K., Khademi, B., Henrich, E., Kronraff, R. *$^{239\,(240)}Pu$, ^{238}Pu, ^{90}Sr, ^{103}Ru and ^{137}Cs concentrations in surface air in Austria due to dispersion of Chernobyl releases over Europe.* Journal of Environmental Radioactivity, 20(2): 133-148, 1993.
[146] Genberg, J., Hyder, M., Stenström, K., Bergström, R., Simpson, D., Fors, E.O., Jönsson, J.Å., et al. *Source apportionment of carbonaceous aerosol in southern Sweden.* Atmos. Chem. Phys., 11(22): 11387-11400, 2011.
[147] Martinsson, J., Abdul Azeem, H., Sporre, M.K., Bergström, R., Ahlberg, E., Öström, E., Kristensson, A., et al. *Carbonaceous aerosol source apportionment using the Aethalometer model – evaluation by radiocarbon and levoglucosan analysis at a rural background site in southern Sweden.* Atmos. Chem. Phys., 17(6): 4265-4281, 2017.
[148] Yttri, K.E., Simpson, D., Nøjgaard, J.K., Kristensen, K., Genberg, J., Stenström, K., Swietlicki, E., et al. *Source apportionment of the summer time carbonaceous aerosol at Nordic rural background sites.* Atmos. Chem. Phys., 11(24): 13339-13357, 2011.
[149] Gilardoni, S., Vignati, E., Cavalli, F., Putaud, J.P., Larsen, B.R., Karl, M., Stenström, K., et al. *Better constraints on sources of carbonaceous aerosols using a combined ^{14}C – macro tracer analysis in a European rural background site.* Atmospheric Chemistry and Physics, 11(12): 5685-5700, 2011.
[150] Larsen, B.R., Gilardoni, S., Stenström, K., Niedzialek, J., Jimenez, J., Belis, C.A. *Sources for PM air pollution in the Po Plain, Italy: II. Probabilistic uncertainty characterization and sensitivity analysis of*

secondary and primary sources. Atmospheric Environment, 50(0): 203-213, 2012.
[151] Flury, T., Völkle, H. *Monitoring of air radioactivity at the Jungfraujoch research station: Test of a new high volume aerosol sampler.* Science of The Total Environment, 391(2-3): 284-287, 2008.
[152] DIGITEL. Accessed: 28 August 2019. Available from: http://www.digitel-ag.com/de/en/products/high-volume-sampler-en/dha-80/.
[153] DIGITEL. *DIGITEL High Volume Aerosol Sampler. Manual, versions Hxx.52.* Report,April 2014.
[154] Goliath, M., Kastlander, J., Meister, M., Olsson, H., Söderström, C. *Radionuclide particles in ground level air in Sweden during 2017.* FOI-R--4621--SE. 2018.
[155] Martinsson, J., Andersson, A., Sporre, M.K., Friberg, J., Kristensson, A., Swietlicki, E., Olsson, P.-A., et al. *Evaluation of $d^{13}C$ in Carbonaceous Aerosol Source Apportionment at a Rural Measurement Site.* Aerosol and Air Quality Research, 17(8): 2081-2094, 2017.
[156] Martinsson, J., Monteil, G., Sporre, M.K., Kaldal Hansen, A.M., Kristensson, A., Eriksson Stenström, K., Swietlicki, E., et al. *Exploring sources of biogenic secondary organic aerosol compounds using chemical analysis and the FLEXPART model.* Atmospheric Chemistry and Physics, 17(18): 11025-11040, 2017.
[157] Malmö stad. *Källbestämning och mätning av sot i gatumiljö, Dalaplan 2015-2016.* https://malmo.se/download/18.3c0b3b6f15965118c0e2a602/1491305560083/Sot+p%C3%A5+Dalaplan+2015-1016.pdf. 2016.
[158] Ene, D., Andersson, K., Jensen, M., Nielsen, S., Severin, G. *Management of Tritium in European Spallation Source.* Fusion Science and Technology, 67(2): 324-327, 2015.
[159] Ene, D., ESHRAQI, M., LINDROOS, M., HAHN, H., BRANDIN, M., PEGGS, S. *Radiation Protection Studies for ESS Superconducting Linear Accelerator.* Prog. Nucl. Sci. Tech., 2: 382-388, 2011.
[160] UNSCEAR. United Nations Scientific COmmittee on Effects of Atomic Radiation, New York. *Sources and effects of ionizing radiation, Report to the General Assembly with scientific annexes Vol I*. 2000.
[161] UNSCEAR. United Nations. *Sources, effects and risks of ionizing radiation. UNSCEAR 2016. Report to the General Assemply, with Scientific Annexes. Annex C. Biological effects of selected internal emitters - tritium*. 2016.
[162] Eyrolle, F., Ducros, L., Le Dizès, S., Beaugelin-Seiller, K., Charmasson, S., Boyer, P., Cossonnet, C. *An updated review on tritium in the environment.* Journal of Environmental Radioactivity, 181(Supplement C): 128-137, 2018.
[163] IAEA/WMO. *Global Network of Isotopes in Precipitation. The GNIP Database. Accessible at: https://nucleus.iaea.org/wiser*. Accessed: 2019-09-23.
[164] *Isotope tracers in catchment hydrology*. Elsevier BV. 978-0-444-50155-X, 1998.
[165] International Atomic Energy Agency (IAEA). International Atomic Energy Agency. *Management of waste containing tritium and carbon-14. Technical report series no 421*. 2004.
[166] Fiévet, B., Pommier, J., Voiseux, C., Bailly du Bois, P., Laguionie, P., Cossonnet, C., Solier, L. *Transfer of tritium released into the marine environment by French nuclear facilities bordering the English*

channel. Environmental Science & Technology, 47(12): 6696-6703, 2013.
[167] Eyrolle-Boyer, F., Antonelli, C., Renaud, P., Tournieux, D. *Origins and trend of radionuclides within the lower Rhône River over the last decades.* Radioprotection, 50(1): 27-34, 2015.
[168] Brunner, P., Schneider, P., Scheicher, H., Seyerl, G., Kurnik, P., Ennemoser, O., Ambach, W. *Tritium intake by exposure to plastic case watches.* Health Physics, 70(4): 484-487, 1996.
[169] Kakiuchi, H., Akata, N., Hasegawa, H., Ueda, S., Tokonami, S., Yamada, M., Hosoda, M., et al. *Concentration of ^{3}H in plants around Fukushima Dai-ichi nuclear power station.* Scientific Reports, 2: 947, 2012.
[170] SSM. *Miljödatabasen/Dricksvatten*. Accessed: 2019-09-18. Available from: https://www.stralsakerhetsmyndigheten.se/omraden/miljoovervakning/sokbara-miljodata/miljodatabasen/dricksvatten/.
[171] SSM. *Miljödatabasen/Havsvatten*. Accessed: 2019-09-18. Available from: https://www.stralsakerhetsmyndigheten.se/omraden/miljoovervakning/sokbara-miljodata/miljodatabasen/havsvatten/.
[172] Åkesson, M., Suckow, A., Visser, A., Sültenfuβ, J., Laier, T., Purtschert, R., Sparrenbom, C.J. *Constraining age distributions of groundwater from public supply wells in diverse hydrogeological settings in Scania, Sweden.* Journal of Hydrology, 528: 217-229, 2015.
[173] IAEA/GNIP. *IAEA/GNIP precipitation sampling guide*. Accessed: Available from: http://www-naweb.iaea.org/napc/ih/documents/other/gnip_manual_v2.02_en_hq.pdf.
[174] SHMI. *SMHI Open Data*. Accessed: Available from: https://www.smhi.se/data/oppna-data.
[175] Ingraham, N.L. *Isotope variations in precipitation*, in *Isotope tracers in catchment hydrology*, C. Kendall and J.F. McDonnell, Editors. 1998, Elsevier BV.
[176] Kortelainen, N.M., Karhu, J.A. *Regional and seasonal trends in the oxygen and hydrogen isotope ratios of Finnish groundwaters: a key for mean annual precipitation.* Journal of Hydrology, 285(1): 143-157, 2004.
[177] VA Syd. *Var kommer ditt drickvatten ifrån?* Accessed: 2019-09-20. Available from: https://www.vasyd.se/Artiklar/Dricksvatten/Var-kommer-dricksvattnet-fran.
[178] Dizman, S., Yilmaz, A., Keser, R. *Determination of tritium concentrations in humans before the development of a nuclear power plant in Turkey.* Isotopes in Environmental and Health Studies, 51(3): 478-484, 2015.
[179] Yoon, S., Ha, W.-H., Lee, S.-S. *Tritium analysis of urine samples from the general Korean public.* Applied Radiation and Isotopes, 81: 276-278, 2013.
[180] Puhakainen, M., Heikkinen, T. *Tritium in the urine in Finnish people.* Radiation protection dosimetry, 128(2): 254-257, 2008.
[181] Pietrzak-Flis, Z., Nidecka, J., Radwan, I. *Estimation of dose to man from environmental tritium based on tritium analysis of hair and urine.* Assessment of Radioactive Contamination in Man, 1984.
[182] Schönhofer, F., Pock, K. *Incorporation of tritium from wrist watches.* Journal of Radioanalytical and Nuclear Chemistry, 197(1): 195-202, 1995.

[183] Klockmaster B. Larssons Klockor. Personal communication. Lund, Sweden. 2019.
[184] Pedehontaa-Hiaa, G., Holstein, H., Mattsson, S., Rääf, C., Eriksson Stenström, K. *Tritium in urine from members of the general public and occupationally exposed workers in Lund, Sweden, prior to operation of the European Spallation Source.* Journal of Environmental Radioactivity, 213: 1-7, 2020.
[185] Balonov, M., Likhtarev, I., Moskalev, I.Y. *The metabolism of ^{3}H compounds and limits for intakes by workers.* Health Physics, 47(5): 761-773, 1984.
[186] Vesanen, R., Mattsson, S. *Tritium in urine from laboratory personnel.* Report GU-RADFYS 85:02 (in Swedish). Department of Radiation Physics, University of Gothenburg, Sahlgrenska Univ Hospital, SE-413 45 Gothenburg, Sweden. 1985.
[187] Mattsson, S. *Internal contamination of hospital staff.* Report MAS-RADFYS 85:08 (in Swedish). Medical radiation physics Malmö, Lund University, SUS Malmö, SE-205 02 Malmö, Sweden. 1985.
[188] VA Syd. *Bulltofta vattenverk*. Accessed: 2019-09-20. Available from: https://www.vasyd.se/Artiklar/Dricksvatten/Bulltofta-vattenverk.
[189] ICRP. *Occupational Intakes of Radionuclides: Part 2.* ICRP Publication, 134, vol. 45, 3-4 vols, 2016.
[190] ICRP. *Compendium of Dose Coefficients based on ICRP Publication 60.* ICRP Publication, 119, vol 41 (Suppl.), 2012.
[191] Feng, B., Chen, B., Zhuo, W., Zhang, W. *A new passive sampler for collecting atmospheric tritiated water vapor.* Atmospheric Environment, 154: 308-317, 2017.

Appendix 1. Review of radionuclides in ESS

Department of Physics
Division of Nuclear Physics
The Biospheric and Anthropogenic Radioactivity (BAR) group

Review of radionuclides in ESS

Vytenis Barkauskas Vytenis.Barkauskas@nuclear.lu.se

Department of Physics
Division of Nuclear Physics
Professorsgatan 1
SE-223 63 Lund, SWEDEN

Report BAR-2019/02

Lund 2019

Content

1. Introduction

1.1. Purpose

The purpose of this report is to review which radionuclides are expected to be produced in and potentially released from the European Spallation Source (ESS) facility, according to the project financed by Swedish Radiation Safety Authority (SSM) “Kompetensutveckling vid Lunds universitet för mätning av ESS-specifika radionuklider”. This is Part 1a report, which includes available literature and data review. The available data was gathered from scientific publications as well as from some ESS reports on radionuclides which may potentially be produced in ESS during operation. This information is based on both modeling and experimental analysis. The list of long-lived radionuclides is given in Appendix A. Only qualitative analysis was performed, the concentrations of radionuclides were not evaluated. The effective dose coefficients of radionuclides were gathered in order to have the possibility to sort radionuclides according to their radiotoxicity. The information provided in this report will be used as a basis for identifying the most important and the most significant radionuclides from a radiation protection point of view. As other tasks of this project are related to identification and development of measurement methods of the most important radionuclides, this report is an integral part of justification of such a list of radionuclides.

1.2. The ESS facility

The European Spallation Source (ESS) is a state-of-the-art neutron source being built in Lund, Sweden [1, 2]. A view of the construction site in September 2018 is given in Fig. 1. As of November 2018, the initial operation of the linear accelerator is planned for 2019, start of instrument commissioning is foreseen in 2022 and the start of a scientific user programme in 2023 [3]. This large-scale user facility will be used for studies of the structure and dynamics of the materials using neutrons. Neutron scattering is a well-developed and extensively used method to investigate the fundamental properties of the materials in the field of physics, chemistry, biology, medicine and geology [4-7]. Until the end of the twentieth century neutron scattering experiments were mainly practiced with a continuous flux of neutrons from nuclear reactors. ESS will offer neutron beams of extremely high brightness for cold (0-5 meV energy) neutrons delivering more neutrons than the world’s most powerful reactor-based neutron sources today, and with higher peak intensity than any other spallation source.

The basic layout of the ESS facility consists of a linear accelerator which delivers proton pulses of 2.86 ms at 14 Hz onto a tungsten target where fast neutrons are produced via spallation reactions [8]. The fast neutrons will be moderated to thermal and cold energies using liquid parahydrogen [9]. These thermal (20-100 meV energy) and cold neutrons will be transported to the beamlines where they will be mainly used for neutron scattering experiments.

Figure 1. ESS construction site on September, 2018 [10].

The worldwide experience from operation of spallation sources is very limited. The main information about operating spallation sources world-wide is given in Table 1. An inevitable side effect of the neutron generation is the production of various radionuclides, resulting from spallation in the proton accelerator and target, as well as from neutron activation of surrounding structures, soil and air. Radionuclides formed in the ESS may be released to the environment during operation and/or accidents. The variety of radionuclides covers α, β and γ-emitting long- and short-lived radionuclides. The main aim of this short report is to analyze available information and present which radionuclides may be formed and released during operation of ESS.

Table 1: Operating Spallation Sources in the world.

Spallation Source	Location	Proton energy	Target material
Los Alamos Neutron Science Center (LANSCE)	Los Alamos, New Mexico, USA	800 MeV	W
Rutherford Appleton Laboratory, ISIS	Chilton, Oxfordshire, UK	800 MeV	W-Ta
Neutron Complex of the INR RAS	Troitsk, Russian Federation	600 MeV	Pb
Paul Scherrer Institute, SINQ	Villigen, Swizerland	590 MeV	Pb
Oak Ridge National Laboratory, SNS	Oak Ridge, Tennessee, USA	940 MeV	Hg
Japan Proton Accelerator Resarch Complex (JPARC)	Tokai-mura, Naka-gun, Ibaraki, Japan	3 GeV	Hg

The target will consist of 10x30x80 mm^3 tungsten bricks distributed on a steel support [11]. The target wheel (total weight – 10 tonnes) will be composed of 36 sectors and will be cooled by pressurized helium gas. For every 2 GeV proton incident on the tungsten target, approximately 56 neutrons will be liberated via nuclear spallation and subsequent reactions. Out of the 56 neutrons, only small part will enter one of the neutron guides with a proper direction and energy to be useful for neutron scattering. The remaining neutrons will activate ESS components (target, moderator, reflector, coolant, constructions etc.) and instruments and will thus contribute to personnel dose in the target building and instrument halls. Most of the radioactivity, however, is confined in the tungsten within the target [2].

2. Radioactivity analysis in accelerator-type facilities and spallation sources

A summary of the most important radiological safety considerations will be provided in this chapter. Most important analysis tools for material composition analysis will be presented here.

2.1. General aspects of radiological safety of the spallation source

The fundamental safety objective, which should be achieved while operating any facility which give rise to radiation risks, is to protect people and the environment from harmful effects of ionizing radiation [12, 13]. The safe operation of the ESS must be clearly evaluated, justified and ensured before the start of the commissioning. The information of the radioactivity produced by ESS must be evaluated to ensure that radiological hazards are minimized to the operating staff, general public, and environment. Readiness for highly unlikely emergency situations has to be based on the comprehensive safety analysis of the ESS facility and its modes of operation [12].

A vast amount of knowledge and operating experience have been gained about radiation protection and safety of proton accelerators during the several decades of studies and operation of such facilities [14-18]. This experience provides basis for the radiological safety analysis of ESS facility.

The ionizing radiation source from ESS may be divided into prompt ("skyshine") radiation that exists only while the accelerator is in operation and induced radioactivity which remains even after the accelerator is shutdown. Neutrons will be the dominant component of the prompt radiation. Several approaches exist to evaluate prompt neutron radiation, see e.g. a report by Thomas and Stevenson (published in 1986) for a detailed discussion [14]. Exposure is also discussed by Moritz (2001) [15] and Mauro (2009) [16]. Our report focuses on the radioactivity arising from radionuclide production, while prompt radiation is out of scope of this report.

As previously stated, a spallation source produces neutrons for the studies of the materials through spallation reactions. Spallation refers to non-elastic nuclear reactions that occur when energetic particles interact with a nucleus. This reaction causes an intra-nuclear cascade and evaporation of the nucleus, emitting various particles such as protons, neutrons, deuterons, etc. These particles later on participate in secondary reactions [19]. The acceleration of the protons which induce the spallation reaction is not totally efficient – lost high energy particles hitting structural components will create radioactive isotopes. Therefore, the accelerator part of a spallation source is also an important source

of radionuclides. Moreover, activation may occur outside the structures of the accelerator – in the soil and groundwater in the vicinity of the accelerator.

In a paper by Stevenson (2001) [20] a few very simple and useful rules of thumb regarding radioactivity induced in accelerators are given. The total quantity of radioactivity produced in an accelerator structure may be related to the energy of initial particle: the total number of inelastic reactions produced by a high-energy proton is approximately equal to its kinetic energy in GeV multiplied by three, almost independent of the target material. About one-third to one-half of all inelastic interactions produces radionuclides with a half-life between several tens of minutes and a few years [20]. A convenient rule then is that the saturated activity for incident proton energies of more than 1 GeV is 1 Bq/GeV.

For example, this approximate method allows us to evaluate the total saturated activity produced by a 2 GeV proton accelerator operating at a proton intensity of 10^{16} per second. The total saturated activity of relatively long-lived radionuclides would be $2 \cdot 10^4$ TBq. In general, if we compare the activities of radionuclides produced by accelerators and spallation sources to the levels in nuclear power plants, the specific activity induced in the accelerator structures is much lower than what is found in reactor irradiated materials [14]. Despite that, analysis of radionuclide production is important for minimizing exposure doses for personnel and general public during operation, possible accidents and radioactive waste management.

The safety of an accelerator-based facility is assured applying the ALARA (As-Low-As-Reasonably-Achievable) principle for exposure doses for personnel and general public. In order to achieve this, it is important to predict the produced radionuclide inventory and residual activity during and after operation and before any handling and maintenance procedures. The quantification of the residual activity is necessary for evaluating the proper time of maintenance and the resulting doses for personnel as well as for optimizing the choice of the construction materials for the accelerator components. This quantification is usually performed using validated (i.e. showing reasonable correspondence between predicted and measured results) computer simulation codes. As there is no direct operating experience from such a unique facility as ESS, simulations before the start of operation are the only reasonable way to predict the activation levels. Comparisons with experimental data from similar spallation sources may be a good method to evaluate if the modeling results are adequate.

The limiting doses are set for normal operation and for postulated accidental scenarios, which may occur during the lifetime of ESS. Different dose limits are set by the Swedish Radiation Safety Authority (SSM) in the regulatory requirements for workers of the facility and for members of the public [21]. For normal operation of ESS, the annual effective dose limit is set to be 0.1 mSv for a member of general public. Higher effective dose limits apply for various postulated accidental scenarios [22]. For those who work with ionising radiation, the general limit on effective dose is set to 20 mSv $year^{-1}$ [21]. Various accident scenarios are analyzed in ESS Preliminary Safety Analysis report [22], and those which could lead to unplanned releases of radionuclides are identified. Effective doses for workers and the members of the public resulting from ESS operation and accidents were estimated performing safety analysis of the facility.

The number of different radionuclides which may be produced in a spallation facility is in principle very large, but in practice a smaller number of radionuclides is of relevance for radiological protection. The main reason is that not all the radioactive nuclei contribute significantly to the effective dose for a worker or for a member of general public, some of them have a very short lifetime, for example. However, radionuclides of shorter half-life than 1 hour may be of concern in radiological protection if produced in very large quantities. For example, some of the radionuclides are relevant only for short-term safety issues (e.g. some accident scenarios). The screening of radionuclides procedure is applied during analysis aimed at excluding clearly insignificant radionuclides. E.g. this procedure was applied by SSM in their document "Underlag till placering i beredskapskategori för ESS och beredskapsplaneringen kring anläggningen" [23], where 49 most important radionuclides were selected for analysis. A very general criterion for including a radionuclide is basically that it cannot be ruled out because it has a non-negligible radiological impact. The importance of a radionuclide is determined by its radiotoxicity, which is based on total activity of the specific radionuclide and the dose conversion factor for inhalation or ingestion:

$$Rtx_n^{inh(ing)}(t) = DCC_n^{inh(ing)} \times A_n(t) \quad (1)$$

where $Rtx_n^{inh(ing)}(t)$ is the inhalation (ingestion) radiotoxicity for nuclide *n* at time *t* in Sv, $DCC_n^{inh(ing)}$is the inhalation (ingestion) dose coefficient for nuclide *n* in Sv/Bq, and $A_n(t)$ is the inventory of radionuclide *n* at time *t* in Bq [24]. In general, the dose coefficient is higher for inhalation than for ingestion of the same radionuclide, meaning that inhalation of the same amount of activity of a specific radionuclide results in a higher dose than ingestion. Considering various exposure scenarios, this fact should be taken into account in order to properly evaluate the resulting doses.

2.2. Calculations of radionuclide concentrations

The basic information needed for the calculation of radionuclide concentrations in the materials irradiated in an operating accelerator (as well as in a spallation source) environment is the reaction cross-sections for the production of a given radionuclide from a material bombarded by protons or neutrons, decay data, material composition and accelerator (spallation target) geometry. The nuclear reactions cross-sections are gathered and compiled into nuclear data libraries. The reaction cross-sections are used as parameters in equations predicting the radionuclide composition. The US Evaluated Nuclear Data File (ENDF/B) [25] and the Europe Joint Evaluated Fission and Fusion File (JEFF) [26] are the most frequently used libraries. For spallation reactions, experimentally validated data in whole energy range is not available. Theoretical models are then used. Different spallation models exist for simulation of spallation reactions, and all models have their own strengths and weaknesses [27]. Benchmarking studies for these models have been performed [28, 29]. These studies were using experimental data from experiments with tungsten [30, 31] for comparison with

theoretical predictions. The information provided in the two papers by Titarenko et al. [30, 31] are extremely important for ESS, which is designed to use tungsten target, as it provides essential experimental data for tungsten target composition evaluation.

The material composition and parameters defining the interaction with particles (protons, neutrons etc.) are vital to solve particle transport problems. Particle transport problems can be described as the calculation of particle and material variables during the interaction of a particle with the surrounding material. This is usually performed using Monte Carlo methods [32]. Once the transport problems are solved the concentration of the radionuclides can be calculated. This is done using a series of coupled differential equations discussed originally by H. Bateman [33]. When solving these equations an operation history has to be assumed, i.e. the length of the periods of irradiation and cooling. To be able to estimate an effective dose to the general public from the installation, the migration of radionuclides to the environment should be performed, taking into account various conditions and scenarios. Migration in different media (air, water and ground) outside the accelerator and target are usually addressed in such analysis [34]. This complex topic is out of scope of this report, as we are intending only to identify the most important radionuclides.

2.3. Modeling tools for computational analysis

The main computation tools used to evaluate particle transport and material activation are MCNP [35], FLUKA [36], MARS [37] and Geant4 [38] codes. Other validated codes may also be used, however, these are less frequently applied. MCNP (Monte Carlo N-Particle) code is a Monte Carlo based code that is used for particle transport problems. This code may successfully be used for spallation source simulations [30, 39, 40], while changes in the material composition may be calculated using Cinder90 code, which is directly integrated in MCNP. FLUKA is a multipurpose transport Monte Carlo code for calculations of particle transport and interactions with matter. The code is also capable of following radioactive inventory evolution. Its capability to predict radioactive inventories of spallation sources has been successfully demonstrated [41]. MARS is used for similar problems as FLUKA. GEANT4 is a highly universal toolkit for the simulation of the passage of particles through matter, including simulation of physical processes relevant for material composition analysis. In a report from 2016, DiJulio et al. [42] presents the results of neutron transport simulations of simple spallation targets and the ESS Technical Report Design (TDR) model using the Monte-Carlo codes Geant4 and MCNP. Overall, there is in general good agreement between the results of calculations of both codes.

3. Review of radionuclide production assessment in spallation facilities

A number of computational and experimental studies have been performed either by ESS or by academic institutions to assess the radionuclide content in European spallation source. Analyzing induced radioactivity in ESS, the spallation source can be divided into two parts: linear accelerator and tungsten spallation target.

This chapter starts with a brief summary of experience from spallation sources in operation, then the predictions for ESS facility is presented. Some considerations regarding radiotoxicity are given in the next section. Extensive experience in the operation of linear accelerators exists worldwide, and this knowledge is much broader than the one of spallation targets. A summary of the experience in induced radioactivity in linear accelerators is given towards the end of the chapter and finally calculations for the linac of ESS are reviewed.

3.1. Experience from some spallation targets world-wide

In a study related to J-Parc Spallation Neutron Source in Japan (study published in 2004), Kai et al. [43] analyze induced radioactivity in a mercury target. Activation of different components was modeled: target, cooling water, moderator, reflector etc. The study presented has no detailed discussion, only the calculation results are given. The radionuclide activities were calculated for the main components of J-PARC spallation neutron source after different times of operation (6, 10 and 30 years). As this is a mercury target spallation source, the principal design is different from ESS, and therefore direct comparison with ESS is not possible.

Experimental measurements of spallation cross-sections of tungsten are limited, due to complicated and costly experiments. However, some experimental data from radioactive spallation product measurements are available. Kelley et al. (studies published in 2004-2005) investigated the ^{148}Gd production cross-sections in tungsten spallation reactions for 600 MeV and 800 MeV energy protons [44, 45]. They also performed modelling and found that the Bertini spallation model predicted the ^{148}Gd production better than the combination of the CEM2k and GEM2 codes. The difference between the experimental data and predictions using the Bertini model was in the range of 2-25 %, while the CEM2k+GEM2 predictions were a factor of two to three higher than the measurements.

In two papers from year 2011, Titarenko et al. [30, 31] summarize modeling and experimental data, and evaluate the validity of theoretical computational models.

The experimentally measured cross sections for nuclide production in thin natural tungsten targets irradiated by various energies (up to 2.6 GeV) protons were determined. It was found that alpha-active nuclides were produced in all heavy target materials irradiated with protons of an energy above about 0.5 GeV. The average experimental accuracy of the cross sections for the observed reaction products for tungsten was 14.8%.

Table 2: Codes and spallation models analyzed in [30].

Code	Physical models
MCNP6/MCNPX	BERTINI
	ISABEL
	CEM03.02
	INCL4.2 + ABLA
	INCL4.5 + ABLA07
PHITS	Not specified
CASCADE	Not specified

In the summary by Titarenko et al.[30], several different theoretical models and codes were used for modeling. They are summarized in Table 2. The high-energy transport codes were based on various versions of nuclear reaction models (generally, an intra-nuclear cascade model (INC) followed by different de-excitation models). An average deviation factor $\langle F \rangle$ between experimental and predictions was used as criteria to quantitatively evaluate the codes. $\langle F \rangle$ is defined as

$$\langle F \rangle = 10^{\frac{1}{N}\sum_{j=1}^{N}(\log \sigma_{code} - \log \sigma_{exp})} \quad (2)$$

where N is number of radionuclides, σ_{code} is predicted cross-section of nuclide production during spallation and σ_{exp} is experimentally measured cross-section of nuclide production during spallation. The average $\langle F \rangle$ values for a tungsten target for different proton energies are given in Fig. 9 of Reference [30]. If $\langle F \rangle$ is equal to 1 it means total agreement between the code prediction and experimental data. The deviation of the calculations from the experimental data was from 50% to 800%. Such deviations significantly exceed the accuracy of 30% required by authors as a reasonable value for practical applications. The discrepancies were particularly large at low proton energies. At the time of publication (2011), the CEM03.02 (as developed during 2004-2006) and the INCL4.5+ABLA07 (as developed during 2008-2009) codes were considered as the most accurate. The main conclusion from these papers is that all intra-nuclear cascade codes should be further developed [31].

In a PhD thesis from 2013, Shetty calculated the radionuclide inventory in the spallation target and other components of a conceptual spallation source designated to transmutation experiments [46]. Geant4 was used in the simulations. A spallation source with 600 MeV energy protons impinging on a tungsten spallation target was modeled. Nuclides contributing most to the activity at shutdown were found to be ^{172}Hf, ^{173}Lu, ^{174}Lu and ^{179}Ta. ^{148}Gd is mentioned as the nuclide significantly contributing to the dose in case of inhalation. Other significant alpha emitters were found to be ^{146}Sm and ^{154}Dy. Experimental analysis was not presented in the publication.

A publication by Findlay et al. (published in 2017) [47] presents Monte Carlo calculations and gamma-ray spectrometry measurements made for a highly irradiated tungsten target from a proton-driven spallation neutron source (ISIS in the UK). In an irradiated proton-driven spallation neutron target, activities of ^{60}Co and ^{172}Lu from a Monte Carlo inventory calculation, fall within uncertainty regions of activities deduced from gamma-ray spectroscopy through the walls of a transport cask.

3.2. Radionuclide assessment of the ESS spallation target

A number of computational studies have been performed either by ESS or by academic institutions to predict the radionuclide composition of the tungsten target. The ESS organization itself has not performed its own direct experimental studies related to evaluation the radionuclide composition of irradiated tungsten targets, however some experimental data is available from the other sources.

In a report published in 2012, Leprince et al. [40] performed INCL4.6-Abla07 MCNPX calculations in a quite detailed ESS geometry (see Fig. 5 of Reference [40]) using Cinder90. The total activity of the target after 5 years of operation was found to be $4.03 \cdot 10^{17}$ Bq and major contributors were ^{187}W (31 %), ^{183m}W (24.1 %), ^{185}W (15.8 %), ^{181}W (3 %) and ^{178}Ta (1 %). The total activity after 5 years of operation and a shut-down of 9 years was found to be $8.95 \cdot 10^{14}$ Bq. The list of contributors to the total activity is greatly reduced in this case due to decay of short-lived radionuclides: ^{3}H is the main one with 76.4 % contribution to total activity. No experimental verification and no uncertainties are given in the paper.

The work carried out by ESS (2013) [48] has relied on two methodologies. Both approaches are discussed in the publications by Leprince et al. [40] and Titarenko et al. [31] already mentioned above. The first used spallation model, INCL4.6-Abla07, and the second relied on an experimental evaluation of nuclear cross section data for p+W reactions at energies up to 3 GeV. The first type of validation involves the use of elementary nuclide production cross-sections and the second relies on nuclide production yields in a thick target. The most important contributors to the total activity according to the ESS calculations are shown in Table 3 [48]. The fractional activity of the radionuclides from beryllium reflector was calculated in this publication as well [48]. Precise values for activity are not given, but the total activity generated in beryllium reflector is approximately two orders of magnitude lower than in the target after five years of irradiation.

Table 3: Fractional contributions (in %) of the most important nuclides to the total activity of the target wheel requiring disposal, as a function of decay time after 5 years of irradiation [48].

Nuclide	Decay time (years)					
	6	40	10^2	10^3	10^4	10^5
^{3}H	83.4	96.4	72	0	0	0
^{14}C	0	0	0	0.3	0.6	0
^{36}Cl	0	0	0	0	0	0.7
^{39}Ar	0	0	0.1	0.7	0	0
^{59}Ni	0	0	0	0	0.2	1.3
^{79}Se	0	0	0	0.1	0.8	2.2
^{81}Kr	0	0	0	0.1	0.9	12.3
^{91}Nb	0	0.1	1.6	31.6	0	0
^{93m}Nb	0	0	0.3	12.6	14.9	0.3
^{94}Nb	0	0	0	0.2	0.8	0.7
^{97}Tc	0	0	0	0	0.2	4
^{99}Tc	0	0	0	0	0.2	2.7
^{137}La	0	0	0	1.4	8.7	57.6
^{148}Gd	0.2	0.9	11.6	0.1	0	0
^{150}Gd	0	0	0	0	0.3	5.6
^{154}Dy	0	0	0	0	0.2	4.3
^{157}Tb	0.1	0.6	9.3	7.2	0	0
^{163}Ho	0	0	0.7	29.7	53.4	0

Some considerations regarding the ESS target composition, without detailed description or justification, are given in a paper by Aguilar et al. (published in 2017) [11]. It was estimated, that the use of a 2.5 mA proton beam would yield an activity of about 4.67×10^{16} Bq after a very long irradiation period. The main radionuclides contributing to residual heat in the target wheel were identified for different cooling periods (^{187}W, ^{185}W, ^{183m}W and ^{176}Ta contribute most after shutdown, while ^{185}Lu, ^{172}Lu and ^{182}Ta are the main radionuclides contributing to residual heat 10 days after shutdown).

In a recent paper (published in 2018) by Kókai et al. [39] different spallation target materials are discussed in the light of the final disposal of the future ESS target, including lead-bismuth, mercury and tungsten. Based on a waste index, the tungsten target was found to be the best alternative. The dimensionless waste index is defined using following equation:

$$WI = \sum_{i=1}^{n} \frac{c_i}{CL} \tag{3}$$

c_i denotes activity concentration in Bq/g, and n is the total number of detectable radioisotopes present in the waste stream. *CL* is the clearance level associated with the negligible dose and is defined as:

$$CL = \frac{10\ \mu Sv/year}{SDC} \tag{4}$$

where *SDC* is the specific dose consequence in units of (μSv/year)/(Bq/g) for a radionuclide for each exposure route.

The modeled tungsten composition in [39] contained impurities before the start of operation, which are specified in the paper (e.g. C, O, Mg, Ca, Fe, Mo). The radionuclide inventory was calculated with MCNPX2.7 using ENDF/B-VII cross-section libraries coupled with Cinder90. Intra-nuclear cascade (INC) models: BERTINI, INCL4.2 and ISABEL were applied. The CEM02 model contained both steps of spallation (INC and evaporation). Kókai et al. [33] found

that after 5 years of irradiation and 10 years of cooling the activity concentrations (excluding tritium) obtained with BERTINI-ABLA and INCL4.2-ABLA showed the maximal (most conservative) values. The CEM02 model gave the most conservative estimate for tritium. The authors do not conclude which model is the most accurate, as experimental results are not presented in the paper. Clearance levels and waste indexes of radionuclides for the tungsten target were calculated. In the case of the tungsten target the overall score was represented by the summarized waste index after a 10-year cooling period --- it was 3.45×10^7 for 2 GeV protons (this value is 2 times lower than the one for mercury and 82 times lower than for lead-bismuth target). Using 1.33 GeV proton energy results in a 40 % lower waste index. It means that from the radiotoxicity point of view, tungsten target is the best option when comparing it with mercury or lead-bismuth targets.

In another recent report (published in 2018), Mora et al. [49] describe the details concerning the generation and accumulation of radionuclides produced by spallation reactions within the tungsten target to be installed at ESS. MCNPX/6 was used for modeling. The selection of the CEM03 model was favored since it has been shown to yield a more complete production spectrum than other models such as BERTINI and is also known to provide more accurate estimates for helium and hydrogen gas production than other computational schemes such as INCL. CEM03 is significantly computationally more efficient than INCL at the expense of some underestimation of the production of light isotopes having masses within 6 and 35. The ACAB code was used to carry out neutron activation and transmutation calculations. All calculations were carried out assuming an incident proton beam with kinetic energy of 2 GeV and 2.5 mA of average proton current. Dominant activity at shutdown resulted from ^{187}W, ^{185}W, ^{181}W and ^{178}Ta. The total activity of the target was found to be 2.19×10^{17} Bq after 5 years of irradiation. A long time after shutdown, the activity would be dominated by ^{179}Ta, ^{172}Lu and ^{172}Hf with significant contributions from tritium and other isotopes such as ^{60}Co and ^{90}Sr becoming more relevant. The calculated inventory showed that a number of very long-lived isotopes such as ^{163}Ho, ^{148}Gd, ^{157}Tb, ^{101}Rh, ^{91}Nb and ^{63}Ni will contribute to the inventory well beyond five years after shutdown. The spatial distribution along the target elements was evaluated.

The main results found in the traces of the publicly available ESS reports are presented in the ESS Preliminary waste management plan [50, 51] (reports from year 2012 and 2017, respectively), and one publication from year 2015 focuses on tritium issues [52]. In the latter report, Ene et al. found that the the total inventory of ^{3}H accumulated in the target within one year of operation was $6.13 \cdot 10^{14}$ Bq [52]. The whole ^{3}H inventory in the target, at the end of its lifetime was evaluated to be $3.2 \cdot 10^{15}$ Bq [52]. 100 kg of tritiated water per year with an activity approaching 600 TBq (6 GBq/ml) will be generated in the helium purification system. The steady state tritium activity in the helium will be under 200 GBq [48].

3.3. Radiotoxicity of nuclides produced in spallation sources

Some research papers are dedicated to radioxicity and dose evaluation. Because our aim is to identify most important radionuclides, these publications are also reviewed.

Toxicity analysis of radionuclides accumulated in different spallation targets, reveals an important role of alpha-emitting rare earths ^{146}Sm, ^{148}Gd, ^{150}Gd and ^{154}Dy – this is a main outcome of a paper by Stankovsky et al. from year 2001 [53]. According to the paper, rare earth alpha-emitters ^{148}Gd, ^{150}Gd and ^{154}Dy contribute to 90% to the total radiotoxicity generated in a tungsten target.

A paper by Moritz et al. (published in 2001) [15] provides a well summarized methodology to evaluate radiation, activation and radioactive effluents to the environment, applicable to a low-energy (up to 1 GeV) proton accelerator. The method for dose calculation is described in Fig. 13 of Reference [15]. Methodology consists of dose evaluation using transfer coefficients from source to atmosphere and surface water, further other transfer coefficients are applied to evaluate radionuclide accumulation in soil, plants and animals. Various pathways of an exposure (external exposure, ingestion and inhalation) are included when evaluating total dose for person.

In the ESS document "Technical Design report" (published in year 2013), the most radiotoxic nuclide in the facility was anticipated to be ^{148}Gd [48]. Analysis of estimated annual dose rate contribution from routine releases to air during normal operation shows that ^{125}I will be the main contributor for the dose to the reference person 660 m away from the facility. Regarding accident scenarios, in case of 0.05% combined volatiles (which cover tritium, iodine isotopes and ^{121}Xe) releases, ^{125}I and ^{3}H are the main contributors to the dose. Other accident scenarios were not presented in the report. Ventilation of the linac tunnel is considered to become the only possible source of immediate, continuous release of activity. The design of the ventilation system, and its performance in mitigating radioactive releases, has not yet been optimized, according to authors [48].

A dose coefficient of $5.82 \cdot 10^{-21}$ Sv/Bq release of ^{3}H was derived 660 m away from the ESS release point [52]. The source term of tritium was evaluated taking into account on-line emissions, and emissions resulting from processing. During normal operation source term of tritium was estimated to be $6.00 \cdot 10^{12}$ Bq/year, while possible release because of design basis accident may reach $3.2 \cdot 10^{15}$ Bq [52]. One publication (from year 2015) is dedicated to tritium migration inside the spallation target [54].

3.4. Experience from linacs

General principles and examples of analysis of radiological safety in operation of proton accelerators are given in an IAEA report by Thomas and Stevenson from year 1988 [14]. In this comprehensive report, a historical context of accelerator development is presented as well as prompt radiation, induced radiation, shielding problems and environmental impact of accelerators. Regarding the induced activity and the activity released to the environment, this report proposes that it is reasonable to study radionuclides with half-lives longer than 10 hours.

The greater part of the radioactivity induced in the soil is confined to regions of high radiation intensity and is typically confined to a few locations close to the accelerator. 95 % of the activity induced in the ground is produced within 2 m from the outer wall of the accelerator tunnel of a proton synchrotron [14]. Of all the radionuclides produced in the soil and groundwater, it is likely that only tritium will move freely in groundwater, without significant holdup due to absorption on rock surfaces. Thomas and Stevenson [14] state that tritium may be the radionuclide that should be most carefully studied in groundwater around accelerators. A model for evaluation of contamination of drinking water is proposed in the report. The conclusion of a crude evaluation is that the magnitude of radioactive contamination of drinking water supplies will be extremely small. Regarding air contamination, the radionuclides of significance for environmental contamination are ^{3}H, ^{7}Be, and perhaps ^{11}C, ^{13}N and ^{15}O. The isotopes ^{7}Be, ^{24}Na, ^{28}Mg, ^{31}Si, ^{32}P, and ^{33}P were identified in the ventilation air around an extracted beam by flow ionization chambers and gamma spectroscopy on filters.

In a report published in 2000, Fasso et al. analyze radionuclides in accelerator stainless steel components using both experimental and modeling techniques [55]. Long-lived radionuclides identified using gamma spectrometry included: ^{48}V, ^{51}Cr, ^{52}Mn, ^{54}Mn, ^{56}Ni, ^{57}Ni, ^{56}Co, ^{57}Co, ^{58}Co, ^{60}Co, ^{88}Y, ^{92m}Nb, ^{95}Nb and ^{99}Mo, and in copper components: ^{51}Cr, ^{54}Mn, ^{56}Co, ^{57}Co, ^{58}Co, ^{60}Co, ^{65}Zn, ^{72}Se, ^{75}Se, ^{74}As and ^{120}Sb.

A comparison between predicted and measured soil activation, performed by Odano et al. [56] for accelerator of Spallation Neutron Source in Oak Ridge National laboratory, US, revealed an agreement between calculated and measured residual soil activation within a factor of from one to three for most of the studied radionuclides. A distribution of radionuclides in the berm is clearly seen, and 85 % of the activation is contained within the first meter of soil surrounding the tunnel concrete wall [56]. Other soil experimental study is presented by Miura et al. in 2003 [57]. ^{3}H, ^{7}Be, ^{22}Na, ^{46}Sc, ^{54}Mn, ^{60}Co, ^{134}Cs, ^{152}Eu and ^{154}Eu were observed in the soil samples. ^{3}H, ^{22}Na and ^{54}Mn, which leached from the soil, were found in the groundwater below the proton beam line.

A brief analysis for the J-PARC accelerator radiation safety design using PHITS, MARS and MCNPX codes for transport calculations is presented in a report by Nakashima et al. (published in 2005) [58]. This report gives a summarized approach of how radiation protection analysis for a large facility should be performed. The calculation flow for radiation and activity analysis for

J-PARC is given in Fig. 1 of Reference [58] .The prompt radiation and activation products are included in this analysis (activation evaluation of air, water and other devices is also performed).

In a report from 2005, Oishi et al. present measurements and analysis work performed at KENS neutron spallation facility in Japan [48]. Induced activities of concrete samples were measured in the large concrete assembly irradiated by high-energy neutrons emitted from the tungsten target bombarded with 500 MeV protons. For the nuclides that were produced by spallation reactions, a large disagreement, up to two orders of magnitude, was observed (NMTC/JAM code was used for calculations). Good agreement within factors of 2 were obtained for the nuclides that were not mainly produced by the spallation reactions: ^{24}Na, ^{47}Sc, ^{47}Ca and ^{54}Mn. While for other nuclides differences up to the factor of 5 were found (^{42}K, ^{43}K, ^{51}Cr and ^{22}Na).

In a report by Mauro (published in 2009) [16] radiation protection studies of linacs in CERN are performed, mainly using the FLUKA code. The main radionuclides in concrete were specified in a PhD thesis by La Torre from year 2014 [17]. Also experimental analysis of soil, soil-water mixture and metal foil samples was performed and comparison with results predicted by FLUKA was performed. Experimental values were estimated to be in a good agreement with FLUKA predicted values (differences between experimental and modeled values for investigated radionuclides did not exceed 65%). Blaha et al. (2014) [18] carried out FLUKA simulations using a detailed geometrical model of the accelerator to predict the induced radioactivity in LINAC4 (CERN) after several years of operation and for various decay times. This publication covers wide variety of relevant radionuclides in the accelerator components, as well as computational prediction of releases.

A paper by Otiougova et al. (published in 2017) presents work performed at PSI in Switzerland [59]. MCNPX2.7.0 was used for transport problems and FISPACT10 code was used to determine the radionuclide inventory as well as the specific activity of the nuclides for part of the PSI accelerator facility [59]. The radionuclide inventory for steel and concrete was evaluated. Measured specific activities in the concrete sample was compared to modeling data. Simulated values for the main nuclides ^{60}Co, ^{152}Eu, ^{154}Eu exceeded the measured ones by a factor of 3 to 4.

3.5. Radionuclide assessment of the linac of ESS

Radiation protection studies for ESS superconducting linear accelerator design are presented by Ene et al. in 2011 [60]. A total activation value of 5.2×10^7 $Bq \cdot cm^{-3}$ (calculated using PHITS and MCNPX codes) coming from the accelerator structure at after 40 years of operation and one-hour decay time is estimated to be due to $^{64,62,61,65}Cu$ radionuclides while at long decay times ^{59}Fe, ^{60}Co, ^{3}H and ^{63}Ni dominate. The main contributor at short times is ^{64}Cu produced from thermal neutron capture in ^{63}Cu (high activation cross section of 4.5 barn). The ^{37}Ar isotope issuing from Ca activation dominates the concrete activity until 6 months while for longer decay time ^{3}H and further ^{238}U together with its ascendants make up majority of activity value. ^{7}Be and ^{3}H are produced by spallation reactions while ^{41}Ar by thermal neutron capture in the natural argon. Activity concentration for the first 100 cm of soil surrounding the concrete wall after 40 years of continuous operation is calculated and presented.

A paper by Bungau et al. (2014) [61] presents activation studies of the magnets and collimators in the High Energy Beam Transport (HEBT) line of ESS due to backscattered neutrons from the target and also due to direct proton interactions and their secondaries. An estimate of the radionuclide inventory and induced activation are predicted using the GEANT4 code. The radionuclide production rate per proton is given in the paper for HEBT components. An interesting part about this paper is it reports some actinides (Am), which were not found in other presentations We assume that uranium impurities were included in the initial material composition, although it is not entirely clear from the report.

A soil activation study by Rakhno et al. from year 2018 [62] addresses distributions of activity of radionuclides produced in the soil around the ESS accelerator tunnel wall after one year and after forty years of normal operation. Spatial migration of the produced radionuclides is not considered. The list of eleven most important comprises the following nuclides: ^{3}H, ^{7}Be, ^{22}Na, ^{24}Na, ^{32}P, ^{35}S, ^{45}Ca, ^{46}Sc, ^{54}Mn, ^{55}Fe, ^{65}Zn.

3.6. ESS reports

There are a number of reports prepared by ESS, which evaluate the radionuclides which may be produced during operation. The most relevant for this purpose seems to be “Source term to the environment from the Target Station” [63]. This report presents annual production and releases of radionuclides during normal operation. This report was used as a source making the radionuclide list in Appendix A.

Predicted radionuclide activities of major ESS components are given in the report “Preliminary safety analysis report” (from 2012) [64]. The activities are given for radionuclides which half-lives are longer than 10 seconds. Mostly short lifetime nuclides were analyzed in the report “Production and Release of Airborne Radionuclides from ESS Linac Tunnel” (from 2013) [65]. In a report

by Ene (from 2015) the radiological impact of the ESS facility on members of the public was assessed and it was demonstrated that the ESS safety objective of not more than 50 μSv/y for personnel during normal operation is met [66]. During this analysis possible radionuclide releases during normal operation were also considered. ESS has estimated the source term for different pathways: radioactivity production and release from the linear accelerator, target, waste treatment facility as well as resulting doses from normal operation and maintenance activities.

4. Conclusions

Available data on radionuclides which may potentially be produced in ESS during operation was gathered from scientific publications as well as from ESS reports. This information is based on both modeling and experimental analysis. The radionuclides analyzed were limited to larger than 10-hour half-life, as this is most relevant half-life for the releases related with normal operation and minor accidents. The short-lived radionuclides were not analyzed. 234 relevant radionuclides were found in the publications. The list of long-lived radionuclides is given in Appendix A. The concentrations of the radionuclides produced were not evaluated. The effective dose coefficients of the radionuclides were gathered in order to have the possibility to sort radionuclides according their toxicity. Information provided in this report may be used as basis for identifying the most important and the most toxic radionuclides. The main conclusions from the review of the available literature are:

- Several different spallation reaction models exist, but deviation of the calculations from the experimental data shows that none of them is significantly more precise in predicting inventory from tungsten spallation target. According to the publication by Titarenko et al. [30] the INCL4.5+ABLA07 model gives the best predicted result for tungsten as target material.
- Experimental data from tungsten spallation targets composition studies exists, but it is limited, and more experimental data is needed to verify existing calculations. Additionally, theoretical spallation models have to be further developed, taking experimental data into account.
- Spallation target composition modeling publications predict radionuclides of highest activity in the target after different cooling times. This information is extremely important when selecting which radionuclides should be emphasized during the most severe accident conditions, target-wheel replacement and maintenance activities.
- The induced radioactivity in linear accelerator is a well-known phenomenon, described in a number of publications. Radionuclides produced in air, structural elements and soil are known and listed in those publications. No unique or very rare radionuclides should be generated in the accelerator structures.
- The radionuclides with the highest inhalation and ingestion dose coefficients are the alpha emitters: $^{241, 243}$Am, ^{228}Th, $^{150, 148}$Gd, ^{146}Sm, and ^{154}Dy. Other radionuclides with high dose coefficients include $^{129, 126, 131, 125}$I and $^{137, 134}$Cs as well as ^{210}Pb, ^{60}Fe, ^{178m}Hf, ^{90}Sr, ^{44}Ti and^{166m}Ho. For most alpha emitters, inhalation dose coefficients are higher than the ingestion ones.
- Production of actinides should be analyzed in more detail since their role is not clear from the existing publications.

Further tasks in this project should be independent modeling for target composition and quantitative comparison of concentrations obtained by other authors and suggestion of analytical methods to measure activities of the radionuclides with highest dose coefficients.

5. References

[1] Lindroos, M., Bousson, S., Calaga, R., Danared, H., Devanz, G., Duperrier, R., Eguia, J., et al. *The European Spallation Source.* Nuclear Instruments and Methods in Physics Research Section B: Beam Interactions with Materials and Atoms, 269(24): 3258-3260, 2011.

[2] Garoby, R., Danared, H., Alonso, I., Bargallo, E., Cheymol, B., Darve, C., Eshraqi, M., et al. *The European Spallation Source Design.* Physica Scripta, 93(1): 014001-014001, 2018.

[3] Genberg, J., Stenström, K., Elfman, M., Olsson, M. *Development of graphitization of µg-sized samples at Lund University.* Radiocarbon, 52: 1270-1276, 2010.

[4] Baker, M.L., Blundell, S.J., Domingo, N., Hill, S. *Spectroscopy Methods for Molecular Nanomagnets*. Springer Berlin Heidelberg. Report, p. 231-291,2015.

[5] Hansen, T.C., Kohlmann, H. *Chemical Reactions followed by in situ Neutron Powder Diffraction.* Zeitschrift für anorganische und allgemeine Chemie, 640(15): 3044-3063, 2014.

[6] Martins, M.L., Gates, W.P., Michot, L., Ferrage, E., Marry, V., Bordallo, H.N. *Neutron scattering, a powerful tool to study clay minerals.* Applied Clay Science, 96: 22-35, 2014.

[7] Andreani, C., Krzystyniak, M., Romanelli, G., Senesi, R., Fernandez-Alonso, F. *Electron-volt neutron spectroscopy: beyond fundamental systems.* Advances in Physics, 66(1): 1-73, 2017.

[8] Appleby, R. *Challenges and goals for accelerators in the XXI century, edited by Oliver Bruning and Stephen Myers.* Contemporary Physics, 58(2): 189-190, 2017.

[9] Zanini, L., Batkov, K., Klinkby, E., Mezei, F., Schönfeldt, T., Takibayev, A. *The neutron moderators for the European Spallation Source.* Journal of Physics: Conference Series, 1021(1): 012066, 2018.

[10] Heinemeier, K.M., Schjerling, P., Heinemeier, J., Magnusson, S.P., Kjaer, M. *Lack of tissue renewal in human adult Achilles tendon is revealed by nuclear bomb (14)C.* FASEB J, 27(5): 2074-9, 2013.

[11] Aguilar, A., Sordo, F., Mora, T., Mena, L., Mancisidor, M., Aguilar, J., Bakedano, G., et al. *Design specification for the European Spallation Source neutron generating target element.* Nuclear Instruments and Methods in Physics Research Section A: Accelerators, Spectrometers, Detectors and Associated Equipment, 856: 99-108, 2017.

[12] *Safety Assessment for Facilities and Activities*. IAEA Safety Standards Series. Vienna. International Atomic Energy Agency. 2016.

[13] *Fundamental Safety Principles*. Vienna. International Atomic Energy Agency. 2006.

[14] Thomas, R.H., Stevenson, G.R., *Radiological Safety Aspects of the Operation of Proton Accelerators*. International Atomic Energy Agency. 1986.

[15] Moritz, L.E. *Radiation protection at low energy proton accelerators.* Radiation Protection Dosimetry, 96: 297-309, 2001.

[16] Mauro, E. *Radiation protection studies for CERN Linac4/SPL accelerator complex.* 199-199, 2009.

[17] La Torre, F.P. *Study of induced radioactivity in proton accelerator facilities*. CERN. Report,2014.

[18] Blaha, J., Torre, F.P.L., Silari, M., Vollaire, J. *Long-term residual radioactivity in an intermediate-energy proton linac.* Nuclear

Instruments and Methods in Physics Research Section A: Accelerators, Spectrometers, Detectors and Associated Equipment, 753: 61-71, 2014.
[19] Filges, D. *Handbook of spallation research theory, experiments and applications*. Wiley-VCH. Report,2009.
[20] Stevenson, G.R. *Induced activity in accelerator structures, air and water.* Radiation Protection Dosimetry, 96: 373-80, 2001.
[21] *The Swedish Radiation Safety Authority's regulations concerning basic provisions for the protection of workers and the general public in practices involving ionising radiation.* SSMFS: 2008:51. SSM. 2008.
[22] *ESS Preliminary Safety Analysis Report.* ESS-0000002. 2012.
[23] *Underlag till placering iberedskapskategori för ESS och beredskapsplaneringen kring anläggningen.* Strålsäkerhetsmyndigheten (SSM). 2018.
[24] Slessarev, I. *Long Term Radiotoxicity.* 2000.
[25] Brown, D.A., Chadwick, M.B., Capote, R., Kahler, A.C., Trkov, A., Herman, M.W., Sonzogni, A.A., et al. *ENDF/B-VIII.0: The 8th Major Release of the Nuclear Reaction Data Library with CIELO-project Cross Sections, New Standards and Thermal Scattering Data.* Nuclear Data Sheets, 148: 1-142, 2018.
[26] A. Santamarina, D.B., Y. Rugama. *The JEFF-3.1.1 Nuclear Data Library.* JEFF Report 22. 2009.
[27] Leray, S., David, J.C., Khandaker, M., Mank, G., Mengoni, A., Otsuka, N., Filges, D., et al. *Results from the IAEA benchmark of spallation models.* Journal of the Korean Physical Society, 59(2): 791-796, 2011.
[28] David, J.C. *Spallation reactions: A successful interplay between modeling and applications.* The European Physical Journal A, 51(6): 68, 2015.
[29] Sharma, S. *Validation of spallation models*. Jagiellonian University. Report,2015.
[30] Titarenko, Y.E., Batyaev, V.F., Butko, M.A., Dikarev, D.V., Florya, S.N., Pavlov, K.V., Titarenko, A.Y., et al. *Verification of high-energy transport codes on the basis of activation data.* Phys. Rev. C, 84: 064612-064612, 2011.
[31] Titarenko, Y.E., Batyaev, V.F., Titarenko, A.Y., Butko, M.A., Pavlov, K.V., Florya, S.N., Tikhonov, R.S., et al. *Measurement and simulation of the cross sections for nuclide production in natW and 181Ta targets irradiated with 0.04- to 2.6-GeV protons.* Physics of Atomic Nuclei, 74(4): 551-572, 2011.
[32] Lux, I., Koblinger, L.s., *Monte Carlo particle transport methods : neutron and photon calculations*. CRC Press. 0849360749, 1991.
[33] Cetnar, J. *General solution of Bateman equations for nuclear transmutations.* Annals of Nuclear Energy, 33(7): 640-645, 2006.
[34] Poinssot, C., Geckeis, H., *Radionuclide behaviour in the natural environment: science, implications and lessons for the nuclear industry*. Cambridge. 9780857091321, 2012.
[35] Dias, C.M., Stenstrom, K., Bacelar Leao, I.L., Santos, R.V., Nicoli, I.G., Skog, G., Ekstrom, P., et al. *$^{14}CO_2$ dispersion around two PWR nuclear power plants in Brazil.* J Environ Radioact, 100(7): 574-80, 2009.
[36] Ferrari, A., Sala, P.R., Fasso, A., Ranft, J. *FLUKA: A Multi-Particle Transport Code.* SLAC-R--773. United States. http://www.slac.stanford.edu/cgi-wrap/pubpage?slac-r-773.html. 2005.
[37] Mokhov, N. *MARS Code Developments, Benchmarking and Applications.* Journal of Nuclear Science and Technology, 37: 167-171, 2000.

[38] Agostinelli, S., Allison, J., Amako, K., Apostolakis, J., Araujo, H., Arce, P., Asai, M., et al. *Geant4—a simulation toolkit.* Nuclear Instruments and Methods in Physics Research Section A: Accelerators, Spectrometers, Detectors and Associated Equipment, 506(3): 250-303, 2003.

[39] Kókai, Z., Török, S., Zagyvai, P., Kiselev, D., Moormann, R., Börcsök, E., Zanini, L., et al. *Comparison of different target material options for the European Spallation Source based on certain aspects related to the final disposal.* Nuclear Instruments and Methods in Physics Research Section B: Beam Interactions with Materials and Atoms, 416: 1-8, 2018.

[40] Leprince, A., David, J.-C., Ene, D., Leray, S. *Reliability and use of INCL4.6-Abla07 spallation model in the frame of European Spallation Source target design*.

[41] Brugger, M., Ferrari, A., Roesler, S., Sala, P.R., *Calculation of radionuclide production cross sections with FLUKA and their application in high energy hadron collider studies*. France. EDP Sciences. 978-2-7598-0090-2, 2008.

[42] DiJulio, D.D., Batkov, K., Stenander, J., Cherkashyna, N., Bentley, P.M. *Benchmarking Geant4 for spallation neutron source calculations.* Journal of Physics: Conference Series, 746(1): 012032-012032, 2016.

[43] Kai, T., Harada, M., Maekawa, F., Teshigawara, M., Konno, C., Ikeda, Y. *Induced-radioactivity in J-PARC Spallation Neutron Source.* Journal of Nuclear Science and Technology, 41(4): 172-175, 2004.

[44] Kelley, K.C. *Gadolinium-148 and other spallation production cross section measurements for accelerator target facilities*. Georgia Institute of Technology. Report,2004.

[45] Kelley, K.C., Hertel, N.E., Pitcher, E.J., Devlin, M., Mashnik, S.G. *148Gd production cross section measurements for 600- and 800-MeV protons on tantalum, tungsten, and gold.* Nuclear Physics A, 760(3): 225-233, 2005.

[46] Shetty, N.V. *Study of particle transport in a high power spallation target for an accelerator driven transmutation system*. Aachen University. Report,2013.

[47] Findlay, D.J.S., Škoro, G.P., Burns, G.J., Ansell, S. *Experimental verification of spallation inventory calculations.* Applied Radiation and Isotopes, 125: 1-3, 2017.

[48] *ESS technical design report.* . http://docdb01.esss.lu.se/DocDB/0002/000274/007/TDR_online_ver_ch10.pdf. 2013.

[49] Mora, T., Sordo, F., Aguilar, A., Mena, L., Mancisidor, M., Aguilar, J., Bakedano, G., et al. *An evaluation of activation and radiation damage effects for the European Spallation Source Target.* Journal of Nuclear Science and Technology, 55(5): 548-558, 2018.

[50] Ene, D. *ESS Preliminary waste management plan.* https://www.ssi.se/Global/ESS/ESS-ans%C3%B6kan/Kompletteringar/SSM2012-131-94%20ESS%20Preliminary%20waste%20management%20plan%20611338_1_1.pdf. 2012.

[51] Ene, D. *Decommissioning Plan for European Spallation Source.* EPJ Web Conf., 153: 05022-05022, 2017.

[52] Ene, D., Andersson, K., Jensen, M., Nielsen, S., Severin, G. *Management of Tritium in European Spallation Source.* Fusion Science and Technology, 67(2): 324-327, 2015.

[53] Stankovsky, A., Saito, M., Artisyuk, V., Shmelev, A., Korovin, Y. *Accumulation and Transmutation of Spallation Products in the Target of Accelerator-Driven System.* Journal of Nuclear Science and Technology, 38(7): 503-510, 2001.

[54] Jørgensen, T., Severin, G., Jensen, M. *Migration of radionuclides in a gas cooled solid state spallation target.* Nuclear Engineering and Design, 282: 28-35, 2015.

[55] Fasso, A., Silari, M., Ulrici, L. *Predicting Induced Radioactivity at High-Energy Electron Accelerators.* Journal of Nuclear Science and Technology, 37(1): 827-834, 2000.

[56] Naoteru Odano, J.O.J., Harrington, R.M., DeVore, J.R. *Shielding and Activation Analyses in Support of The Spallation Neutron Source (SNS) ES&H Requirements.* http://citeseerx.ist.psu.edu/viewdoc/download;jsessionid=BEC89FE8E4714CACBE444F0229CD2313?doi=10.1.1.539.8779&rep=rep1&type=pdf.

[57] Miura, T., Bessho, K., Ishihama, S., Ohtsuka, N. *Migration of radionuclides induced in the soil below the 12 GeV proton accelerator facility at KEK.* Journal of Radioanalytical and Nuclear Chemistry, 255(3): 543-546, 2003.

[58] Nakashima, H., Nakane, Y., Masukawa, F., Matsuda, N., Oguri, T., Nakano, H., Sasamoto, N., et al. *Radiation safety design for the J-PARC project.* Radiation Protection Dosimetry, 115: 564-568, 2005.

[59] Otiougova, P., Bergmann, R., Kiselev, D., Talanov, V., Wohlmuther, M. *Induced radioactivity studies of the shielding and beamline equipment of the high intensity proton accelerator facility at PSI.* EPJ Web Conf., 146: 03017-03017, 2017.

[60] Ene, D., Mathias, B., Mohammad, E., Mats, L., Steve, P., Hakan, H.A.H.N. *Radiation Protection Studies for ESS Superconducting Linear Accelerator.* Progress in NUCLEAR SCIENCE and TECHNOLOGY, 2: 382-388, 2011.

[61] Bungau, C., Bungau, A., Cywinski, R., Barlow, R., Edgecock, T.R., Carlsson, P., Danared, H., et al. *Induced activation in accelerator components.* Phys. Rev. ST Accel. Beams, 17: 084701-084701, 2014.

[62] Rakhno, I.L., Mokhov, N.V., Tropin, I.S., Ene, D. *Activation assessment of the soil around the ESS accelerator tunnel.* ArXiv e-prints, 2018.

[63] Ene, D. *Source Term to the environment from the Target Station.* ESS-0018859. ESS. 2016.

[64] Schoeller, D.A. *Isotope Fractionation: Why Aren't We What We Eat?* Journal of Archaeological Science, 26(6): 667-673, 1999.

[65] Robinson, D. *$\delta^{15}N$ as an integrator of the nitrogen cycle.* Trends in Ecology & Evolution, 16(3): 153-162, 2001.

[66] Georgiadou, E., Stenström, K. *Bomb-pulse dating of human material – modelling the influence of diet* Radiocarbon, 52: 1351-1357, 2010.

Appendix A

Nuclide	A	Z	Half-life	Decay	Effective dose coefficients (e) for ingestion of radionuclides for members of the public. Adults. (Sv/Bq) [1]	Effective dose coefficients (e) for inhalation of radionuclides for members of the public. Adults. (Sv/Bq) [1]	Source	ESS ref
H3	3	1	12.32 years	beta-	1.8E-11	2.6E-10	[2], [3], [4], [5], [6], [7], [8], [9]	[10]
Be7	7	4	53.12 days	EC, gamma	2.8E-11	5.5E-11	[2], [11] , [4], [12], [8], [9], [13] , [14]	[10]
Be10	10	4	1.39e6 years	beta-	1.1E-09	3.5E-08	[2], [3] , [13] , [4]	[10]
C14	14	6	5730 years	beta-	5.8E-10	5.8E-09	[2] , [3] , [13] , [4]	[10]
Na22	22	11	2.6 years	beta+	3.2E-09	1.3E-09	[11], [15] , [3] , [4] , [5] , [6], [7] , [8] , [9] , [13] , [14]	[10]
Na24	24	11	15 hours	beta-, gamma	4.3E-10	2.7E-10	[11] , [8]	[10]
Al26	26	13	7.17e5 years	beta+, EC, gamma	3.5E-09	2.0E-08	[3] , [13]	
P32	32	15	14.28 days	beta-	2.4E-09	3.4E-09	[4] , [8]	[10]
P33	33	15	25.3 days	Beta-	2.4E-10	1.5E-09	[4]	[10]
S35	35	16	87.3 days	Beta-	7.7E-10	1.9E-09	[8] , [4]	[10]
Cl36	36	17	3e5 years	beta-, EC	9.3E-10	7.3E-09	[2] , [3]	[10]
Ar37	37	18	35 days	EC		4.1E-15		[10]
Ar39	39	18	269 years	beta-		1.1E-11	[13]	[10]
K40	40	19	1.25e9 years	beta-, EC	6.2E-09	2.1E-09	[3]	[10]
K42	42	19	12.36 hours	beta-	4.3E-10	1.2E-10	[11]	[10]
K43	43	19	22.3 hours	beta-	2.5E-10	1.4E-10	[11] , [4]	[10]
Ca41	41	20	1e5 years	EC	1.9E-10	1.8E-10	[3]	[10]
Ca45	45	20	162.7 days	beta-	7.1E-10	3.7E-09	[15] , [4] , [8]	[10]
Ca47	47	20	4.5 days	beta-, gamma	1.6E-09	2.1E-09	[4]	[10]
Ti44	44	22	63 years	EC, gamma	5.8E-09	1.2E-07	[5] , [7] , [12]	
Sc44m	44	21	58.6 hours	IC, gamma, EC	2.4E-09	1.4E-09	[11] , [5]	[10]
Sc46	46	21	83.8 days	beta-, gamma	1.5E-09	6.8E-09	[11] , [15] , [4] , [12] , [8] , [9] , [14]	[10]
Sc47	47	21	80.4 hours	beta-, gamma	5.4E-10	7.3E-10	[11] , [4]	[10]
Sc48	48	21	43.7 hours	beta-, gamma	1.7E-09	1.1E-09	[11]	[10]
V48	48	23	16 days	beta+	2.0E-09	2.4E-09	[11] , [4], [14]	[10]
V49	49	23	330 days	EC	1.8E-11	3.4E-11	[5] , [6]	[10]
Cr51	51	24	27.7 days	EC, gamma	3.8E-11	3.7E-11	[11] , [4] , [5] , [12] , [8] , [14]	[10]
Mn52	52	25	5.6 days	EC, beta+, gamma	1.8E-09	1.4E-09	[11] , [5]	[10]
Mn53	53	25	3.7e6 years	EC	3.0E-11	5.4E-11	[3]	[10]

Mn54	54	25	312 days	EC, gamma	7.1E-10	1.5E-09	[2] , [11] , [15] , [3] , [4] , [5] , [12] , [8] , [9] , [14]	[10]
Fe55	55	26	2.73 years	EC	3.3E-10	1.8E-10	[2] , [11], , [3] , [4] , [5], [6] , [8]	[10]
Fe59	59	26	44.6 days	beta-, gamma	1.8E-09	4.0E-09	[2] , [11] , [4] , [12]	[10]
Fe60	60	26	2.6e6 years	Beta-	1.1E-07	2.8E-07	[13]	
Co56	56	27	77.3 days	EC	2.5E-09	6.7E-09	[11] , [12] , [14]	[10]
Co57	57	27	272 days	EC	2.1E-10	1.0E-09	[11] , [5] , [12] , [14]	[10]
Co58	58	27	70.9 days	EC	7.4E-10	2.1E-09	[11] , [4] , [5] , [12] , [14]	[10]
Co60	60	27	5.3 years	beta-, gamma	3.4E-09	3.1E-08	[11], [15] , [4] , [5] , [6] , [7] , [12] , [8] , [9] , [13] , [14]	[10]
Ni56	56	28	6 days	Beta+, gamma	8.6E-10	1.0E-09	[14]	[10]
Ni57	57	28	35.6 hours	beta+, gamma	8.7E-10	5.3E-10	[11]	[10]
Ni59	59	28	7.6e4 years	EC	6.3E-11	4.4E-10	[2]	[10]
Ni63	63	28	100 years	beta-	1.5E-10	1.3E-09	[5] , [6] , [8] , [13]	[10]
Ni66	66	28	54.6 hours	Beta-	3.0E-09	1.8E-09		[10]
Cu67	67	29	61.8 hours	Beta-	3.4E-10	6.1E-10		[10]
Zn65	65	30	244 days	EC, gamma	3.9E-09	2.2E-09	[11] , [6] , [12] , [8]	[10]
Zn72	72	30	46.5 hours	Beta-	1.4E-09	1.3E-09		[10]
Ga67	67	31	3.3 days	EC, gamma	1.9E-10	2.4E-10		[10]
Ge68	68	32	271 days	EC	1.0E-10	1.4E-08		[10]
Ge69	69	32	39 hours	Beta+, gamma	2.4E-10	2.9E-10		[10]
Ge71	71	32	11.3 days	EC	1.2E-11	1.1E-11		[10]
As71	71	33	65.3 hours	Beta+, gamma	4.6E-10	4.0E-10		[10]
As72	72	33	26 hours	Beta+, gamma	1.8E-09	9.0E-10		[10]
As73	73	33	80.3 days	EC, gamma	2.6E-10	1.0E-09		[10]
As74	74	33	17.8 days	EC, gamma, beta+, beta-	1.3E-09	2.1E-09		[10]
As76	76	33	1.1 days	Beta-, gamma	1.6E-09	7.4E-10		[10]
As77	77	33	38 hours	Beta-	4.0E-10	3.9E-10		[10]
Se72	72	34	8.4 days	EC, gamma				[10]
Se75	75	34	120 days	EC, gamma	2.6E-09	1.3E-09	[12]	[10]
Se79	79	34	3.3e5 years	beta-	2.9E-09	6.8E-09	[2] , [13]	[10]
Br82	82	35	35.2 hours	Beta-	5.4E-10	6.3E-10		[10]
Kr79	79	36	35 hours	Beta+, gamma		9.7E-10		[10]
Kr81	81	36	2.3e5 years	EC, gamma		2.1E-11	[13]	[10]
Kr85	85	36	11 years	beta-		2.2E-11	[2] , [5] , [6] , [13]	[10]
Rb83	83	37	86.2 days	EC, gamma	1.9E-09	6.9E-10		[10]
Rb84	84	37	33 days	EC, beta+, beta-, gamma	2.8E-09	1.0E-09	[12]	[10]
Rb86	86	37	18.7 days	Beta-, gamma	2.8E-09	9.3E-10		[10]
Sr82	82	38	25.4 days	EC	6.1E-09	8.9E-09		[10]
Sr83	83	38	1.4 days	EC, beta+, gamma	4.9E-10	1.1E-08		[10]

Sr85	85	38	65 days	EC, gamma	5.6E-10	8.1E-10	[12]	[10]
Sr90	90	38	28.9 years	beta-	2.8E-08	1.6E-07	[5] , [6] , [7] , [13]	[10]
Y87	87	39	3.4 days	EC, gamma	5.5E-10	3.9E-10		[10]
Y88	88	39	107 days	EC, gamma	1.3E-09	4.4E-09	[12]	[10]
Y90	90	39	2.7 days	beta-	2.7E-09	1.5E-09	[6]	[10]
Y91	91	39	58.5 days	Beta-	2.4E-09	8.9E-09		[10]
Zr93	93	40	1.5e6 years	Beta-	1.1E-09	2.5E-08	[13]	[10]
Zr95	95	40	64 days	Beta-, gamma	9.5E-10	5.9E-09	[12]	[10]
Nb90	90	41	14.6 hours	Beta+, gamma	1.2E-09	6.6E-10		[10]
Nb91 [16]	91	41	680 years	EC	4.2E-11	1.1E-09	[2] , [6] , [13]	[10]
Nb92 [16]	92	41	10 days	EC, gamma	9.7E-10	2.5E-08		[10]
Nb93m	93	41	16 years	IC	1.2E-10	1.8E-09	[2] , [6] , [13]	
Nb94	94	41	20.3e3 years	beta-, gamma	1.7E-09	4.9E-08	[2] , [12] , [13]	[10]
Nb95	95	41	35 days	Beta-, gamma	5.8E-10	1.8E-09	[12]	[10]
Mo93	93	42	4000 years	EC	3.1E-09	2.3E-09	[13]	[10]
Mo99	93	42	66 years	Beta-, gamma	6.0E-10	9.9E-10		[10]
Tc96	96	43	4.3 days	EC, gamma	1.1E-09	7.0E-10		[10]
Tc97	97	43	4.2e6 years	EC	6.8E-11	1.8E-09	[2] , [13]	[10]
Tc99	99	43	2.1e5 years	beta-	6.4E-10	1.3E-08	[2], [17] , [13]	[10]
Ru97	97	44	2.9 days	EC, gamma	1.5E-10	1.1E-10		[10]
Ru103	103	44	39.3 days	Beta-, gamma	7.3E-10	3.0E-09		[10]
Ru106	106	44	374 days	Beta-	7.0E-09	6.6E-08	[12]	[10]
Rh99	99	45	16.1 days	EC, gamma	5.1E-10	8.7E-10		[10]
Rh101	101	45	3.3 years	EC, gamma	5.5E-10	2.3E-09	[5], [6], [7] , [13]	[10]
Rh102	102	45	207 days	EC, beta+, beta-, gamma	2.6E-09	1.7E-08	[6]	[10]
Rh102m	102	45	3.7 years	EC, gamma	1.2E-09	7.1E-09		[10]
Rh105	105	45	35.4 hours	Beta-, gamma	3.7E-10	3.5E-10		[10]
Pd100	100	46	3.6 days	EC, gamma	9.4E-10	8.5E-10		[10]
Pd103	103	46	17 days	EC	1.9E-10	3.8E-10		[10]
Pd107	107	46	6.5e6 years	Beta-	3.7E-11	5.9E-10	[13]	[10]
Ag105	105	47	41.2 days	EC, gamma	4.7E-10	8.1E-10		[10]
Ag110m	110m	47	250 days	Beta-, gamma	2.8E-09	1.2E-08		[10]
Ag111	111	47	7.5 days	Beta-	1.3E-09	1.7E-09		[10]
Cd109	109	48	462 days	EC	2.0E-09	8.1E-09	[12]	[10]
Cd115	115	48	53.5 hours	Beta-	1.4E-09	1.1E-09		[10]
Cd115m	115	48	44.6 days	Beta-	3.3E-09	7.7E-09		[10]
In111	111	49	2.8 days	EC	2.9E-10	2.3E-10	[12]	[10]
In114m	114	49	49.5 days	IC, gamma	4.1E-09	9.3E-09		[10]
Sn113	113	50	115 days	EC	7.3E-10	2.7E-09	[12]	[10]
Sn117m	117	50	13.8 days	IC	7.1E-10	2.4E-09		[10]
Sn119m	119	50	293 days	IC	3.4E-10	2.2E-09		[10]
Sn121	121	50	27 hours	Beta-	2.3E-10	2.3E-10		[10]

Sn125	125	50	9.6 days	Beta-, gamma	3.1E-09	3.1E-09	[12]	
Sb120m	120	51	5.7 days	EC, gamma	1.2E-09	1.1E-09		[10]
Sb122	122	51	2.7 days	Beta-, gamma	1.7E-09	1.1E-09		[10]
Sb124	124	51	60 days	Beta-, gamma	2.5E-09	8.6E-09	[12]	[10]
Sb125	125	51	2.7 years	Beta-, gamma	1.1E-09	1.2E-08	[12]	[10]
Sb126	126	51	12.4 days	Beta-, gamma	2.4E-09	3.2E-09		[10]
Sb127	127	51	3.9 days	Beta-, gamma	1.7E-09	1.9E-09		[10]
Te118 [16]	118	52	6 days	EC	2.8E-09	2.3E-09		[10]
Te119m [16]	119	52	4.7 days	EC, gamma	6.7E-10	6.8E-10		[10]
Te121	121	52	16.8 days	EC, gamma	4.3E-10	4.1E-10		[10]
Te121m	121	52	154 days	IC	2.3E-09	5.7E-09		[10]
Te123m	123	52	119 days	IC	1.4E-09	5.1E-09		[10]
Te125m	125	52	57.4 days	IC	8.7E-10	4.2E-09		[10]
Te127m	127	52	109 days	IC, beta-	2.3E-09	9.8E-09		[10]
I125	125	53	59.4 days	EC	1.5E-08	5.1E-09	[2] , [12]	[10]
I126	126	53	12.9 days	Beta+, beta-, gamma	2.9E-08	9.8E-09		[10]
I129	129	53	1.6e7 years	Beta-	1.1E-07	3.6E-08	[17]	[10]
I131	131	53	8 days	Beta-, gamma	2.2E-08	7.4E-09		[10]
Xe127	127	54	36.3 days	EC		9.7E-10	[15]	[10]
Cs129	129	55	32 hours	EC, gamma	6.0E-11	7.7E-11		[10]
Cs131	131	55	9.7 days	EC	5.8E-11	4.7E-11		[10]
Cs132	132	55	6.4 days	Beta+, beta-, gamma	5.0E-10	3.0E-10	[12]	[10]
Cs134	134	55	2.1 years	EC, beta-, gamma	1.9E-08	2.0E-08	[15] , [6] , [12] , [9] , [14]	[10]
Cs136	136	55	13.2 days	beta-, gamma	3.0E-09	2.8E-09	[15]	[10]
Cs137	137	55	30.2 years	beta-, gamma	1.3E-08	3.9E-08	[15] , [12]	[10]
Ba128	128	56	2.4 days	EC, gamma	2.7E-09	1.4E-09		[10]
Ba131	131	56	11.5 days	EC, gamma	4.5E-10	8.7E-10	[15], [14]	[10]
Ba133	133	56	10.5 years	EC, gamma	1.5E-09	1.0E-08	[15] , [5] , [6] , [7] , [12]	[10]
Ba135m	135	56	28.7 hours	IC	4.3E-10	3.6E-10		[10]
La137	137	57	6e4 years	EC	8.1E-11	8.7E-09	[2] , [13]	[10]
La140	140	57	1.7 days	Beta-, gamma	2.0E-09	1.1E-09		[10]
Ce134	134	58	3.2 days	EC	2.5E-09	1.3E-09		[10]
Ce137m	137	58	34.4 hours	IC, beta+	5.4E-10	4.4E-10		[10]
Ce139	139	58	138 days	EC, gamma	2.6E-10	1.9E-09	[12]	[10]
Ce141	141	58	32.5 days	Beta-, gamma	7.1E-10	3.8E-09	[12]	[10]
Nd140	140	60	3.4 days	EC				[10]
Pm143	143	61	265 days	EC, gamma	2.3E-10	1.5E-09	[5] , [6]	[10]
Pm144	144	61	363 days	EC, gamma	9.7E-10	8.2E-09	[7]	[10]
Pm145	145	61	17.7 years	EC	1.1E-10	3.6E-09	[5] , [6] , [7] , [13]	[10]
Pm146	146	61	5.5 years	EC, beta-	9.0E-10	2.1E-08	[7] , [13]	[10]
Pm147	147	61	2.6 years	Beta-	2.6E-10	5.0E-09		[10]

Pm148	148	61	5.3 days	Beta-, gamma	2.7E-09	2.2E-09		[10]
Pm148m	148	61	41.3 days	Beta-, IC	1.7E-09	5.7E-09		[10]
Pm149	149	61	53 hours	Beta-	9.9E-10	7.3E-10		[10]
Sm145	145	62	340 days	EC	2.1E-10	1.6E-09	[5] , [6]	[10]
Sm146	146	62	6.8e7 years	alpha	5.4E-08	1.1E-05	[17] , [13]	[10]
Sm151	151	62	89 years	Beta-	9.8E-11	4.0E-09	[13]	[10]
Sm153	151	62	46.3 hours	Beta-	7.4E-10	6.3E-10		[10]
Eu145	145	63	5.9 days	Beta+, gamma	7.5E-10	5.5E-10		[10]
Eu146	146	63	4.6 days	beta+, gamma	1.3E-09	8.0E-10	[6]	[10]
Eu147	147	63	24.1 days	beta+, alpha, gamma	4.4E-10	1.1E-09	[5] , [6]	[10]
Eu148	147	63	54.5 days	Beta+, alpha, gamma	1.3E-09	2.6E-09	[14]	[10]
Eu149	149	63	93.1 days	EC	1.0E-10	2.9E-10	[6]	[10]
Eu150	150	63	36.9 years	EC, gamma	1.3E-09	5.3E-08	[7] , [13]	[10]
Eu152	152	63	13.5 years	EC, beta-, gamma	1.4E-09	4.2E-08	[15] , [5] , [7] , [12] , [9] , [14]	[10]
Eu154	154	63	8.6 years	beta-, gamma	2.0E-09	5.3E-08	[15] , [5] , [7] , [12] , [9] , [13]	[10]
Gd146	146	64	48.3 days	EC	9.6E-10	6.4E-09	[6]	[10]
Gd147	147	64	38.1 hours	Beta+, gamma	6.1E-10	4.0E-10		[10]
Gd148	148	64	75 years	alpha	5.6E-08	2.6E-05	[2] , [5] , [6] , [7] , [17] , [13]	[10]
Gd149	149	64	9.3 days	beta+, alpha	4.5E-10	7.3E-10	[6]	[10]
Gd150 [16]	150	64	1.8e6 years	alpha	5.3E-08	2.9E-05	[2] , [17] , [13]	[10]
Gd151	151	64	124 days	EC, alpha	2.0E-10	8.6E-10		[10]
Gd153	153	64	240 days	EC, gamma	2.7E-10	2.1E-09	[5] , [6] , [12]	[10]
Tb153	153	65	2.3 days	Beta+, gamma	2.5E-10	1.9E-10		[10]
Tb155	155	65	5.3 days	EC, gamma	2.1E-10	2.2E-10	[5]	[10]
Tb156	156	65	5.4 days	EC, gamma	1.2E-09	1.2E-09		[10]
Tb157	157	65	71 years	EC	3.4E-11	1.2E-09	[2], [5], [6] , [13]	[10]
Tb158	158	65	180 years	EC, beta-, gamma	1.1E-09	4.6E-08	[5], [7] , [13]	[10]
Tb160	160	65	72 days	Beta-, gamma	1.6E-09	7.0E-09	[12]	[10]
Tb161	161	65	6.9 days	Beta-	7.2E-10	1.3E-09	[12]	
Dy154 [16]	154	66	3e6 years	Alpha	5.7E-08	1.1E-05	[2] , [17] , [13]	[10]
Dy159	159	66	144 days	EC	1.0E-10	3.7E-10		[10]
Dy166	166	66	81.6 hours	Beta-, gamma	1.6E-09	1.9E-09		[10]
Ho163 [16]	163	67	4570 years	EC	6.8E-12	2.4E-10	[2], [5], [6] , [13]	[10]
Ho166m	166	67	1.2 years	Beta-, gamma	1.6E-11	1.2E-07		[10]
Er160	160	68	28.6 h	EC			[5]	[10]
Er169	169	68	9.4 days	Beta-	3.7E-10	1.0E-09		[10]
Tm165 [16]	165	69	30 hours	beta+, gamma	3.4E-10	3.0E-10	[5] , [6]	[10]
Tm167	167	69	9.3 days	EC	5.6E-10	1.1E-09	[5] , [6]	[10]
Tm168 [16]	168	69	93.1 days	Beta+, gamma	1.0E-09	3.1E-09		[10]
Tm170	170	69	129 days	Beta-	1.3E-09	7.0E-09	[12]	[10]

Tm171	171	69	1.9 years	beta-	1.1E-10	1.4E-09	[5] , [6] , [13]	[10]
Tm172	172	69	63.6 hours	Beta-	1.7E-09	1.1E-09		[10]
Yb166	166	70	56.7 hours	EC, gamma	9.5E-10	7.7E-10	[5] , [6]	[10]
Yb169	169	70	32 days	EC, gamma	7.1E-10	3.0E-09	[5] , [6] , [12]	[10]
Yb175	175	70	4.2 days	Beta-, gamma	4.4E-10	7.3E-10		[10]
Lu169	169	71	34 hours	beta+, gamma	4.6E-10	3.8E-10	[5] , [6]	[10]
Lu170	170	71	2 days	EC	9.9E-10	6.6E-10	[5] , [6]	[10]
Lu171	171	71	8.2 days	beta+, gamma	6.7E-10	8.8E-10	[5] , [6]	[10]
Lu172	172	71	6.7 days	beta+, gamma	1.3E-09	1.6E-09	[2] , [5] , [6] , [7]	[10]
Lu173	173	71	1.37 years	EC, gamma	2.6E-10	2.4E-09	[2] , [5] , [6] , [7] , [13]	[10]
Lu174	174	71	3.3 years	EC	2.7E-10	4.2E-09	[5] , [6] , [7] , [13]	[10]
Lu174m	174	71	142 days	IC, EC	5.3E-10	4.2E-09		[10]
Lu177	177	71	6.6 days	Beta-, gamma	5.3E-10	1.2E-09		[10]
Lu177m	177	71	160 days	Beta-, IC	1.7E-09	1.6E-08		[10]
Hf172	172	72	1.9 years	EC, gamma	1.0E-09	3.2E-08	[2] , [5] , [6] , [7] , [12] , [13]	[10]
Hf173	173	72	24 hours	Beta+, gamma	2.3E-10	1.6E-10	[5] , [6]	[10]
Hf175	175	72	70 days	EC, gamma	4.1E-10	1.2E-09	[2] , [5] , [6]	[10]
Hf178m	178	72	31 years	gamma	4.7E-09	2.6E-07	[6]	[10]
Hf181	181	72	42.4 days	Beta-, gamma	1.1E-09	5.0E-09		[10]
Ta177	177	73	56.6 hours	EC	1.1E-10	1.1E-10	[5] , [6]	[10]
Ta179	179	73	1.8 years	EC	6.5E-11	5.6E-10	[2] , [5] , [6] , [7] , [13]	[10]
Ta182	182	73	114 days	beta-, gamma	1.5E-09	1.0E-08	[5] , [6] , [12]	[10]
Ta183	183	73	5.1 days	beta-, gamma	1.3E-09	2.1E-09	[5] , [6]	[10]
W178	178	74	21.6 days	EC	2.2E-10	7.2E-11	[5] , [6]	[10]
W181	181	74	121 days	EC	7.6E-11	2.7E-11	[2] , [5] , [6]	[10]
W185	185	74	75.1 days	beta-	4.4E-10	1.2E-10	[2] , [5] , [6]	[10]
W187	187	74	23.7 hours	beta-, gamma	6.3E-10	1.9E-10	[5] , [6]	[10]
W188	188	74	69.8 days	Beta-	2.1E-09	5.7E-10		[10]
Re182	182	75	64 hours	Beta+, gamma	1.4E-09	1.2E-09		[10]
Re183 [16]	183	75	70 days	EC, gamma	3.2E-10	2.4E-09		[10]
Re184	184	75	38 days	EC, gamma	1.0E-09	1.9E-09		[10]
Re184m	184	75	169 days	IC, beta+	1.5E-09	6.5E-09		[10]
Re186	186	75	3.7 days	Beta-. EC	1.5E-09	1.1E-09		[10]
Os185	185	76	93.6 days	EC	5.1E-10	1.6E-09	[12]	[10]
Ir192	192	77	73.8 days	Beta-, EC	1.4E-09	6.6E-09	[12]	
Au198	198	79	2.7 days	Beta-, gamma	1.0E-09	8.6E-10	[12]	
Au199	199	79	3.2 days	Beta-, gamma	1.3E-09	7.9E-10	[12]	
Hg203	203	80	46.6 days	Beta-, gamma	1.9E-09	2.4E-09	[12]	
Pb210	210	82	22.3 years	Beta-, gamma	6.9E-07	5.6E-06	[12]	
Bi207	207	83	31.5 years	Beta+, gamma	1.3E-09	5.6E-09	[12]	
Th228	228	90	1.9 years	alpha	7.2E-08	4.0E-05	[12]	

Np239	239	93	2.4 days	Beta-, gamma	8.0E-10	1.0E-09	[12]	
Am241	241	95	432 years	SF, alpha	2.0E-07	9.6E-05	[12]	
Am243	243	95	7370 years	SF, alpha	2.0E-07	9.6E-05	[12]	

[1] Eckerman K Fau - Harrison, J., Harrison J Fau - Menzel, H.G., Menzel Hg Fau - Clement, C.H., Clement, C.H. *ICRP Publication 119: Compendium of dose coefficients based on ICRP Publication 60.* 2012.

[2] *ESS technical design report.* . http://docdb01.esss.lu.se/DocDB/0002/000274/007/TDR_online_ver_ch10.pdf. 2013.

[3] Naoteru Odano, J.O.J., Harrington, R.M., DeVore, J.R. *Shielding and Activation Analyses in Support of The Spallation Neutron Source (SNS) ES&H Requirements.* http://citeseerx.ist.psu.edu/viewdoc/download;jsessionid=BEC89FE8E4714CACBE444F0229CD2313?doi=10.1.1.539.8779&rep=rep1&type=pdf.

[4] Thomas, R.H., Stevenson, G.R., *Radiological Safety Aspects of the Operation of Proton Accelerators*. International Atomic Energy Agency. 1986.

[5] Findlay, D.J.S., Škoro, G.P., Burns, G.J., Ansell, S. *Experimental verification of spallation inventory calculations.* Applied Radiation and Isotopes, 125: 1-3, 2017.

[6] Mora, T., Sordo, F., Aguilar, A., Mena, L., Mancisidor, M., Aguilar, J., Bakedano, G., et al. *An evaluation of activation and radiation damage effects for the European Spallation Source Target.* Journal of Nuclear Science and Technology, 55(5): 548-558, 2018.

[7] Kókai, Z., Török, S., Zagyvai, P., Kiselev, D., Moormann, R., Börcsök, E., Zanini, L., et al. *Comparison of different target material options for the European Spallation Source based on certain aspects related to the final disposal.* Nuclear Instruments and Methods in Physics Research Section B: Beam Interactions with Materials and Atoms, 416: 1-8, 2018.

[8] Ene, D., Mathias, B., Mohammad, E., Mats, L., Steve, P., Hakan, H.A.H.N. *Radiation Protection Studies for ESS Superconducting Linear Accelerator.* Progress in NUCLEAR SCIENCE and TECHNOLOGY, 2: 382-388, 2011.

[9] Miura, T., Bessho, K., Ishihama, S., Ohtsuka, N. *Migration of radionuclides induced in the soil below the 12 GeV proton accelerator facility at KEK.* Journal of Radioanalytical and Nuclear Chemistry, 255(3): 543-546, 2003.

[10] Ene, D. *Source Term to the environment from the Target Station.* ESS-0018859. ESS. 2016.

[11] Mauro, E. *Radiation protection studies for CERN Linac4/SPL accelerator complex.* 199-199, 2009.

[12] Bungau, C., Bungau, A., Cywinski, R., Barlow, R., Edgecock, T.R., Carlsson, P., Danared, H., et al. *Induced activation in accelerator components.* Phys. Rev. ST Accel. Beams, 17: 084701-084701, 2014.

[13] Shetty, N.V. *Study of particle transport in a high power spallation target for an accelerator driven transmutation system*. Aachen University. Report,2013.

[14] Oishi, K., Nakao, N., Kosako, K., Yamakawa, H., Nakashima, H., Kawai, M., Yashima, H., et al. *Measurement and analysis of induced activities in concrete irradiated using high-energy neutrons at KENS*

neutron spallation source facility. Radiation Protection Dosimetry, 115(1-4): 623-629, 2005.

[15] La Torre, F.P. *Study of induced radioactivity in proton accelerator facilities*. CERN. Report,2014.

[16] Endo, A., Yamaguchi, Y. *Dose coefficients for intakes of radionuclides by workers: Coefficients for radionuclides not listed in ICRP Publication 68.* JAERI-Data/Code--99-047. Japan. http://inis.iaea.org/search/search.aspx?orig_q=RN:31026890. 1999.

[17] Stankovsky, A., Saito, M., Artisyuk, V., Shmelev, A., Korovin, Y. *Accumulation and Transmutation of Spallation Products in the Target of Accelerator-Driven System.* Journal of Nuclear Science and Technology, 38(7): 503-510, 2001.

Appendix 2. Procedure tritium in air and precipitation

Department of Physics
Division of Nuclear Physics
The Biospheric and Anthropogenic Radioactivity (BAR) group

Procedure: Collection of precipitation and air humidity and subsequent measurement of waterborne tritium (HTO)

Authors	Kristina Eriksson Stenström	Professor Division of Nuclear Physics Lund University
	Guillaume Pedehontaa-Hiaa	PhD, Researcher Division of Nuclear Physics Medical Radiation Physics, ITM Lund University
	Vytenis Barkauskas	PhD, Post-doc Division of Nuclear Physics Lund University
Reviewed by	Christopher Rääf	Associate Professor Medical Radiation Physics, ITM
	Daniela Ene	PhD, Senior Scientist Environment, Health and Safety European Spallation Source ESS-ERIC
Approved by	Dirk Rudolph	Professor, Head of Division Division of Nuclear Physics

Department of Physics
Division of Nuclear Physics
Professorsgatan 1
SE-223 63 Lund, SWEDEN

Report BAR-2018/02

Lund 2018

Contents

1. Purpose

The purpose of the procedure is to describe the necessary steps for measurement of the activity of tritium (^{3}H) in the atmospheric water vapour and in precipitation, i.e.:

- sampling of atmospheric water vapour and sampling of precipitation;
- sample preparation;
- measurement of tritium using Liquid Scintillation Counting (LSC);
- data analysis to produce the final results as activity concentration of tritium in precipitation and air humidity.

The procedure was applied to the background measurements of tritium reported in Ref [1]. The procedure may be applied to future measurements of tritium-containing water in air and precipitation at the ESS site and surroundings in the frame of the ESS Ambient Control Program to be endorsed by the Swedish Radiation Safety Authority (SSM).

2. Procedure applicability

The procedure is applicable to environmental sampling of water from precipitation (continuous sampling) and air (occasional sampling). The activity concentration of waterborne tritium (HTO) is measured with LSC. The procedure is applicable to measurements of tritium in the ESS site area both prior to and after start of operation of the ESS facility in order to assess the background and the radiological impact of ESS.

The air humidity sampler must not be used during rainy weather conditions. For continuous monitoring of tritium in air during operation of the ESS facility, a commercially available tritium air sampler, collecting water vapour as well as hydrogen gas, is recommended.

3. Sampling of water from air and precipitation

3.1. Procedure map

The procedure map is shown in Figure 1.

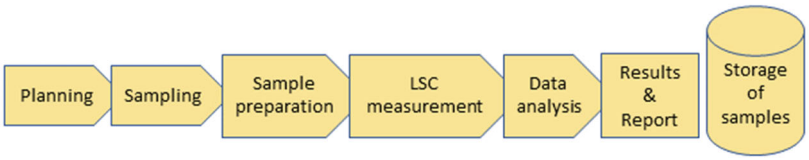

Figure 1: Procedure map.

3.2. Procedure details

Details of the procedure map (planning and sampling) are shown in Figure 2.

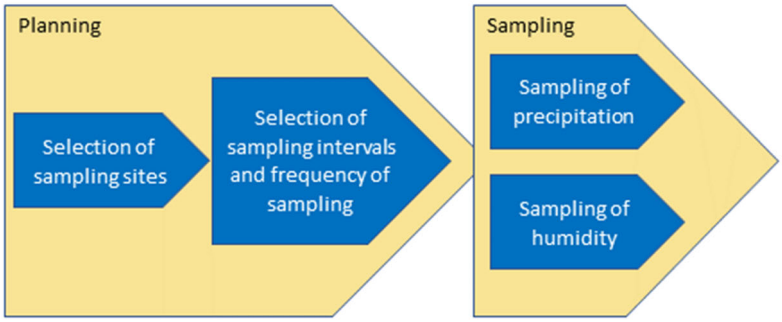

Figure 2: Details of the procedure map (planning and sampling).

3.2.1. Input

The input to the procedure is water-borne tritium in precipitation and air.

3.2.2. Planning	
Several criteria for selection of the sampling sites and time intervals are analysed prior to sampling. For sampling of precipitation, the sampling site within the ESS area should be selected considering the recommendations in the IAEA/GNIP precipitation sampling guide [2]. In	**Responsible:** Radiological expert

particular, the influence from structures should be minimized, e.g. by keeping trees and buildings at least as far away as they are high [2]. The sampling location should preferably be within the fenced area to minimize the risk of e.g. theft.

For sampling of air humidity, the site should preferably not be in the immediate vicinity of very busy roads (to reduce influence from water vapour produced in combustion engines). The sampling of air humidity requires access to 230 V. Sampling of air humidity for background measurements should strive to cover different weather conditions, wind directions and seasons. During operation of the facility, it is recommended to sample air humidity in the upwind as well as in the downwind direction of the ESS site.

Preferably, precipitation samples as well as air humidity samples should also be collected occasionally at an urban background site.

Intervals for continuous sampling of precipitation are preferably 1 month as recommended by GNIP [2], unless the purpose of the measurements gives rise to another sampling frequency (e.g. at changes in operating conditions of the facility).

For sampling of air humidity, it should not rain, since the sampler is not designed for such weather conditions. Therefore, the weather forecast must be consulted when deciding the sampling date. If possible, sampling of air humidity should be performed at the monthly emptying of the precipitation collector.

Output/product	Selection of sites. Selection of sampling intervals for precipitation. Selection of dates for collection of air humidity.

3.2.3. Sampling

Sampling of precipitation

Responsible:

Radiological expert and/or technician

Sampling

Equipment: Precipitation is sampled using a rain collector from Palmex (Croatia) (Standard Rain Sampler RS1, including a siphon inlet) [3]. The sampler can be equipped with a funnel of diameter 13.5 cm or 23 cm for rain sampling. The larger funnel is commonly being used for rain sampling. During winter months a snow tube (diameter 15 cm, height 52 cm) is placed on top of the smaller funnel to assure representative sampling of snow. Water from the precipitation enters a 3 L plastic bottle through the funnel and the plastic siphon tube (reaching the bottom of the 3 L flask). A spare bottle with lid is available and used when emptying the sampler (bottles are switched). This dip-in sampler (and the sampling site) fulfils the recommendations of the IAEA/GNIP precipitation sampling guide [2]. The sampler is mounted on a metal stand (see Figure 3).

Figure 3: The Palmex rain sampler RS1, equipped with the 23 cm funnel.

Sampling of precipitation

Method: At the time of retrieving a precipitation sample, the bottle with the precipitation is unscrewed from below, and the flask is closed with the associated lid. The spare bottle is attached to the sampler. The water is taken to the lab where it is transferred to one or several 500 ml water collection bottles (water sampling bottle, sterile, VWR collection, art no 331-0063) using a dedicated funnel. The water is weighed. The sterile water flask is labelled with sampling date interval, amount of collected water, sampling site (T#), sample number (P#) and signature of the person performing the task. The sterile water flasks with the precipitation is stored in a refrigerator at 4°C at the sample preparation laboratory. The 3 L plastic flask

is washed with distilled water and dried. All sampling data should be stored.

Sampling of air humidity

Responsible: Radiological expert and/or technician

Sampling of humidity

Equipment: For sampling of air humidity, a dehumidifier from Wood's (Wood's MRD10, Woods, Canada) [4] is used, see Figure 4. A 24 cm long plastic tubing (inner diameter 8 mm) is connected to the water outlet of the dehumidifier. A sterile 500 ml water collection bottle (VWR collection, art no 331-0063) is used for collection of condensed water vapour. A cable approved for outdoor use shall be used to connect the dehumidifier to a 230 V power supply. Temperature and air humidity are monitored during sampling.

Figure 4: The air humidity sampler Wood's MRD10 located in front of the Palmex rain sampler.

Method: The sampler is transported to the sample collections site by car at the time of sampling. The sampler is placed in a plastic storage box (the red box in Figure 4), which also have space available for the sample collection flask. When sampling at the rain collector, a tray is placed at the base of the metal rack of the rain collector to stabilize the box with the humidity sampler. The dehumidifier is secured onto the metal rack by using straps. If the sampler is used elsewhere, it is suitable to place the sampler and the plastic storage box on a portable table.

The free end of the plastic tubing (the tubing that is attached to the water outlet of the dehumidifier) is put into a 500 ml sample collection bottle (also placed in the red storage box in Figure 4). Care should be taken to protect the socket (connecting the dehumidifier and extension cable) from any water (e.g. by keeping the socket in a water-tight plastic bag).

The dehumidifier is started by pressing the start button (ON/OFF). The mode should be “Continue” (select at HUM ID button), which refers to continuous sampling. Air humidity and temperature are noted at the beginning and at the end of the sampling. The time of sampling depends on the temperature and relative humidity (and possibly on wind speed). In general: sample for 1 hour and then check the amount of water collected, either by visually inspecting the sample or by weighing the sample (at least 20 g of water should be collected).

Switch off the dehumidifier when the sampling is complete. Wait for at least 5 minutes, and then carefully tilt the dehumidifier towards the water sampling bottle to allow water condensed inside the dehumidifier to enter the water sample bottle. The water inside the dehumidifier may also be frozen, which require some additional time for thawing (the dehumidifier is however equipped with a defrosting function, which may be activated during sampling). Remove the water sampling flask, put on the lid, weigh the sample and label the flask with sampling date, sampling interval, amount of collected water, sampling site (T#), sample number (H#) and signature of the person performing the task. The sterile water flasks with the condensed water vapour are stored in a refrigerator at 4°C in the sample preparation laboratory until analysis. All sampling data should be stored, including temperature, air humidity, wind speed and wind direction at the time at sampling (the two latter obtained from a nearby weather station).

Output/product	Water samples from precipitation (integrated sampling). Samples of air moisture (occasional sampling).

3.2.4. Sample preparation

The precipitation samples are filtrated using filter paper to remove small plant or soil pieces that could have entered the collection bottle. The humidity samples are filtrated if collected at very dry and windy conditions.

10 mL of the filtrate is mixed with 10 mL of Ultima Gold LLT LSC cocktail in a 20 mL LSC plastic vial, the vial is shaken for 2 min and stored for 48 h in the dark to reduce chemical quenching before LSC measurement.

Background samples are prepared following the same procedure but with 10 mL of tritium depleted water (also called old water). Such water can be obtained from a deep well at Grevie (N55.6131, E13.1970) - operated by VA Syd - with a well-documented low HTO concentration (well 8 in Ref [5]).

Responsible:

Technician

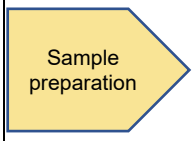

Standard samples are prepared using 10 mL of the same tritium depleted water added with known amounts of tritium from a reference solution (TRY44 number R8/12/123 by Eckert and Ziegler, Germany).	
Output/product	Filtered water samples mixed with scintillation cocktail, ready for measurement.

3.2.5. LSC analysis

The samples are analyzed in a LSC liquid scintillation counter according to the instructions given by the manufacturer of the instrument. The basic output of the analysis is instrument-dependant. However, in general an LSC instrument provides counts per minute (cpm), the statistical uncertainty of this count (%) and the counting efficiency. Measurements of the standards serve as quality insurance of the LSC results.

Responsible:

Radiological expert

LSC measure-ment

Output/product	Counts per minute (cpm) including statistical uncertainty and counting efficiency of the measurements of unknowns, standards and background.

3.2.6. Calculations

The following should be performed with an external computer if the LSC instrument is not equipped to post-process the results.

Responsible:

Radiological expert

MDA

The minimum detectable activity, *MDA* (Bq/L), is calculated according to equation (2) [6]:

$$MDA = \frac{3.29 \cdot \sqrt{\left(\frac{cpm_b}{t_s}\right) + \left(\frac{cpm_b}{t_b}\right) + \left(\frac{2.71}{t_s}\right)}}{60 \cdot E \cdot V} \qquad (1)$$

where cpm_b is the count rate of the background (cpm), t_s is the measurement time of the sample (min), t_b is the measurement time of the background (min), E is the efficiency and V is the sample volume (L).

Data analysis

Results & Report

Tritium activity concentration in precipitation

The tritium activity concentration A in precipitation in Bq/L is calculated according to equation (1):

$$A = \frac{cpm_s}{60 \cdot V \cdot E_s} - \frac{cpm_b}{60 \cdot V \cdot E_b} \quad (2)$$

where cpm_s is the count rate of the sample, E_s is the counting efficiency of the sample, cpm_b is the count rate of the background, E_b is the counting efficiency of the background and V is the volume (L).

Tritium activity concentration in air humidity

The relative humidity RH is given by:

$$RH = \frac{p}{p_{sat}} \quad (3)$$

where p is the partial water vapour pressure in air (Pa) and p_{sat} is the saturated vapour pressure over water (Pa). Tetens' equation provides the saturated vapour pressure over water, p_{sat}, given in Pa [7]:

$$p_{sat} = 610.78 \cdot e^{\left(\frac{17.27 \cdot T_{°C}}{T_{°C}+237.3}\right)} \quad (4)$$

where $T_{°C}$ is the temperature in °C.

The ideal gas law states

$$p \cdot V = \frac{m}{M} \cdot R \cdot T \quad (5)$$

where V is the volume, m is the mass, M is molar mass of water vapour ($18.015 \cdot 10^{-3}$ kg/mol), R is the gas constant (8.314 J/(mol·K)) and T is the temperature in K.

The absolute humidity AH is given by:

$$AH = \frac{m}{V} \quad (6)$$

Using equations (3)-(6) above, AH (kg/m^3) can be written as:

$$AH = \frac{m}{V} = \frac{p \cdot M}{R \cdot T} = \frac{RH \cdot p_{sat} \cdot M}{R \cdot T}$$
$$= \frac{RH \cdot M}{R \cdot T} \cdot 610.78 \cdot e^{\left(\frac{17.27 \cdot T_{°C}}{T_{°C}+237.3}\right)} \quad (7)$$

The tritium activity concentration in air humidity, A_{air} (Bq/m^3) is finally given by:

$$A_{air} = \frac{AH \cdot A}{\rho} \quad (8)$$

where A is the measured activity concentration of water (Bq/L) and ρ is the density of water (1.0 kg/L).

Uncertainty in LSC measurement

The uncertainty in the results is dominated by the statistical uncertainty in the count rates of the sample and background. Uncertainties introduced in volume and efficiency measurements are negligible compared to the statistical uncertainty in the number of counts. The total calculated uncertainty (σ_{calc}) in the activity concentration considers the uncertainty of the sample as well as the background:

$${\sigma_A}^2 = \left(\frac{\partial A}{\partial cpm_s}\right)^2 \cdot {\sigma_{cpm_s}}^2 + \left(\frac{\partial A}{\partial cpm_b}\right)^2 \cdot {\sigma_{cpm_b}}^2 \quad (9)$$

Thus,

$$\sigma_A = \frac{1}{60 \cdot V}\left(\left(\frac{\sigma_{cpm_s}}{E_s}\right)^2 + \left(\frac{\sigma_{cpm_b}}{E_b}\right)^2\right)^{0.5} \quad (10)$$

The statistical uncertainty in counts *(cpm·t)* of a measurement equals *(cpm·t)*$^{0.5,}$ thus:

$$\sigma_{cpm} = \frac{(cpm \cdot t)^{0.5}}{t} = \left(\frac{cpm}{t}\right)^{0.5} \quad (11)$$

and

$$\sigma_A = \frac{1}{60 \cdot V}\left(\frac{cpm_s/t_s}{{E_s}^2} + \frac{cpm_b/t_b}{{E_b}^2}\right)^{0.5} \quad (12)$$

Uncertainty in activity concentration of air humidity The uncertainty in the calculation of A_{air} is believed to be associated with a) the measurement of the relative humidity *RH*, and b) isotope fractionation during the condensation process. a) The uncertainty in the measurement of the relative humidity RH is conservatively estimated to be 10 % (depending on the instrument used). b) Isotope fractionation during condensation depends on several factors, such as relative humidity and condensation temperature [8]. In laboratory tests on condensation of water vapour, performed by Deshpande et al [8], the molar concentration of deuterium (^{2}H) was on average 1.5% higher in the condensate than in the vapour of ambient air (condensation temperature 0 °C). Maximum observed relative molar excess of ^{2}H was 4% [8]. Assuming that the isotope fractionation of tritium is of the same order of magnitude as for ^{2}H, the concentration of tritium may be up to 8% higher in the liquid phase than in the vapour (with the experimental conditions of Ref. [8]). Using a conservative approach, the uncertainty due to isotope fractionation during condensation is estimated to be 15%. The final uncertainty in the HTO activity concentration of air humidity includes the uncertainty of the LSC measurement as well as in *RH* and isotope fractionation.	
Output/product	Activity concentrations of tritium in precipitation (in Bq/L) and air (in Bq/m^3). If the sample activity concentration is below the *MDA*, the value is presented as "< *MDA*"). The results shall be presented in a written report, which includes quality assessment of the measurements and interpretation of the results.

3.2.7. Storage of samples	
Sample material remaining after LSC analysis is stored according to recommendations by SSM [9].	**Responsible:** Radiological expert 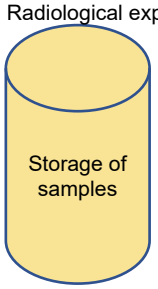
Output/product	The procedure guarantees that sample material is available until the data has been disseminated.

4. Acknowledgement

The authors thank Associate Professor Christopher Rääf, Medical Radiation Physics (Malmö) and Dr Daniela Ene, ESS, for constructive reviewing of the report.

5. References

[1] Eriksson Stenström, K., Pedehontaa-Hiaa, G., Barkauskas, V. *Tritium in precipitation and air humidity at the European Spallation Source (ESS) site: results from measurements in the spring of 2018.* BAR-2018/03. Lund University, Department of Physics, Division of Nuclear Physics. 2018.

[2] IAEA/GNIP. *IAEA/GNIP precipitation sampling guide.* Accessed: 2018-05-02. Available from: http://www-naweb.iaea.org/napc/ih/documents/other/gnip_manual_v2.02_en_hq.pdf.

[3] Palmex. Accessed: 2018-06-13. Available from: http://www.rainsampler.com/portfolio-page/rain-sampler-rs1/.

[4] Wood's. Accessed: 2018-06-13. Available from: https://woods.se/en/Produkter/dehumidifiers/woods-mrd10/.

[5] Åkesson, M., Suckow, A., Visser, A., Sültenfuβ, J., Laier, T., Purtschert, R., Sparrenbom, C.J. *Constraining age distributions of groundwater from public supply wells in diverse hydrogeological settings in Scania, Sweden.* Journal of hydrology, 528: 217-229, 2015.

[6] Currie, L.A. *Limits for qualitative detection and quantitative determination. Application to radiochemistry.* Analytical chemistry, 40(3): 586-593, 1968.

[7] Tetens, O. *Über einige meteorologische Begriffe.* Zeitschrift für Geophysik, 6: 207-309, 1930.
[8] Deshpande, R.D., Maurya, A.S., Kumar, B., Sarkar, A., Gupta, S.K. *Kinetic fractionation of water isotopes during liquid condensation under super-saturated condition.* Geochimica et Cosmochimica Acta, 100: 60-72, 2013.
[9] *Special conditions for the ESS facility in Lund.* Vers. 2, ESS-0018828. Swedish Radiation Safety Authority. 2015.

Appendix 3. Isotope fractionation to take into account in analysis of tritium

Department of Physics
Division of Nuclear Physics
The Biospheric and Anthropogenic Radioactivity (BAR) group

Isotope fractionation to take into account in analysis of tritium

Kristina Eriksson Stenström	kristina.stenstrom@nuclear.lu.se
Guillaume Pedehontaa-Hiaa	Guillaume.pedehontaa-hiaa@med.lu.se

Department of Physics
Division of Nuclear Physics
Professorsgatan 1
SE-223 63 Lund, SWEDEN

Report BAR-2019/01

Lund 2019

Contents

Terminology

Isotopes: Atoms of the same element (the same number of protons, i.e. atomic number *Z*) with different number of neutrons (*N*), i.e. with different mass numbers (*A*). E.g., three isotopes of hydrogen occur in nature: protium (^{1}H or H, with one proton and no neutrons), deuterium (^{2}H or D, with one proton and one neutron) and tritium (^{3}H or T, one proton and two neutrons).

Isotopologue: Molecules that differ only in isotopic composition. E.g., water has 18 naturally occurring isotopologues ($H_2{}^{16}O$, $H_2{}^{17}O$, $H_2{}^{18}O$, $HD^{16}O$, $HD^{17}O$, $HD^{18}O$, $HT^{16}O$, $HT^{17}O$, $HT^{18}O$, $DD^{16}O$, $DD^{17}O$, $DD^{18}O$, $DT^{16}O$, $DT^{17}O$, $DT^{18}O$, $TT^{16}O$, $TT^{17}O$, $TT^{18}O$)

Mass isotopomers: isotopologues that have the same mass (e.g. $H_2{}^{18}O$, $HD^{17}O$, $HT^{18}O$).

1. Introduction

In an ongoing project entitled “Strengthening competence at Lund University for measurement and analysis of ESS-specific radionuclides” - financed by the Swedish Radiation Safety Authority, SSM (project number SSM2018-1636) - we assess the tritium concentrations in various environmental matrixes in the Lund area before start of the ESS facility. Sample types include drinking water, precipitation and air humidity, and previous measurements have also been performed on water from sewage sludge and vegetation. We also measure tritium in human urine. The purpose of this brief report is to assess to what extent isotope fractionation that can influence the results of measurements of tritium. The isotope fractionation may be due to natural processes or result from the sample preparation. The main focus of the report is on isotope fractionation that can occur during collection of water vapour using methods employing condensation [1]. Furthermore, it presents results of isotope fractionation during distillation of urine and freeze-drying of sewage sludge.

The report also briefly describes isotope fractionation of water in the hydrological cycle.

2. Isotope fractionation

Isotopes of the same elements are characterized by differences in the number of neutrons in the nucleus. This results not only in differences in mass between the various isotopes, but also in slightly different physical and chemical properties. Isotope fractionation, partly favouring the transfer of one isotope to another of a specific element, occurs in various processes in nature, such as physical phase transitions (e.g. evaporation and condensation in the hydrological cycle), chemical reactions (e.g. oxidation of hydrogen gas to water), diffusion and uptake in biological systems (e.g. uptake of hydrogen isotopes in man). Light elements, such as hydrogen, with a large mass difference between its isotopes, generally suffer more from the isotope fractionation effect than heavier elements. Thus, for the lightest element of the periodic table, hydrogen, isotope fractionation can be significant [2, 3].

Two types of fractionation processes mainly occur: a) equilibrium fractionation (or isotope exchange) and b) kinetic fractionation [3]. Since isotope fractionation occurring in nature is a combination of equilibrium and kinetic fractionation, it should be treated as non-equilibrium fractionation [2].

2.1. Equilibrium fractionation

Equilibrium fractionation is of quantum mechanical origin and occurs only at chemical equilibrium, i.e. in reversible reactions, and varies with the strength of the chemical bonding and the temperature [4]. Equilibrium fractionation can occur between two different substances and between separate phases of the same substance.

The total energy of a molecule, E_{tot}, is given by:

$$E_{tot} = E_{elec} + E_{trans} + E_{rot} + E_{vib} \quad (1)$$

where E_{elec} is the electronic energy, E_{trans} is the translational energy, E_{rot} is the rotational energy and E_{vib} is the vibrational energy, respectively. The latter, molecular vibration, is the main cause of equilibrium isotope fractionation [2]. The vibrational bond energy depends on the masses of the atoms in a molecule, and generally increases with increasing mass. A molecule containing a light isotope thus possesses a higher vibrational energy than a heavier isotope, and the lighter isotope is not as strongly bound as the heavy one. This drives lighter isotopologues to react slightly more frequent than heavier isotopologues.

The isotope fractionation between two phases (e.g. liquid and gas) is, in certain cases, depending only on temperature [5]. The isotopic ratios of raindrops in clouds are mainly determined by equilibrium fractionation. Generally, increasing temperature leads to decreasing fractionation ($\propto 1/T^2$) [5]. Isotope exchange reactions are typical equilibrium reactions.

2.2. Kinetic fractionation

Kinetic fractionation is irreversible, and occurs in processes such as diffusion, evaporation and in chemical reactions when chemical bonds are broken. Furthermore, the kinetic isotope effects are often larger than the equilibrium effects [5]. The processes leading to kinetic fractionation are generally fast, incomplete and proceeding only in one direction (one reservoir suffers from continuous losses) [5]. Photosynthesis is a typical such example. The condensation method of collection air moisture in Refs [1, 6] is a typical example where kinetic fractionation can occur.

According to kinetic gas theory, the average kinetic energy per atom or molecule is equal for all gases at a specific temperature. Consequently, a heavier isotopologue has – due to its higher mass – a lower molecular speed than the lighter isotopologue. The lower speed of the heavier isotopologue leads to slower diffusion and relatively fewer collisions with other molecules than for the lighter isotopologue. Therefore, the heavier isotopologue generally reacts slower than the lighter isotope.

One example relates to evaporation of water into unsaturated air. Due to its higher speed, a lighter isotopologue evaporates more easily than a heavier isotopologue. Thus, a heavier isotopologue becomes enriched in the liquid phase, whereas the lighter isotopologue is more abundant in gaseous phase. For water, this means that the liquid phase becomes enriched in the heavier isotopes. This is reflected in various vapour pressures of molecules with different hydrogen isotopes of water [4, 7]: the vapour pressure is lower for HTO than for HDO, which in turn is lower than the vapour pressure for H_2O. Consequently, the boiling point at normal pressure is thus higher for $HD^{16}O$ (100.75±0.05 °C) as well as for $HT^{16}O$ (100.8±0.1 °C) than for H_2O [8].

3. Isotope fractionation units and standards

3.1. Isotope fractionation units

Several quantities and units are used related to isotope fractionation (Table 1).

Table 1: Some quantities related to isotope fractionation.

Quantity	Denotation/definition	Eq.
Number of atoms	N	
Isotope ratio (R)	$R = \frac{N(heavier\ isotope)}{N(lighter\ isotope)}$	(2)
Relative difference of isotope ratios (isotope delta or δ)	$\delta = \left(\frac{R_{reactant} - R_{product}}{R_{product}}\right) \cdot 1000$	(3)
Relative difference of isotope ratios in sample x relative a standard (std)	$\delta = \left(\frac{R_x - R_{std}}{R_{std}}\right) \cdot 1000$	(4)
For hydrogen: Relative difference of isotope ratios relative a standard, VSMOW, Vienna Standard Mean Ocean Water (δD, δ^2H)	$\delta D = \frac{R_{sample} - R_{VSMOW}}{R_{VSMOW}} \cdot 1000$	(5)
For equilibrium fractionation, isotopic fractionation factor (α)	$\alpha = \frac{R_{product}}{R_{reactant}}$	(6)
For equilibrium fractionation, isotopic fractionation between any two phases	$\alpha_{A-B} = \frac{R_A}{R_B} = \frac{\delta_A + 1000}{\delta_B + 1000}$	(7)
For equilibrium isotopic fractionation, isotopic enrichment factor, discrimination, isotopic discrimination or isotopic fractionation constant (ε):	$\varepsilon = \alpha - 1$	(8)

3.2. Standards for δD measurements

Some commonly used standard materials for δD assessments are listed in Table 2.

Table 2: Common standards for δD measurements.

Standard	$R = {}^2H/{}^1H$ (10^6 x isotope amount ratio)	δD (‰)
VSMOW (Vienna Standard Mean Ocean Water)	155.76	0
SLAP (Standard Light Antarctic Precipitation, water)	89.02	-428
GISP (Greenland Ice Sheet Precipitation)	89.12	-189.7

4. The hydrological cycle

4.1. δD values found in precipitation and waters

The δD value in precipitation mainly depends on a) the temperature and b) the proportion of the original water vapour that remains in the air parcel water and that is being precipitated [9]. This leads to the so-called continental effect: the greater distance from the source of the vapour, the more depleted in δD the precipitation becomes. The heavier isotopes are thus rained out as the air parcel is moving inlands, making the vapour isotopically lighter, and thus also the precipitation more depleted in δD. The principle of the continental effects is visualized in Figure 1.

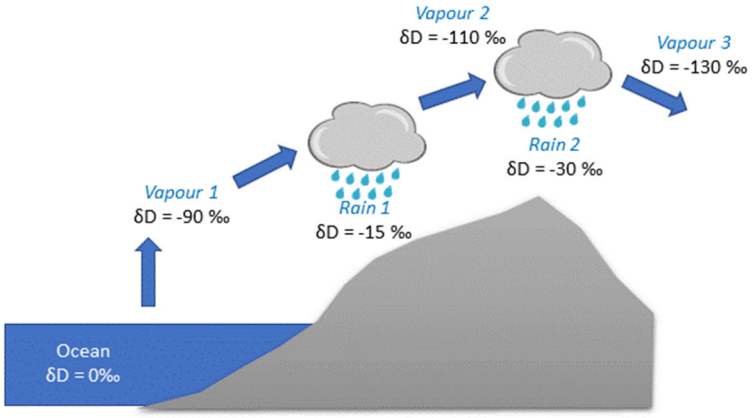

Figure 1: Principle of the continental effect, modified from [10].

Other isotope fractionation effects are due to elevation, latitude and amount of precipitation [9]. In natural waters, the D/H ratio typically varies as shown in Figure 2. The temporal variation in isotopic composition, due to weather conditions and season, can be very large [9]. The relative humidity is also known to affect the degree of isotope fractionation [11-13].

An example of monthly variations of the D/H ratio in precipitation is shown in Figure 3, displaying data from Espoo, Finland [14]. Correlation between the D/H ratio and temperature is very high.

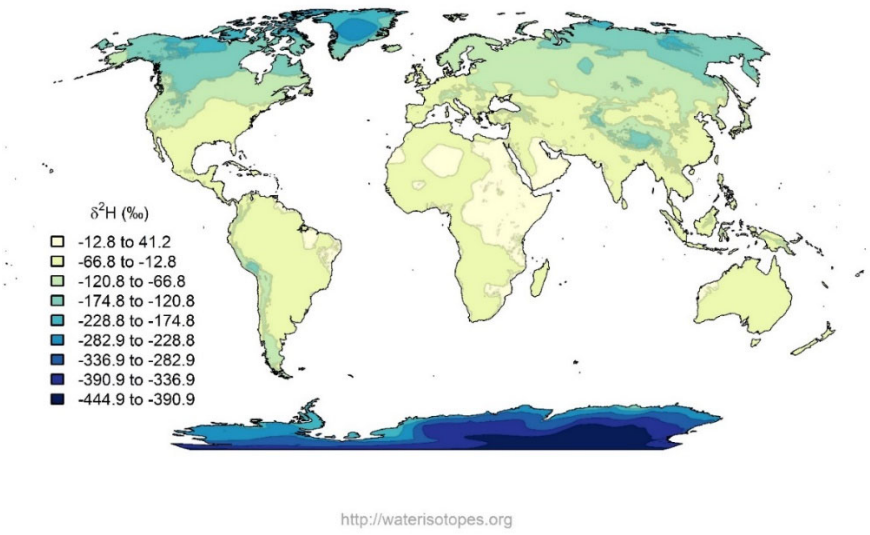

Figure 2: Average annual D/H ratios worldwide [15]. δ^2H=-444.9‰ (lower value) corresponds to a molar D/H ratio of $86 \cdot 10^{-6}$ and δ^2H=41.2‰ (upper value) corresponds to a molar D/H ratio of $162 \cdot 10^{-6}$ (see above about units of isotope ratios).

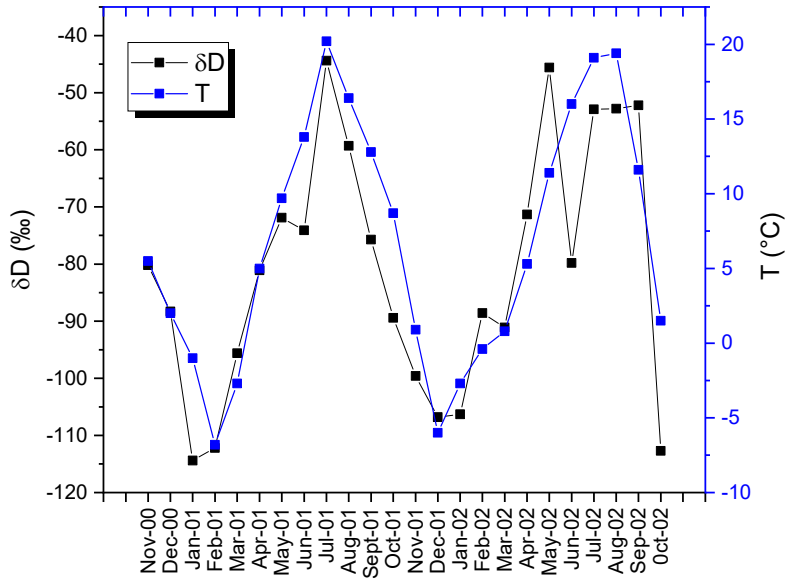

Figure 3: Monthly average δD values in precipitation and monthly average temperature in Espoo, Finland, during year 2000 and 2001. Data from Kortelainen and Karhu [14].

4.2. Bottled waters

Ref [16] presents a comprehensive database of δD values of 234 samples of bottled waters from various parts of world. δD varied between -147‰ and + 15‰, with a mean of -58‰. Examples of δD values of bottled water in Europe

are given in Table 3. Bottled waters with high δD values are probably originating from sources suffered from evaporation (e.g. some bottled waters from India display enrichment in ^2H [16]).

Table 3: Examples of δD in bottled water according to Bowen et al [16].

Country	Number of samples	δD (‰)	$R=^2H/^1H$ (10^6 x isotope amount ratio)
Denmark	1	-54	147
Finland	3	-82 to -78	143-144
France	4	-74 to -42	144-149
Germany	3	-68, -62, -20[a]	145, 146,153[a]

[a] Bad Adelholzen, source suffered from evaporation?

4.3. Laboratory tests on condensation

In laboratory tests on condensation of water vapour, performed by Deshpande et al [17], the concentration of ^2H was on average 1.5% higher in the condensate than in the vapour of ambient air (condensation temperature 0 °C). Maximum observed relative excess of ^2H was 4% [17]. Isotope fractionation during condensation depended on several factors, such as relative humidity and condensation temperature [17].

5. Isotope fractionation tests performed at Lund University

5.1. Collection of air humidity using the condensation method

For tritium analysis using LSC, >10 ml of water needs to be collected. The condensation method using an ice bath, as described in Kamath et al [1], is not applicable to samples at ESS due to the dry Swedish air. Instead commercial air dehumidifiers were tested.

Initial tests were performed on a small dehumidifier, Renkforce mini (Figure 4a). The sampling capacity of the Renkforce mini dehumidifier was too low when tested in a conservatory in March 2018 (temperatures about 10 °C and RH ~50%): to obtain 10 ml of water sampling times >12 hours were needed.

A privately-owned larger dehumidifier was then tested, Wood's 28 (Figure 4b). This one had a sampling capacity of 61 ml water for a sampling time of <1 h at ~18 °C and RH ~30%. A more portable version (Wood's MRD10, Figure 4c), was purchased, demonstrating a sampling capacity of 57 ml of water for < 4 hours at ~10 °C and RH ~50%.

Figure 4: Tested air dehumidifiers a) Renkforce mini; b) Wood's 28; c) Wood's MRD10.

The $^{2}H/^{1}H$ ratio was measured for some of the water samples generated during the testing of the sampling capacity of the dehumidifiers (the Renkforce mini and the Wood's 28 dehumifiers). 3x1 ml of water from each sample was transferred to a 1.5 ml HPLC thread vial (VWR1548-1488) using a pipette. The samples were analysed for their isotopic composition at the Stable isotope service lab, Department of Biology, Lund University, Sweden. SLAP, GISP and VSMOW were used as standards. The results, shown in Table 4, are in line with the Finnish data of Figure 3.

Table 5 shows δD values of snow that fell during the same period as the data of Table 4. The snow is enriched in ^{2}H compared to the condensed water from air humidity. This is consistent with the principles of kinetic fractionation: the heavier isotopologues are precipitated and the lighter isotopologues are enriched in the gaseous phase.

Table 4: δD in water samples collected by the dehumidifers Renkforce mini and Wood's 28. SEM: Standare error of mean.

Sampler	Date	Time (h)	Temp (°C)	RH (%)	ID	δD (‰)	MEAN (‰)	STDEV (‰)	SEM (‰)	$^{2}H/^{1}H$
Renkforce Mini	15-16 March 2018	14,5	6	50	KS1	-83.2				
					KS2	-80.2				
					KS3	-82.6	-82.0	1.6	0.9	0.000143
Renkforce Mini	16-17 March 2018	16,3	10	39	KS4	-66.8				
					KS5	-65.3				
					KS6	-68.9	-67.0	1.8	1.0	0.000145
Renkforce Mini	17-18 March 2018	23	6	44	KS16	-63.5				
					KS17	-61.3				
					KS18	-65.8	-63.5	2.2	1.3	0.000146
Renkforce Mini	18-19 March 2018	15	13	44	KS22	-57.4				
					KS23	-60.5				
					KS24	-61.6	-59.8	2.2	1.2	0.000146
Wood's 28	19 March 2018	2	11	40	KS25	-72.1				
					KS26	-72.8				
					KS27	-68.7	-71.2	2.2	1.3	0.000145
Wood's 28	19 March 2018	1	18	30	KS28	-60.5				
					KS29	-61.3				
					KS30	-61.1	-60.9	0.4	0.2	0.000146

Table 5: δD in snow (sampled 16-18 March 2018). SEM: Standare error of mean.

ID	δD (‰)	MEAN (‰)	STDEV (‰)	SEM (‰)	$^{2}H/^{1}H$
KS19	-43.9				
KS20	-55.3				
KS21	-53.7	-51.0	6.2	3.6	0.000148

A very simple test was performed in a domestic cooking oven to estimate the effects of isotope fractionation during the condensation method using an ice bath. A 500 ml glass jar with plastic lid was filled with tap water and placed in a freezer -18°C overnight. The jar was placed on a deep plate (see Figure 5) in a domestic oven set to 30°C with circulating air. A deep baking plate filled with 1 litre of tap water was also placed in the oven (see Figure 5). After 3 hours the ice was completely melted, the temperature of the oven showed 30°C and the relative humidity was 73%. About 1 dl of the water on the baking plate had evaporated, and 31 g water vapour had condensed on the 500 ml glass jar.

Figure 5: Experimental setup for test of isotope fractionation during evaporation/condensation.

Table 6 shows δD values from IRMS measurements of the original tap water, the condensate (the water condensed on the 500 ml jar with the ice) and the water remaining on the deep baking plate after the test (referred to as ”remaining tap water”). The δD value of the tap water remaining on the baking plate after evaporation is higher than the original tap water, showing that the lighter isotopologues have evaporated to a higher extent than the heavier. The condensate displays the lowest δD value, verifying that the water that has evaporated from the deep baking plate (and then condensed on the ice bath) is fractionated favouring the evaporation of the lighter isotopologues. The $^{2}H/^{1}H$ ratio of the condensate is approximately 4% lower than the original tap water. This includes two steps: evaporation from the deep baking plate followed by condensation on the ice bath. To estimate the fractionation during the condensation, a simple mass balance calculation can be performed, showing that the water vapour that has not been condensed should have a $^{2}H/^{1}H$ ratio of about 0.000138. Condensation of water vapour would then roughly increase the $^{2}H/^{1}H$ ratio with a few percent. This value is of the same order of magnitude as the tests performed by Deshpande et al [17].

Table 6: IRMS results of evaporation/condensation test performed 17 March 2018.

Sample	ID	δD (‰)	MEAN (‰)	STDEV (‰)	SEM (‰)	$^{2}H/^{1}H$
Original tap water	KS7	-48.9				
17 March 2018	KS8	-52.9				
	KS9	-49.4	-50.4	2.2	1.3	0.000148
Condensate on ice bath	KS10	-89.6				
	KS11	-88.7				
	KS12	-90.0	-89.4	0.7	0.4	0.000142
Remaining tap water	KS13	-46.1				
	KS14	-46.3				
	KS15	-47.3	-46.6	0.6	0.4	0.000149

5.2. Distillation of urine

Table 7 shows results from tests of distillation of urine samples in task 3b in the ongoing project SSM2018-1636. Isotope fractionation does not seem to be an issue in the distillation procedure.

Table 7: IRMS results of urine samples. SEM: Standard error of mean.

Individual	Date	ID	Description	δD (‰)	MEAN (‰)	STDEV (‰)	SEM (‰)	$^2H/^1H$
A	2018-05-30	GP34	Filtrated with charcoal	-63.1				
		GP35		-69.6				
		GP36		-63.2	-65.3	3.7	2.2	0.000146
A	2018-05-02	GP1	Filtrated and distilled at atmospheric pressure	-65.2				
		GP2		-70.6				
		GP3		-67.7	-67.8	2.7	1.6	0.000145
A	2018-05-02	GP4	Filtrated and distilled at lowered pressure (water jet pump)	-69.3				
		GP5		-70.9				
		GP6		-66.1	-68.8	2.5	1.4	0.000145
B	2018-05-XX	GP22	Filtrated and distilled at lowered pressure (water jet)	-70.4				
		GP23		-70.6				
		GP24		-74.4	-71.8	2.2	1.3	0.000145
C	2018-05-23	GP31	Filtrated and distilled at lowerest pressure (vacuum pump)	-70.7				
		GP32		-66.4				
		GP33		-70.1	-69.1	2.3	1.3	0.000145

5.3. Freeze drying of sewage sludge

Table 8 shows results from tests of water extracted in freeze drying of sewage sludge. The drying process was not complete. The low δD values indicate a higher degree of lighter isotopes leaving the sludge and ending up in the extracted water. Incomplete freeze drying may thus e.g. lead to an underestimation of the tritium concentration in the sewage sludge.

Table 8: IRMS results of water extracted from sewage sludge. The sludge was collected in April 2018. SEM: Standard error of mean.

ID	Description	δD (‰)	MEAN (‰)	STDEV (‰)	SEM (‰)	$^2H/^1H$
GP25	Freeze drying 1	-117.0				
GP26	Freeze drying 2	-110.1				
GP27	Freeze drying 3	-113.2	-113.4	3.46	2.00	0.000138

6. Production of tritium

The natural production of tritium mainly takes place in the upper atmosphere in cosmic ray-induced nuclear reactions (involving neutrons from spallation reactions) with atmospheric nitrogen and oxygen (e.g. $^{14}N + n \rightarrow ^{12}C + ^{3}H$). The vast majority of the tritium produced in the atmosphere is oxided to water (HTO). Tritium is also produced in the crust of the Earth in neutron-induced reactions with ^{6}Li.

Anthropogenic sources of tritium include atmospheric nuclear weapon's testing, nuclear power plants, tritium as tracer in research, hospitals and industry, and the use of tritium in luminous objects.

6.1. Tritium units

1 TU = 1 Tritium Unit, which equals 1 tritium atom per 10^{18} ^{1}H atoms, corresponding to 0.118 Bq/L of water.

6.2. Tritium isotope fractionation

Tritium in e.g. the hydrological cycle will be subjected to isotope fractionation, just like deuterium.

The fractionation factor for tritium has been shown to obey [4]:

$$\frac{\ln(\alpha_{T-H})}{\ln(\alpha_{D-H})} = 1.33 - 1.40 \quad (9)$$

where α_{T-H} is the fractionation factor for tritium to protium and α_{D-H} is the fractionation factor for deuterium to protium.

6.3. Tritium variations

The seasonal variations are also known as the spring leak. Each spring, the tropopause breaks up between 30° and 60° north, allowing water vapour from the stratosphere (higher tritium concentration) to enter the troposphere (lower tritium content). Annual differences are less pronounced [9]. These effects are shown in Figure 6.

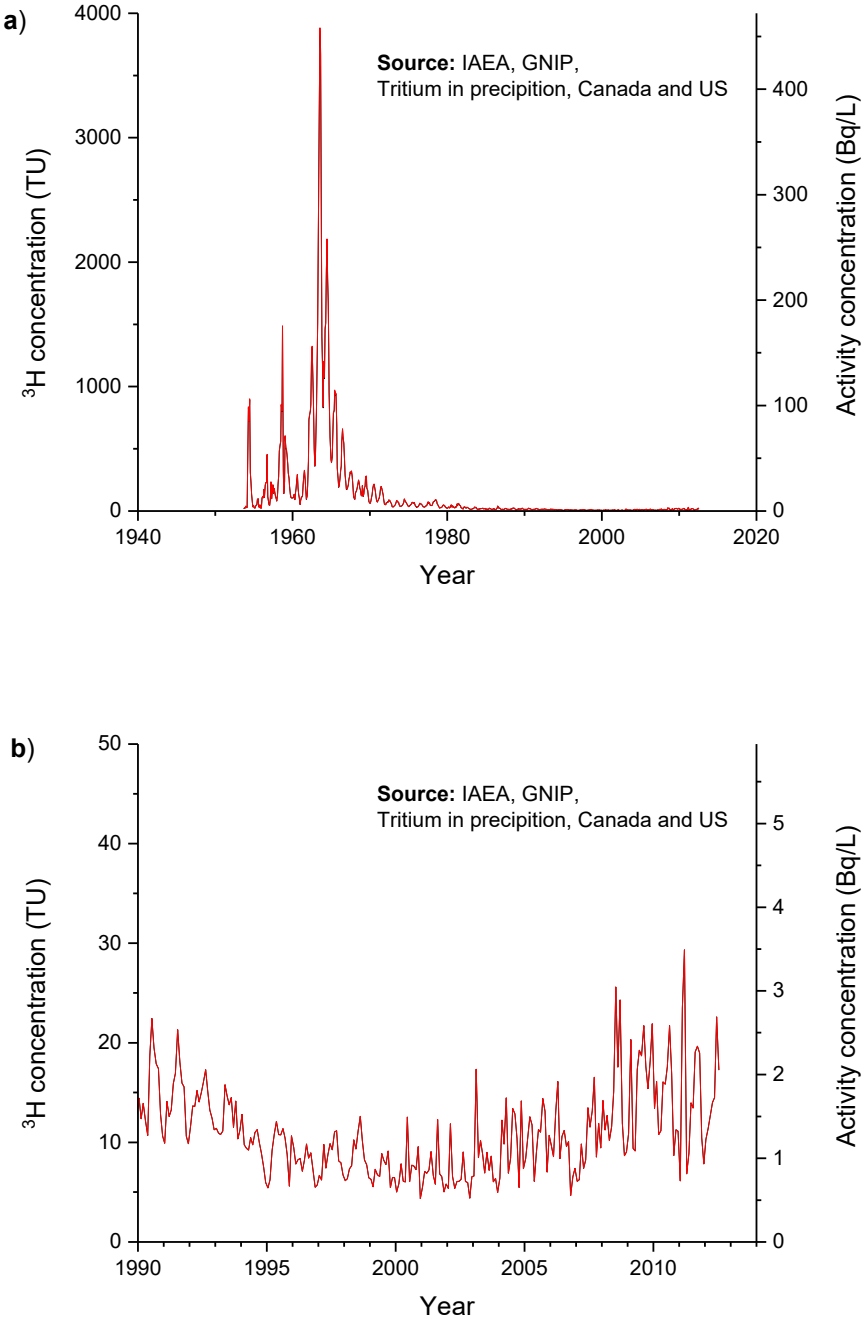

Figure 6: Tritium concentration in precipitation in Canada and the US [18] a) during the bomb-pulse era, b) from 1990 to 2012. 1 TU = 1 Tritium Unit, which equals 1 tritium atom per 10^{18} ^{1}H atoms, corresponding to 0.118 Bq/L of water.

Oceans have a low tritium content due to the long residence time of this reservoir: thus water vapour over the oceans also are low in tritium concentration (due to exchange with the surface water). As an air mass travels from the ocean and inlands, tritium is added not only from the stratosphere, but

also from evapotranspiration. Apart from distance from ocean (the continental effect), latitude and season are factors that influence the tritium concentration in precipitation [9].

6.4. Uncertainty in activity concentration of air humidity

Assuming that the isotope fractionation of tritium relative deuterium is of the same order of magnitude as for ^{2}H [19], the concentration of tritium may be up to 8% higher in the liquid phase than in the vapour (with the experimental conditions of Ref. [17]). Using Eq. (2) [4], taking into account that the mass difference and hence isotope fractionation decreases with increasing mass, the concentration of tritium may be up to 6% higher in the liquid phase than in the vapour.

7. Summary and conclusions

Isotope fractionation, resulting in changes in isotope ratios, may occur during processes in nature, such as evaporation and condensation in the hydrological cycle, as well as in sampling and sample preparation. The effect is more pronounced the larger the mass difference between the isotopes/isotopologues and may thus become an issue for specific activity assessments of light radionuclides such as tritium. The purpose of this brief report was to assess to what extent isotope fractionation can influence the results of measurements of tritium in the project SSM2018-1636. In particular, the report focussed on isotope fractionation occurring during collection of water vapour using an air dehumidifier, which has been used to collect water vapour from air for LCS measurements of waterborne tritium in air in Lund and close to the ESS facility.

Since heavier isotopologues (e.g. HTO) condensate more easily than lighter ones (e.g. H_2O), the specific activity of water collected from vapour using the condensation method may be higher than the original water vapour in gas phase. Using literature data as well as own experimental data, we estimate that the concentration of tritium may be up to several percent higher in the liquid phase collected than in the vapour when using the condensation method.

The distillation procedure used for water samples and urine in the project SSM2018-1636 did not seem to affect the hydrogen isotope ratios.

The report shows that measurements of the stable isotope ratio $^2H/^1H$ may serve as quality control of isotope fractionation effects in sample preparation prior to tritium measurements. $^2H/^1H$ measurements may also reveal information about the source and the natural history of various waters.

8. References

[1] Kamath, S.e.a. *Tritium concentration in ambient air around Kaiga Nuclear Power Plant.* Radiation Protection and Environment, In press, 2018.

[2] Le Goff, P., Fromm, M., Vichot, L., Badot, P.-M., Guétat, P. *Isotopic fractionation of tritium in biological systems.* Environment international, 65: 116-126, 2014.

[3] Hoefs, J., *Stable Isotope Geochemistry. [Elektronisk resurs]*. Cham : Springer International Publishing : Imprint: Springer, 2015. 7th ed. , 2015.

[4] Bigeleisen, J. *Correlation of tritium and deuterium isotope effects*. in *Tritium in the Physical and Biological Sciences. V. 1. Proceedings of a Symposium*. 1962.

[5] Sharp, Z. *Principles of stable isotope geochemistry.* 2017.

[6] Reji, T., Ravi, P., Ajith, T., Dileep, B., Hegde, A., Sarkar, P. *Environmental transportation of tritium and estimation of site-specific model parameters for Kaiga site, India.* Radiation protection dosimetry, 149(3): 304-308, 2011.

[7] Van Hook, W.A. *Vapor pressures of the isotopic waters and ices.* The Journal of Physical Chemistry, 72(4): 1234-1244, 1968.

[8] Horita, J., Cole, D.R. *Stable isotope partitioning in aqueous and hydrothermal systems to elevated temperatures*, in *Aqueous Systems at Elevated Temperatures and Pressures*. 2004, Elsevier. p. 277-319.

[9] Ingraham, N.L. *Isotope variations in precipitation*, in *Isotope tracers in catchment hydrology*, C. Kendall and J.F. McDonnell, Editors. 1998, Elsevier BV.

[10] Atzrodt, J., Derdau, V., Kerr, W.J., Reid, M. *Deuterium- and Tritium-Labelled Compounds: Applications in the Life Sciences.* Angewandte Chemie International Edition, 57(7): 1758-1784, 2018.

[11] Cappa, C.D., Hendricks, M.B., DePaolo, D.J., Cohen, R.C. *Isotopic fractionation of water during evaporation.* Journal of Geophysical Research: Atmospheres, 108(D16), 2003.

[12] Craig, H., Gordon, L., Horibe, Y. *Isotopic exchange effects in the evaporation of water: 1. Low-temperature experimental results.* Journal of Geophysical Research, 68(17): 5079-5087, 1963.

[13] Stewart, M.K. *Stable isotope fractionation due to evaporation and isotopic exchange of falling waterdrops: Applications to atmospheric processes and evaporation of lakes.* Journal of Geophysical Research, 80(9): 1133-1146, 1975.

[14] Kortelainen, N.M., Karhu, J.A. *Regional and seasonal trends in the oxygen and hydrogen isotope ratios of Finnish groundwaters: a key for mean annual precipitation.* Journal of Hydrology, 285(1): 143-157, 2004.

[15] http://waterisotopes.org. *Waterisotopes Database*. Accessed: Available from: http://waterisotopes.org.

[16] Bowen, G.J., Winter, D.A., Spero, H.J., Zierenberg, R.A., Reeder, M.D., Cerling, T.E., Ehleringer, J.R. *Stable hydrogen and oxygen isotope ratios of bottled waters of the world.* Rapid communications in mass spectrometry, 19(23): 3442-3450, 2005.

[17] Deshpande, R.D., Maurya, A.S., Kumar, B., Sarkar, A., Gupta, S.K. *Kinetic fractionation of water isotopes during liquid condensation under super-saturated condition.* Geochimica et Cosmochimica Acta, 100: 60-72, 2013.

[18] IAEA/WMO. *Global Network of Isotopes in Precipitation. The GNIP Database. Accessible at:* http://www.iaea.org/water. Accessed: 2018-02-02.
[19] Kaufman, S., Libby, W. *The natural distribution of tritium.* Physical Review, 93(6): 1337, 1954.

Appendix 4. Example of material to participants in tritium-in-man study (neighbours)

FÖRFRÅGAN OM DELTAGANDE

”Kartläggning av tritium i människor i Lund före start av European Spallation Source (ESS)”

Lund, oktober 2018

Bästa Lundabo/boende i Lundatrakten,

Lunds universitet söker frivilliga försökspersoner till en studie som kartlägger dagens nivåer av ämnet tritium i människor boende i Lundatrakten. Tritium förekommer naturligt i ytterst låga koncentrationer i allt vatten. Tritium bildas också t ex i kärnkraftsreaktorer och i vissa forskningsanläggningar: European Spallation Source (ESS) kommer att vara en sådan. För att i framtiden kunna säkerställa att ESS uppfyller de strikta krav som tillståndsmyndigheten Strålsäkerhetsmyndigheten (SSM) ställer, genomförs nu miljömätningar av tritium och andra radioaktiva ämnen runt ESS för att kartlägga dagens bakgrundsnivåer av strålning.

I en utökad studie vill vi på Lunds universitet nu bestämma halten av tritium i människa i Lundatrakten, så att vi i framtiden har ett bakgrundsvärde att jämföra nya mätningar med.

- Du måste vara myndig för att delta i studien.
- Du kan när som helst avbryta din medverkan i studien utan att uppge skäl.
- Du får om du önskar ta del av resultatet av tritiumanalysen.
- All information som ingår i studien hanteras enligt gällande sekretessbestämmelser.
- När resultaten från studien publiceras kommer alla resultat från enskilda individer att presenteras med en kodning, och kan inte spåras till ursprungsindividen.

Som medverkande lämnar du ett urinprov vid ett tillfälle. Provinsamlingen gör du själv i hemmet och provet hämtas i hemmet om du så önskar.

Är du intresserad av att delta? Skicka i så fall in bifogad intresseanmälan inom en vecka. Använd det medföljande svarskuvertet (porto är betalt). Vi kommer att välja ut 30 personer att delta i studien. Urvalet sker med avsikten att få jämn spridning av ålder, kön och geografisk bosättning. Lunds universitet kommer att kontakta dig per brev för att meddela om du valts ut till att medverka i studien.

Om du har några frågor eller synpunkter får du gärna höra av dig till undertecknad!

Vänliga hälsningar,

Kristina Stenström

PÅ NÄSTA SIDA HITTAR DU EN KORTFATTAD BAKGRUND TILL STUDIEN!

Kristina Eriksson Stenström, professor

Lunds universitet
Fysiska institutionen
Avdelningen för kärnfysik
Sölvegatan 14
223 62 Lund
Telefon: 046-2227643
Email: kristina.stenstrom@nuclear.lu.se

Bakgrund till studien

Människokroppen innehåller en liten mängd radioaktiva ämnen. Vanligtvis kommer merparten av de radioaktiva ämnena i kroppen från helt naturliga källor. Människan har sedan förra århundradet också framställt radioaktivitet på konstgjord väg, t ex för att användas inom forskning, industri och sjukvård. Tritium (supertungt väte) är ett sådant radioaktivt ämne, som också bildas naturligt i atmosfären. Genom att tritiumet binds in i vattenmolekyler sprids det genom vattnets kretslopp även till människans kropp. Den stråldos som människan får från naturligt tritium är bara ca 0,001% av den naturliga strålningen från rymden, marken och oss själva.

Människans framställning av tritium kommer främst från atmosfäriska kärnvapentest på 1950- och 1960-talen, men också från kärnkraftsreaktorer, forskningsreaktorer och -laboratorier. Tritium används t ex som spårämne inom forskning. Tritium används också som ingrediens i viss självlysande färg, som finns i en del armbandsklockor och i kikarsikten. Tritium kan leta sig ut från alla dessa källor och även hamna i människokroppen i ytterst låga, men varierande, koncentrationer. Vi vill nu kartlägga tritium i människa i Lundatrakten före start av forskningsanläggningen European Spallation Source (ESS).

INFORMATION TILL FRIVILLIGA DELTAGARE

”Kartläggning av tritium i människor i Lund före start av European Spallation Source (ESS)”

Bäste Lundabo,

Tack för att du ställer upp som frivillig försöksperson i kartläggningen av dagens nivåer av tritium i människa i Lundatrakten!

Nedan sammanfattas studiens bakgrund och upplägg, samt villkoren för medverkan i studien.

1. Bakgrund och syfte

Det radioaktiva ämnet tritium förekommer naturligt i ytterst låga koncentrationer i allt vatten. Tritium bildas också t ex i kärnkraftsreaktorer och i vissa forskningsanläggningar: European Spallation Source (ESS) kommer att vara en sådan. För att i framtiden kunna säkerställa att ESS uppfyller de strikta krav som tillståndsmyndigheten Strålsäkerhetsmyndigheten (SSM) ställer, genomförs nu miljömätningar av tritium och andra radioaktiva ämnen runt ESS för att kartlägga dagens bakgrundsnivåer av strålning.

I en utökad studie vill vi på Lunds universitet nu bestämma halten av tritium i människa i Lundatrakten, så att vi i framtiden har ett bakgrundsvärde att jämföra nya mätningar med.

2. Förfrågan om deltagande

I studien ingår såväl allmänhet som personer som hanterar och eventuellt exponeras för tritium på sina arbetsplatser. Vi har utifrån inkomna intresseanmälningar gjort ett urval av vilka personers urin vi önskar analysera. Du är en av de personer från allmänheten vars tritiumhalt vi gärna vill analysera. Genom att ha fyllt i och lämnat in intresseanmälan har du gett ditt samtycke till att medverka i studien.

3. Hur går studien till?

När vi fått enkäten kommer vi att kontakta dig per epost för att avtala lämpliga datum för provinsamling. Du kommer sedan att förses med ett provtagningskit som också innehåller instruktioner för urininsamling. Dagen före provinsamling ombeds du föra protokoll över vad du dricker. Själva provtagningen kommer att vara mycket enkel, där du vid ett tillfälle ombeds samla morgonurin i en plastburk.

Vi hämtar gärna upp ditt urinprov i din bostad.

Vi hämtar gärna upp ditt urinprov i din bostad: placera då kylväskan med urinprovet utanför din bostad senast kl 08.00 samma dag som provinsamlingen. Forskarlaget hämtar kylväskan under förmiddagen. Alternativt hämtas/lämnas provet på annan plats (om så är avtalat).

En delmängd av urinprovet analyseras sedan för kreatininhalt (ett mått på vätskeintaget). En annan delmängd av urinprovet mäts med hjälp av en vätskescintillator för att bestämma halten av tritium. Analyserna görs snarast efter det att provet anlänt, antingen vid Lunds universitet eller vid Mangalore University i Indien. Efter analys destrueras provet, och ingen urin kommer att sparas.

4. Vilka är riskerna?

Studien medför inte något fysiskt obehag eftersom det enda vi kommer att be dig om är att själv ta ett urinprov, samt att dagen före provinsamlingen bokföra ditt intag av vätska i ett protokoll. Med största sannolikhet förekommer ingen tritiumhalt som medför stråldoser av betydelse.

5. Finns det några fördelar?

Resultaten av studien kommer att ligga till grund för att i framtiden kontrollera att stråldosbidraget från ESS ligger inom tillåtna gränser. Du får genom att delta i studien också veta vilken nivå av tritium som du utsätts för idag.

Om du utsätts för tritium i ditt yrkesliv kan resultaten av studien påvisa hur säker och god din arbetsmiljö är ur strålskyddssynpunkt, eller peka på yrkesmässiga förhållanden som kan behöva förbättras.

6. Hantering av data och sekretess

All information som ingår i studien hanteras enligt gällande sekretessbestämmelser. Ansvarig för dina personuppgifter är Lunds universitet. I projektet kommer personuppgifter om dig att behandlas i enlighet med den europeiska Dataskyddsförordningen (GDPR) och Dataskyddslagen (SFS 2018:218). Personuppgiftsansvarig för detta projekt är Lunds universitet (Box 117, 221 00 LUND, tel. 046-2220000, registrator@lu.se, org.nr. 202100-3211).

Dina svar och ditt resultat kommer att behandlas så att obehöriga inte kan ta del av dem. Detta sker genom att dina enkätsvar och prov kodas, och att enkätsvar och kodnyckel förvaras inlåsta, och därmed oåtkomliga för obehöriga, vid Avdelningen för kärnfysik vid Lunds universitet. Din provburk kommer att vara märkt med en pseudonym för att garantera sekretessen. När resultaten från studien publiceras kommer alla resultat från enskilda individer att presenteras med en kodning, och kan inte spåras till ursprungsindividen.

Du har rätt att gratis, en gång per kalenderår, efter skriftligt undertecknad ansökan ställd till oss, få besked om vilka personuppgifter om dig som vi behandlar och hur vi behandlar dessa. Du har också rätt att begära rättelse i fråga om personuppgifter som vi behandlar om dig.

7. Hur får jag information om studiens resultat?

Resultat av undersökningen kommer att skickas direkt till dig om så önskas (ange i bifogad enkät). Detta kommer att ske i god tid innan resultaten av undersökningen avses att publiceras i vetenskaplig tidskrift.

8. Ersättning

Ingen ekonomisk ersättning kan erbjudas för deltagande i studien.

9. Frivillighet

Samtyckte till studien sker genom att du skickar in enkäten. Deltagande i studien är helt frivilligt, och du kan när som helst, utan särskild förklaring, avbryta deltagandet genom att kontakta undertecknad. Du kan då också begära att dina samtliga inlämnade data destrueras och att du stryks ur kodnyckeln. Resultat som redan publicerats i vetenskaplig tidskrift kan däremot inte destrueras.

10. Ansvarig för studien

Ansvarig för studien är:

Kristina Eriksson Stenström, professor

Lunds universitet

Fysiska institutionen

Avdelningen för kärnfysik

Sölvegatan 14

223 62 Lund

Telefon: 046-222 76 43

Epost: kristina.stenstrom@nuclear.lu.se

INSTRUKTIONER FÖR PROVTAGNING

”Kartläggning av tritium i människor i Lund före start av European Spallation Source (ESS)”

Du har fått ett kit bestående av:

- Kylväska
- Penna (behåll gärna denna!)
- Kylklamp
- Enkät
- Protokoll för dokumentation av vätskeintag
- 1 st 100 ml burk
- 2 st plastpåsar
- 1 st klämma

Dagen före provinsamling:

1. Ta fram kylväskan.
2. Lägg kylklampen i frysen.
3. Fyll i enkäten.
4. Dokumentera allt du dricker i protokollet.

Nästa dag (provinsamling direkt på morgonen):

5. Direkt på morgonen: samla morgonurin i aktuell provburk. Förslut burken ordentligt efter insamling.
6. Ställ burken med urinprovet i dubbla plastpåsar och förslut påsarna med klämman.
7. I kylväskan: Lägg i den frysta kylklampen, urinprovet (burken med dubbla plastpåsar om), ifylld enkät samt ifyllt protokoll om föregående dags vätskeintag.
8. Stäng kylväskan och placera utanför din bostad senast kl 08.00. Forskarlaget hämtar kylväskan under förmiddagen. Alternativt hämtas/lämnas provet på annan plats (om så är avtalat).

PROTOKOLL FÖR VÄTSKEINTAG

”Kartläggning av tritium i människor i Lund före start av European Spallation Source (ESS)”

Ditt namn:_____

Datum för förande av vätskeprotokoll: _____

Datum för insamling av urin: _____

Pseudonym (fylls i av Lunds universitet):_____

Fyll i protokollet så noga som möjligt!

Klockslag	Dryck	Om tillämpligt: Vatten till drycken kom från… (t ex vattenkran i hemmet)	Ungefärlig mängd (deciliter)

ENKÄT

”Kartläggning av tritium i människor i Lund före start av European Spallation Source (ESS)”

Genom att lämna in denna enkät ger du ditt samtycke till att vi analyserar din urin med avseende på tritiumhalten samt även kreatininhalten (för att få en uppskattning om vätskeintaget).

Du har rätt att när som helst avbryta din medverkan i studien utan att uppge skäl. Om du vill kontakta oss senare efter studiens slut är det viktigt att du behåller kontaktinformationen i det medföljande brevet.

Som medverkande lämnar du ett urinprov vid ett tillfälle. Provinsamlingen av urin gör du själv i hemmet och provet hämtas i hemmet om du så önskar.

Vänligen fyll i medföljande frågeformulär och lägg i kylväskan tillsammans med urinprovet.

Din pseudonym (fylls i av Lunds universitet):_____

1. Ange ditt namn: _____
2. Vilket är ditt födelseår? _____
3. Vilken är din ungefärliga vikt (kg)? _____
4. Vilken är din bostadsadress (inkl postnummer)?

   _____
5. Vilken är din epost-adress?

   _____
6. Är du kvinna eller man (eller vill inte uppge)?

   ☐ Kvinna ☐ Man ☐ Vill inte uppge

7. Tritiumhalten i kroppen kan påverkas av om man använder vissa armbandsur med självlysande färg. Använder du ett armbandsur med självlysande färg?

☐ Ja ☐ Nej

Om ja, vilket märke/modell? (gärna så detaljerat som möjligt):

_____

_____

8. Hanterar din arbetsplats någon form av tritiumhaltigt material?

☐ Ja, nämligen

_____

_____

☐ Nej

☐ Vet inte

9. Jag önskar ta del av resultatet av tritiumanalysen

☐ Ja ☐ Nej

RESULTAT

”Kartläggning av tritium i människor i Lund före start av European Spallation Source (ESS)”

Hej!

Stort tack för din medverkan i studien ”Kartläggning av tritium i människor i Lund före start av European Spallation Source (ESS)”!

Vi har nu analyserat urinprov från dig och från över 50 andra frivilliga försökspersoner i Lundatrakten. Såväl personer från allmänheten som arbetstagare som hanterar tritiumhaltiga material i sitt arbete på laboratorier och sjukhus har ingått i studien. Här kommer resultaten av analysen av ditt urinprov:

Namn:_____

Ditt resultat (koncentration av vattenbundet tritium i urin, Bq/liter): _____ Bq/liter

Generellt sett var tritiumhalten i samtliga analyserade urinprov ytterst låga. För att få ett perspektiv på nivåerna kan du jämföra ditt värde med följande siffror:

- Uppmätt värde på tritium i dricksvatten i Lund (denna studie): 1,5 ± 0,4 Bq/liter
- EU:s riktvärde[2] för tritium i dricksvatten: 100 Bq/liter
- WHO:s vägledande gränsvärde[3] för tritium i dricksvatten: 10 000 Bq/L

Vi kommer nu att sammanställa resultaten i en vetenskaplig artikel. Din anonymitet är garanterad i publikationen.

[2] Detta är inte ett gränsvärde, utan innebär att orsakerna till ett överskridande ska utredas (Livsmedelsverkets föreskrift SLVFS 2001:30).

[3] Det vägledande gränsvärdet är beräknat utifrån en effektiv stråldos på 0,1 mSv/år, ett intag av 2 liter vatten per dag, och med doskoefficienten för vattenburet tritium satt till $1{,}8 \cdot 10^{-11}$ Sv/Bq. 0,1 mSv/år motsvarar en ytterst låg risknivå som inte förväntas ge någon mätbar negativ hälsoeffekt. En person (aldrig-rökare) som bor i Sverige får i medeltal stråldosen 2,4 mSv/år från olika källor, se https://www.stralsakerhetsmyndigheten.se/publikationer/rapporter/stralskydd/2007/200702/.

- ✓ Om du inte vill att ditt anonymiserade resultat publiceras, är du välkommen att kontakta undertecknad senast 2019-03-15.

- ✓ Om du vill läsa artikelutkastet före det skickas in för publicering, meddela undertecknad senast 2019-03-15.

Du är välkommen att kontakta undertecknad om du har några frågor!

Vänliga hälsningar

Kristina Eriksson Stenström, professor
Lunds universitet
Fysiska institutionen
Avdelningen för kärnfysik
Sölvegatan 14
223 62 Lund
Telefon: 046-222 76 43
Epost: kristina.stenstrom@nuclear.lu.se

Appendix 5. Procedure: Sample preparation of tritium samples and measurement by liquid scintillation counting

Department of Physics
Division of Nuclear Physics
The Biospheric and Anthropogenic Radioactivity (BAR) group

Procedure: Sample preparation of tritium samples and measurement by liquid scintillation counting

Guillaume Pedehontaa-Hiaa
Guillaume.pedehontaa-hiaa@med.lu.se

Department of Physics
Division of Nuclear Physics
Professorsgatan 1
SE-223 63 Lund, SWEDEN

Report BAR-2019/03

Lund 2019

Procedure: Sample preparation of tritium samples and measurement by liquid scintillation counting

1. Purpose

This procedure describes the preparation of water-based samples prior to the analysis of their tritiated water (HTO) content using Liquid Scintillation Counting (LSC). The purpose of the pre-treatments is to decrease the colour quenching of the sample and to decrease the amount of other beta emitters that could be detrimental for the analytical results.

The sample preparation consists of two steps:

- A filtration on activated charcoal
- A distillation

The measurements are performed on a Beckmann LS 6500 LSC liquid scintillation counter at Medical Radiation Physics, Malmö. The operating conditions described here were optimised to lower the minimum detectable activity (MDA).

2. Procedure applicability

The procedure is applicable to water and urine sample with a volume of at least 50 mL.

Urine, ground water and surface water samples require a pre-treatment before measurement. In addition, the urine samples should be stored in a fridge at 4 °C.

Precipitation and air humidity samples can be analysed directly without pre-treatment.

3. Sample preparation

3.1. Procedure map

The procedure map is shown in Figure 1.

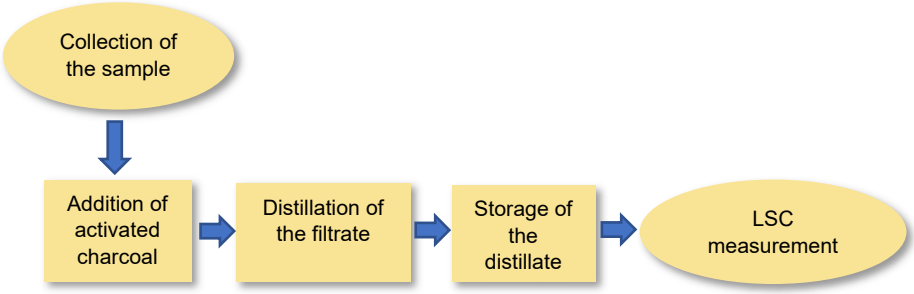

Figure 1: Procedure map.

The filtrate is the liquid phase collected after filtration of the sample. The distillate is the liquid phase collected after distillation.

3.2. Risk assessment

Full personal protective equipment (PPE) should to be worn, including: lab coat, gloves and safety googles, long sleeve trousers and closed shoes. Collective protective equipment such as ventilation and fume-hoods must also be operating. Filtration and distillation must be performed under a fume-hood. The use of water and electrical devices creates a risk of electrocution. Safety sheets of the chemicals must be available in the laboratory.

3.3. Filtration

The filtration should be performed according to the following steps:

- Urine samples are stored at 4 °C in a fridge, water samples can be stored at room temperature
- Mixing 50 mL of the sample with 2.5 g of activated charcoal for a concentration of 50 g L^{-1}
- Shaking vigorously the mixture for at least 2 minutes (if some white foam still forms shaking 2 additional minutes)
- Placing the filter on the funnel and place the funnel on an appropriate container such as a beaker (V > 50 mL)
- Pouring the sample solution on the filter progressively, the mixture may need to be shortly agitated again to put the charcoal in suspension in the liquid phase
- Collecting the filtrate for distillation (see Figure 2)

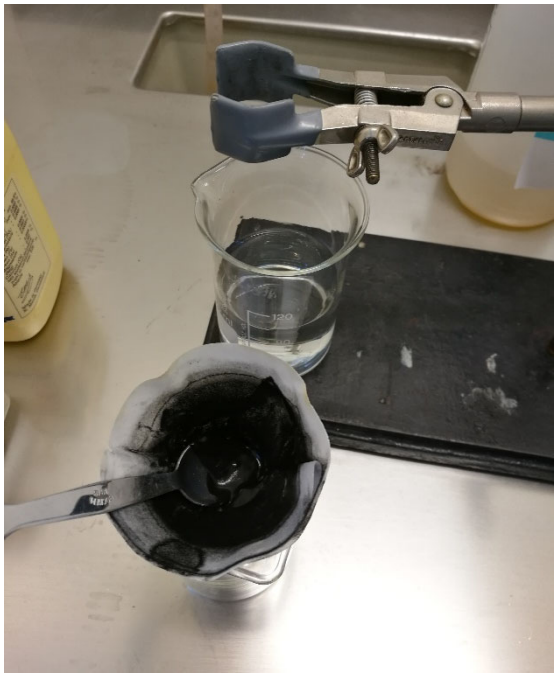

Figure 2: Example of filtration setup

3.4. Distillation at lowered pressure

The distillation set-up is a classical one with a membrane pump and a valve to control the pressure in order to limit the combustion of residues. The chosen operating conditions for this distillation set-up are 40 °C and 0.1 bar.

3.4.1. Material

Figure 3 is a diagram of the distillation set-up. The set-up requires one electric outlet for the heating mantel, one for the pump and one tap for the cooling system.

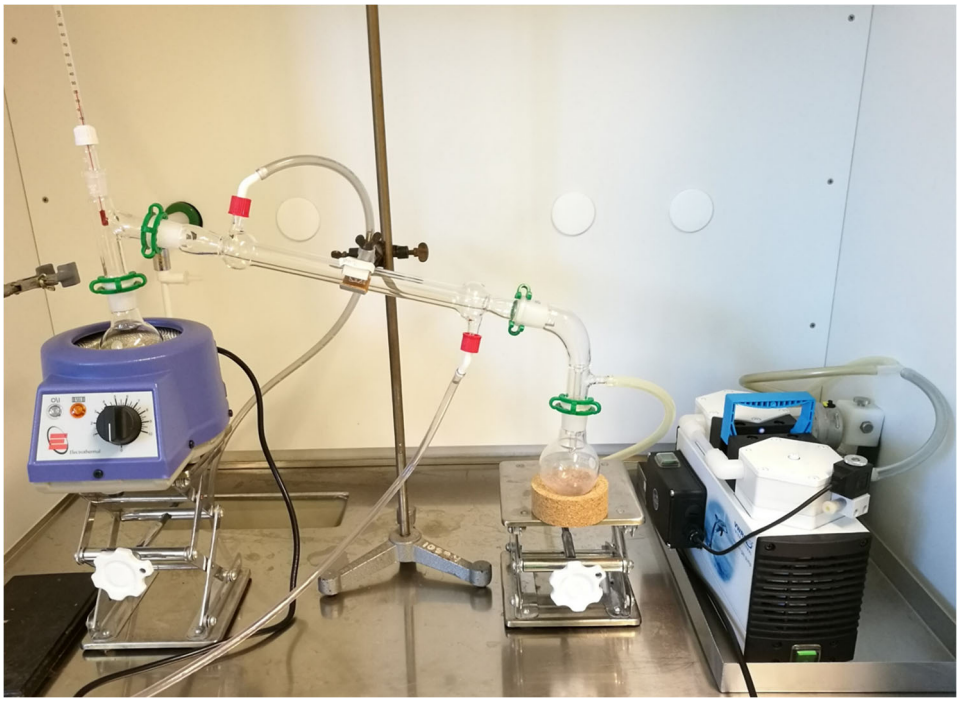

Figure 3: Photo of the glassware of the distillation setup.

3.4.2. Method

The filtration should be performed according to the following steps:

- Weighing the two empty round bottom flasks.
- Adding about 100 mg of pumice stone in the distilling round bottom flask and weighing the flask again.
- Adding the distillate and weighing the flask. Those masses will be used to calculate the percentage of water loss and the percentage of residues after the distillation
- Installing the elements of the set-up according to Figure 3. Air tightness between glassware pieces is obtained thanks to Teflon sleeves. It is important to verify that the inlet and outlet of the liebig condenser are correctly plugged (the water must flow from the bottom to the top of the condenser).
- Starting the water flow through the condenser.
- Starting the membrane pump and set the pressure to 0.1 bar.
- Turning on the heating mantel. The temperature should be about 40 °C, if too high or too low, the pressure can be adjusted with the valve.
- The distillation should be completed up to dryness to avoid isotope fractionation but the residues should not burn inside the distilling flask to avoid combustion impurities in the receiving flask
- When the distillation is finished, turning off the heating mantel and removing it.
- Switching off the pump and removing the plastic tube from the vacuum adapter when the atmospheric pressure is reached.
- Removing the receiving flask, weighing it and transfering the distillate to a storage container.

- Once the distilling flask has cooled down, removing it and weighing it to calculate the percentage of residue.

3.5. Cleaning

All reusable consumables that were in contact with activated charcoal must be cautiously cleaned with a filter brush then rinsed with ultrapure water.

The distilling flask must firstly be rinsed with tap water and put in an ultrasonic bath several minutes to dissolve part of the residues. Limestone tends to appear in the flasks after several distillations. They should regularly be rinsed with acetic acid in order to dissolve this limestone layer.

All the other pieces of the distillation set-up in contact with the urine sample (glassware, Teflon sleeves, thermometer…) must be successively rinsed with tap water, ultrapure water and ethanol.

4. Measurement

The HTO activity concentration of the urine samples was determined using a Beckmann LS 6500 LSC multi-purpose liquid scintillation counter. The efficiency of each measurement is determined using Horrocks' method for quenching correction.

From each sample, 2 subsamples are analysed. Each subsample consists of 10 mL distillate mixed with 10 mL Ultima Gold LLT cocktail (PerkinElmer) in a 20 mL LSC polyethylene vial (Wheaton). The vials are shaken for 2 min and stored at 48 h in the dark to reduce chemical quenching before analysis. The water/scintillation cocktail ratio is optimised to 1:1 to lower the level of minimal detectable activity (MDA).

The activity in each subsample is measured five times, consecutively, for 120 min each, giving a total detection time of 1200 min for each sample.

Background samples are prepared using Grevie well water, a water with a well-documented low tritium concentration, from a deep well situated at the Grevie-Bulltofta Waterworks (N55.61418, E13.18418), operated by VA Syd. Standard samples are prepared using a reference tritium solution (TRY44 number R8/12/123 by Eckert and Ziegler, Germany) with a reported uncertainty in the activity concentration of 1.5%.

The Swedish Radiation Safety Authority has a comprehensive responsibility to ensure that society is safe from the effects of radiation. The Authority works from the effects of radiation. The Authority works to achieve radiation safety in a number of areas: nuclear power, medical care as well as commercial products and services. The Authority also works to achieve protection from natural radiation an to increase the level of ratiation safety internationally.

The Swedish Radiation Safety Authority works proactively and presentively to protect people and the environment from the harmful effects of radiation, now and in the future.
The Authority issues regulations and supervises compliance, while also supporting research, providing training and information, and issuing advice. Often, activities involving radiation require licences issued by the Authority. The Swedish Radiation Safety Authority maintains emergency preparedness around the clock with the aim of limiting the aftermath of radiation accidents and the unintentional spreading of radioactive substances. The Authority participates in international co-operation in order to promote radiation safety and finances projects aiming to raise the level of radiation safety in certain Eastern European countries.

The Authority reports to the Ministry of the Environment and has around 300 employees with competencies in the fields of engineering, natural and behavioral sciences, law, economics and communications. We have recieved quality, environmental and working environment certification.

Publikationer utgivna av Strålsäkerhetsmyndigheten kan laddas ned via stralsäkerhetsmyndigheten.se eller beställas genom att skicka e-post till registrator@ssm.se om du vill ha broschyren i alternativt format, som punktskrift eller daisy.

Strålsäkerhetsmyndigheten
Swedish Radiation Safety Authority
SE-171 16 Stockholm
Phone: 08-799 40 00
Web: ssm.se
E-mail: registrator@ssm.se

E-print AB, 2020